

CERN-PH-EP-2012-300

Submitted to: JHEP

Measurement of isolated-photon pair production in pp collisions at $\sqrt{s} = 7$ TeV with the ATLAS detector

The ATLAS Collaboration

Abstract

The ATLAS experiment at the LHC has measured the production cross section of events with two isolated photons in the final state, in proton-proton collisions at $\sqrt{s} = 7$ TeV. The full data set collected in 2011, corresponding to an integrated luminosity of 4.9 fb^{-1} , is used. The amount of background, from hadronic jets and isolated electrons, is estimated with data-driven techniques and subtracted. The total cross section, for two isolated photons with transverse energies above 25 GeV and 22 GeV respectively, in the acceptance of the electromagnetic calorimeter ($|\eta| < 1.37$ and $1.52 < |\eta| < 2.37$) and with an angular separation $\Delta R > 0.4$, is $44.0^{+3.2}_{-4.2}$ pb. The differential cross sections as a function of the di-photon invariant mass, transverse momentum, azimuthal separation, and cosine of the polar angle of the largest transverse energy photon in the Collins–Soper di-photon rest frame are also measured. The results are compared to the prediction of leading-order parton-shower and next-to-leading-order and next-to-next-to-leading-order parton-level generators.

Measurement of isolated-photon pair production in pp collisions at $\sqrt{s} = 7$ TeV with the ATLAS detector

ATLAS Collaboration

G. Aad *et al.* (full author list given at the end of the article in Appendix)

ABSTRACT: The ATLAS experiment at the LHC has measured the production cross section of events with two isolated photons in the final state, in proton-proton collisions at $\sqrt{s} = 7$ TeV. The full data set collected in 2011, corresponding to an integrated luminosity of 4.9 fb^{-1} , is used. The amount of background, from hadronic jets and isolated electrons, is estimated with data-driven techniques and subtracted. The total cross section, for two isolated photons with transverse energies above 25 GeV and 22 GeV respectively, in the acceptance of the electromagnetic calorimeter ($|\eta| < 1.37$ and $1.52 < |\eta| < 2.37$) and with an angular separation $\Delta R > 0.4$, is $44.0^{+3.2}_{-4.2}$ pb. The differential cross sections as a function of the di-photon invariant mass, transverse momentum, azimuthal separation, and cosine of the polar angle of the largest transverse energy photon in the Collins–Soper di-photon rest frame are also measured. The results are compared to the prediction of leading-order parton-shower and next-to-leading-order and next-to-next-to-leading-order parton-level generators.

Contents

1	Introduction	1
2	The ATLAS detector	2
3	Data and Monte Carlo samples	3
4	Event selection	4
5	Signal yield extraction	5
5.1	Jet background subtraction	5
5.2	Electron background subtraction	9
6	Cross section measurement	10
6.1	Efficiency and unfolding	10
6.2	Trigger efficiency correction	12
6.3	Results	12
7	Comparison with theoretical predictions	13
8	Conclusion	15
A	Experimental differential cross section	21

1 Introduction

The measurement at the LHC of the production cross section, in pp collisions, of two isolated photons not originating from hadronic decays, $pp \rightarrow \gamma\gamma + X$, provides a tool to probe perturbative Quantum Chromodynamics (QCD) predictions and to understand the irreducible background to new physics processes involving photons in the final state. These processes include Higgs boson decays to photon pairs ($H \rightarrow \gamma\gamma$) or graviton decays predicted in some Universal Extra-Dimension models [1, 2].

Recent cross section measurements for di-photon production at hadron colliders were performed by the DØ [3] and CDF [4] collaborations at the $\sqrt{s} = 1.96$ TeV Tevatron $p\bar{p}$ collider, and by ATLAS [5] and CMS [6] using $\sqrt{s} = 7$ TeV pp collisions recorded at the LHC in 2010.

In this paper, the production cross section of two isolated photons with transverse energies (E_T) above 25 GeV and 22 GeV respectively, in the acceptance of the ATLAS electromagnetic calorimeter ($|\eta| < 1.37$ and $1.52 < |\eta| < 2.37$) and with an angular separation $\Delta R > 0.4$, is measured. The results are obtained using the data collected by the ATLAS

experiment in 2011, which corresponds to an integrated luminosity¹ of $(4.9 \pm 0.2) \text{ fb}^{-1}$, thus increasing the sample size by more than a factor of 100 compared to the previous measurement. The transverse energy thresholds for the two photons are higher than in the previous measurement (16 GeV).

The integrated di-photon production cross section is measured, as well as the differential cross sections as a function of four kinematic variables: the di-photon invariant mass ($m_{\gamma\gamma}$), the di-photon transverse momentum ($p_{T,\gamma\gamma}$), the azimuthal² separation between the photons in the laboratory frame ($\Delta\phi_{\gamma\gamma}$), and the cosine of the polar angle of the highest E_T photon in the Collins–Soper di-photon rest frame ($\cos\theta_{\gamma\gamma}^*$) [9]. The first distribution is of obvious interest for resonance searches; the second and the third provide important information in the study of higher-order QCD perturbative effects and fragmentation, especially in some specific regions such as the small $\Delta\phi_{\gamma\gamma}$ limit; the fourth can be used to investigate the spin of di-photon resonances. For this purpose, the Collins-Soper rest frame is preferred to other frame definitions because of its robustness with respect to initial state radiation. The results are compared to the predictions from: parton-shower Monte Carlo generators, PYTHIA [10] and SHERPA [11]; parton-level calculations with next-to-leading-order (NLO) QCD corrections using the DIPHOX [12] program complemented by GAMMA2MC [13]; and at next-to-next-to-leading-order (NNLO), using 2γ NNLO [14]. The contribution from the di-photon decays of the particle recently discovered by ATLAS [15] and CMS [16] in the search for the Standard Model Higgs boson is not included in the theoretical calculations. It is expected to contribute around 1% of the signal in the $120 < m_{\gamma\gamma} < 130$ GeV interval, and negligibly elsewhere.

2 The ATLAS detector

ATLAS [17] is a multipurpose detector with a forward-backward symmetric cylindrical geometry and nearly 4π coverage in solid angle. The most relevant subdetectors for the present analysis are the inner tracking detector (ID) and the calorimeters.

The ID consists of a silicon pixel detector and a silicon microstrip detector covering the pseudorapidity range $|\eta| < 2.5$, and a straw tube transition radiation tracker covering $|\eta| < 2.0$. It is immersed in a 2 T magnetic field provided by a superconducting solenoid. The ID allows efficient reconstruction of converted photons if the conversion occurs at a radius of up to ≈ 0.80 m.

The electromagnetic calorimeter (ECAL) is a lead/liquid-argon (LAr) sampling calorimeter providing coverage for $|\eta| < 3.2$. It consists of a barrel section ($|\eta| < 1.475$) and two end-caps ($1.375 < |\eta| < 3.2$). The central region ($|\eta| < 2.5$) is segmented into

¹The 3.9% uncertainty in the integrated luminosity for the complete 2011 data set is based on the calibration described in refs. [7, 8] including an additional uncertainty for the extrapolation to the later data-taking period with higher instantaneous luminosity.

²ATLAS uses a right-handed coordinate system with its origin at the nominal interaction point (IP) in the centre of the detector and the z -axis coinciding with the axis of the beam pipe. The x -axis points from the IP to the centre of the LHC ring, and the y -axis points upward. Cylindrical coordinates (r, ϕ) are used in the transverse plane, ϕ being the azimuthal angle around the beam pipe. The pseudorapidity is defined in terms of the polar angle θ as $\eta = -\ln \tan(\theta/2)$.

three longitudinal layers. The first (inner) layer, covering $|\eta| < 1.4$ in the barrel and $1.5 < |\eta| < 2.4$ in the end-caps, has high granularity in the η direction (between 0.003 and 0.006 depending on η), sufficient to provide event-by-event discrimination between single-photon showers and two overlapping showers from a π^0 decay. The second layer, which collects most of the energy deposited in the calorimeter by the photon shower, has a cell granularity of 0.025×0.025 in $\eta \times \phi$. The third layer is used to correct high energy showers for leakage beyond the ECAL. In front of the electromagnetic calorimeter a thin presampler layer, covering the pseudorapidity interval $|\eta| < 1.8$, is used to correct for energy loss before the ECAL.

The hadronic calorimeter (HCAL), surrounding the ECAL, consists of an iron/scintillator tile calorimeter in the range $|\eta| < 1.7$, and two copper/LAr calorimeters spanning $1.5 < |\eta| < 3.2$. The ECAL and HCAL acceptance is extended by two LAr forward calorimeters (using copper and tungsten as absorbers) up to $|\eta| < 4.9$.

Di-photon events are recorded using a three-level trigger system. The first level, implemented in hardware, is based on towers defined with a coarser granularity (0.1×0.1 in $\eta \times \phi$) than that of the ECAL. They are used to search for electromagnetic deposits in $\eta \times \phi$ regions of 2×1 and 1×2 towers, within a fixed window of size 2×2 and with a transverse energy above a programmable threshold. The second- and third-level triggers are implemented in software and exploit the full granularity and energy calibration of the calorimeter to refine the first-level trigger selection.

3 Data and Monte Carlo samples

The data set analysed consists of the 7 TeV proton-proton collisions recorded by the ATLAS detector in 2011. Only events where the beam conditions are stable and the trigger system, the tracking devices, and the calorimeters are operational, are considered.

Monte Carlo (MC) samples are produced using various generators as described below. Particle interactions with the detector material and the detector response are simulated with GEANT4 [18]. The events are reconstructed with the same algorithms used for collision data. More details of the event generation and simulation infrastructure are provided in ref. [19].

Simulated di-photon events are generated with both PYTHIA 6.4.21 and SHERPA 1.3.1. PYTHIA uses the modified leading-order MRST2007 [20] parton distribution functions (PDFs) while SHERPA uses the CTEQ6L1 [21] PDFs. The PYTHIA event-generator parameters are set according to the ATLAS AMBT2 [22] tune, while the SHERPA parameters are the default ones of the SHERPA 1.3.1 distribution. Photons originating from the hard scattering and quark bremsstrahlung are included in the analysis. The MC di-photon signal is generated with a photon E_T threshold of 20 GeV; one million events are produced both with PYTHIA and SHERPA. They are used to model the transverse isolation energy (see section 4) distribution of signal photons, to compute the reconstruction efficiency and to study the systematic uncertainties on the reconstructed quantities. Background γ -jet events are generated using ALPGEN [23] with the CTEQ6L1 PDF set.

4 Event selection

Events are collected using a di-photon trigger with a nominal transverse energy threshold of 20 GeV for both photon candidates. The photon trigger objects are required to pass a selection based on shower shape variables computed from the energy deposits in the second layer of the electromagnetic calorimeter and in the hadronic calorimeter. The requirements are looser than the photon identification criteria applied in the offline selection. In order to reduce non-collision backgrounds, events are required to have a reconstructed primary vertex with at least three associated tracks and consistent with the average beam spot position. The signal inefficiency of this requirement is negligible.

Photons are reconstructed from electromagnetic energy clusters in the calorimeter and tracking information provided by the ID as described in ref. [24]. Photons reconstructed near regions of the calorimeter affected by read-out or high-voltage failures are not considered.³ The cluster energies are corrected using an in-situ calibration based on the Z boson mass peak [25], and the determination of the pseudorapidities is optimized using the technique described in ref. [15]. In order to benefit from the fine segmentation of the first layer of the electromagnetic calorimeter to discriminate between genuine prompt photons and fake photons within jets, the photon candidate pseudorapidity must satisfy $|\eta| < 1.37$ or $1.52 < |\eta| < 2.37$. We retain photon candidates passing loose identification requirements, based on the same shower shape variables – computed with better granularity and resolution – and the same thresholds used at trigger level. The highest- E_T (“leading”) and second highest- E_T (“subleading”) photons within the acceptance and satisfying the loose identification criteria are required to have $E_{T,1} > 25$ GeV and $E_{T,2} > 22$ GeV, respectively. The fraction of events where the two selected photon candidates are not matched to the photon trigger objects is negligible. The angular separation between the two photons, $\Delta R = \sqrt{(\Delta\eta)^2 + (\Delta\phi)^2}$, is required to be larger than 0.4, in order to avoid one photon candidate depositing significant energy in the isolation cone of the other, as defined below.

Two further criteria are used to define the signal and background control regions. Firstly the tight photon selection [24] (abbreviated as **T** in the following) is designed to reject hadronic jet background, by imposing requirements on nine discriminating variables computed from the energy leaking into the HCAL and the lateral and longitudinal shower development in the ECAL. Secondly the transverse isolation energy E_T^{iso} is computed from the sum of the positive-energy topological clusters with reconstructed barycentres inside a cone of radius $\Delta R = 0.4$ around the photon candidate. The algorithm for constructing topological clusters suppresses noise by keeping only those cells with a significant energy deposit and their neighbouring cells. The cells within 0.125×0.175 in $\eta \times \phi$ around the photon are excluded from the calculation of E_T^{iso} . The mean value of the small leakage of the photon energy from this region into the isolation cone, evaluated as a function of the photon transverse energy, is subtracted from the measured value of E_T^{iso} (meaning that E_T^{iso} can be negative). The typical size of this correction is a few percent of the photon transverse energy. The measured value of E_T^{iso} is further corrected by subtracting the

³This requirement leads to a typical loss of 0.8% to 1.4% on the photon reconstruction efficiency, depending on the data-taking period.

estimated contributions from the underlying event and additional pp interactions. This correction is computed on an event-by-event basis, by calculating the transverse energy density from low-transverse-momentum jets, as suggested in refs. [26, 27]. The median transverse energy densities of the jets in two η regions, $|\eta| < 1.5$ and $1.5 < |\eta| < 3.0$, are computed separately, and the one for the region containing the photon candidate pseudorapidity is multiplied by the total area of all topological clusters used in the calculation of the isolation variable in order to estimate the correction. Signal photons are required to pass the tight selection (“tight photons”) and the isolation requirement **I**, $-4 < E_T^{\text{iso}} < 4$ GeV. A total of 165 767 pairs of tight, isolated photons are selected. The fraction of events in which an additional photon pair passes all the selection criteria, except for the requirement on the two photons being the leading and subleading E_T candidates, is less than 1 per 100 000. The non-tight ($\tilde{\mathbf{T}}$) photon candidates are defined as those failing the tight criteria for at least one of the shower-shape variables that are computed from the energy deposits in a few cells of the first layer of the electromagnetic calorimeter adjacent to the cluster barycentre. Photon candidates with $4 < E_T^{\text{iso}} < 8$ GeV are considered non-isolated ($\tilde{\mathbf{I}}$).

5 Signal yield extraction

After the selection, the main background is due primarily to γ -jet and secondarily to di-jet (jj) final states, collectively called “jet background” in the following. Two methods, the two-dimensional sidebands and the two-dimensional fit, already exploited in ref. [5], are used to perform an in-situ statistical subtraction of the jet background from the selected photon candidate pairs, as described in section 5.1.

After the jet background contribution is subtracted, a small residual background contamination arises from events where isolated electrons are misidentified as photons. This contribution is estimated as described in section 5.2.

5.1 Jet background subtraction

Both the two-dimensional sidebands and the two-dimensional fit methods use the photon transverse isolation energy and the tight identification criteria to discriminate prompt photons from jets. They rely on the fact that the correlations between the isolation and the tight criteria in background events are small, and that the signal contamination in the non-tight or non-isolated control regions is low.

The two-dimensional sidebands method counts the numbers of photon candidate pairs where each of the candidates passes or fails the tight and the isolation criteria. Four categories are defined for each photon, resulting in 16 categories of events. The inputs to the method are the numbers of events in the categories and the signal efficiencies of the tight and isolation requirements. The correlation between these two requirements is assumed to be negligible for background events. The method allows the simultaneous extraction of the numbers of true di-photon signal, γj , $j\gamma$ ⁴ and jj background events, and the tight and isolation efficiencies for fake photon candidates from jets (“fake rates”). The

⁴Here and in the following, γj ($j\gamma$) denotes the events where the leading (subleading) candidate is a true photon, and the other candidate a true jet.

expected number of events in each category is written as a function of the parameters (yields, efficiencies, fake rates and correlation factors) and the system of 16 equations is solved with a χ^2 minimization procedure. This method is an extension of the one used in our previous di-photon analysis [5]. It allows the extraction of different isolation fake rates for jets in $j\gamma$ or jj events as well as a correlation factor for the isolation of jet pairs.

The two-dimensional fit method consists of an extended maximum likelihood template fit to the two-dimensional distribution of the transverse isolation energies $E_{T,1}^{\text{iso}}$ and $E_{T,2}^{\text{iso}}$ of the two photon candidates in events belonging to the **T-T** sample, *i.e.* where both photons satisfy the tight identification criteria. The fit is performed in the isolation range $-4 < E_{T,i}^{\text{iso}} < 8$ GeV ($i = 1, 2$). The correlations between the transverse isolation energies of the two candidates in di-photon, γj , and $j\gamma$ events are found to be negligible in MC samples, and the products of two one-dimensional templates for $E_{T,1}^{\text{iso}}$ and $E_{T,2}^{\text{iso}}$ are used for each of the three event species. For the jj component, large correlations are observed in data, and a two-dimensional template is used. The two-dimensional fit is described in detail in our previous paper [5]. There are two differences between the present and previous analyses: the use now of binned distributions instead of smooth parametric functions for the photon and jet templates, and the correction for signal leakage in the background templates, as described below.

The transverse isolation energy distributions of the signal photons and the corresponding efficiencies of the signal requirement $-4 < E_T^{\text{iso}} < 4$ GeV are obtained from the SHERPA di-photon sample, separately for the leading and the subleading candidates. In the two-dimensional fit method, the templates are shifted by +160 and +120 MeV respectively in order to maximize the likelihood, as determined from a scan as a function of the shifts. These values are also used to compute the signal efficiencies of the isolation requirement needed in the two-dimensional sidebands method. Shifts of similar size between ATLAS data and MC simulation have been observed in the transverse isolation energy distribution, computed with the same technique (based on topological clusters inside a cone of radius 0.4), of electron control samples selected from $Z \rightarrow ee$ decays with a tag-and-probe method. The E_T^{iso} distributions of prompt photons in γj and $j\gamma$ events are assumed to be identical to that of prompt photons in di-photon events, as found in simulated samples. The tight identification efficiencies for prompt photons, needed in the two-dimensional sidebands method and in the final cross section measurement, are estimated using the same di-photon MC sample. The shower shape variables are corrected for the observed differences between data and simulation in photon-enriched control samples. Residual differences between the efficiencies in the simulation and in data are corrected using scale factors determined from control samples of photons from radiative Z boson decays, electrons selected with a tag-and-probe technique from $Z \rightarrow ee$ decays, and photon-enriched control samples of known photon purity [28]. After applying these corrections, the photon identification efficiency in the simulation is estimated to reproduce the efficiency in data to within 2%. For the two-dimensional fit, the transverse isolation energy template of the leading (subleading) jet in $j\gamma$ (γj) events is extracted directly from data where one candidate passes the non-tight and the other passes both the tight identification and isolation (**TI**) requirements. For jj events, the two-dimensional template is obtained from data in which the two candidates are required

to be non-tight. The correlation is found to be about 8%. The jet background templates are corrected for signal leakage in the control samples, estimated from the SHERPA sample.

Figure 1 shows the projections of the two-dimensional fit to the transverse isolation energies of the leading and subleading photon candidates. The yields for each of the four components extracted with the two-dimensional sidebands method and the two-dimensional fit are given in table 1. The di-photon purity is around 68% and the di-photon yields agree within 1.5% between the two methods.

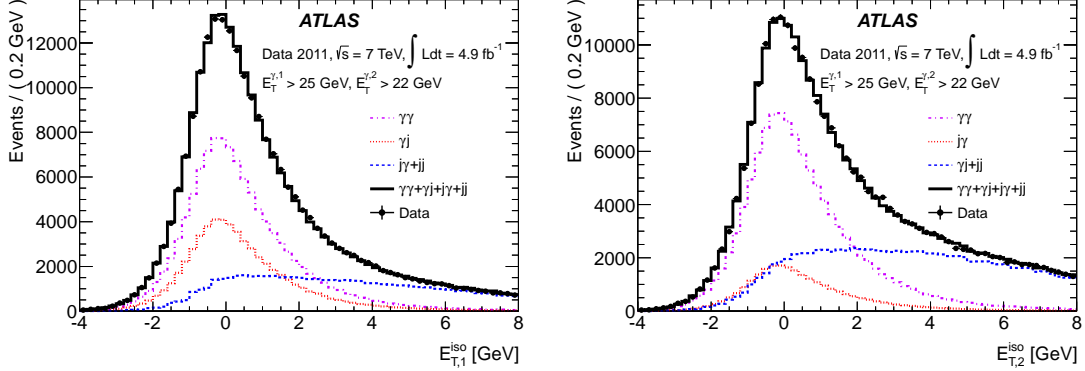


Figure 1. Projections of the two-dimensional fit to the transverse isolation energies of the two photon candidates: leading photon (left) and sub-leading photon (right). The photon templates from SHERPA are shifted by +160 MeV (+120 MeV) for the leading (subleading) photon. Solid circles represent the observed data. The (black) solid line is the fit result, the (violet) dash-dotted curve shows the $\gamma\gamma$ component. The (red) dotted line shows in the left (right) figure the contribution from γj ($j\gamma$) events. In both figures, the (blue) dashed line represents a broad background component in the photon candidates' sample: for the leading candidate this is due to $j\gamma$ and jj final states, whereas for the sub-leading candidate it comes from γj and jj final states.

Yield	two-dimensional sidebands results			two-dimensional fit results		
$N_{\gamma\gamma}$	113 200	± 600 (stat.)	$+5000$ (syst.) -8000 (syst.)	111 700	± 500 (stat.)	$+4500$ (syst.) -7600 (syst.)
$N_{\gamma j}$	31 500	± 400 (stat.)	$+3900$ (syst.) -3100 (syst.)	31 500	± 300 (stat.)	$+4800$ (syst.) -3600 (syst.)
$N_{j\gamma}$	13 000	± 300 (stat.)	$+2500$ (syst.) -800 (syst.)	13 900	$+300$ (stat.) -200 (stat.)	$+3400$ (syst.) -2100 (syst.)
N_{jj}	8 100	± 100 (stat.)	$+1900$ (syst.) -1400 (syst.)	8 300	± 100 (stat.)	$+300$ (syst.) -2100 (syst.)

Table 1. Total yields for two candidates satisfying the tight identification and the isolation requirement $-4 < E_T^{\text{iso}} < 4$ GeV. Both statistical and total systematic uncertainties are listed.

To obtain the differential signal yields as a function of the di-photon kinematic variables, such as $m_{\gamma\gamma}$, $p_{T,\gamma\gamma}$, $\Delta\phi_{\gamma\gamma}$ and $\cos\theta_{\gamma\gamma}^*$, the above methods are applied in each bin of the variables. Figure 2 shows the differential spectra of the signal and background components obtained with the two-dimensional fit. In some regions of the di-photon spectra, discrepancies with the two-dimensional sidebands results are larger than those observed for the integrated yield. The results from the two-dimensional fit are used to extract the

nominal cross sections, while differences between the results obtained with the two methods are included in the final systematic uncertainty.

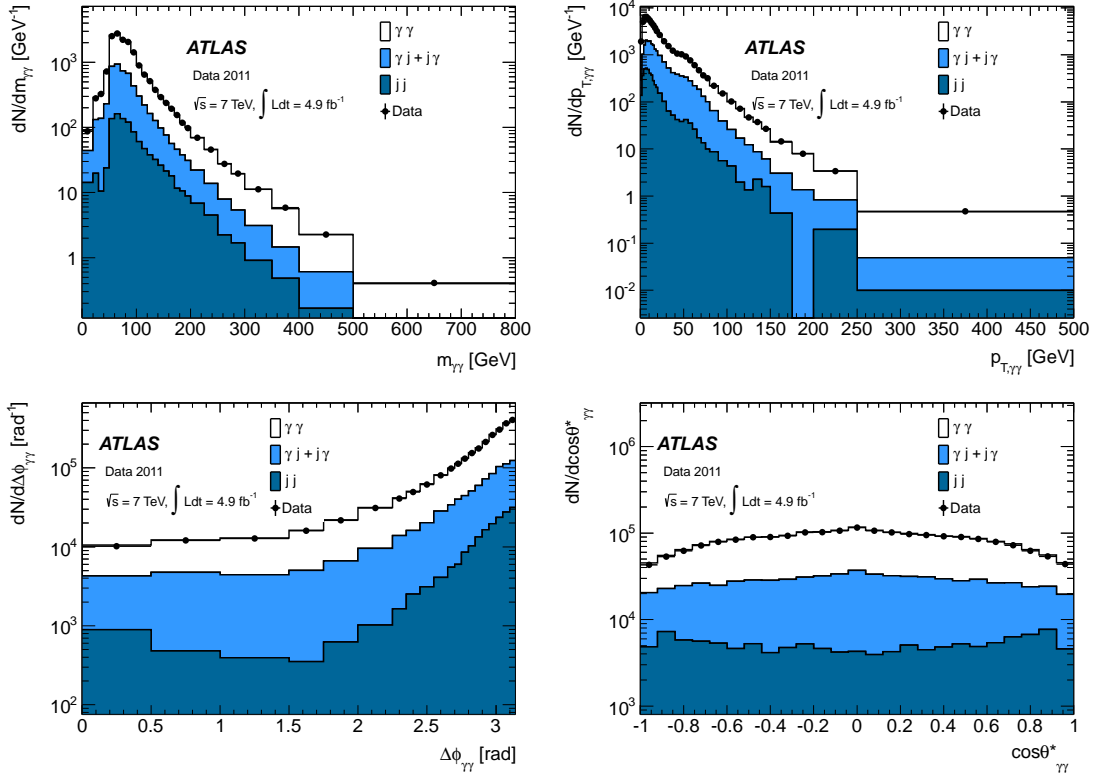


Figure 2. Differential spectra in data (solid circles) and from the two-dimensional fit, for the $\gamma\gamma$ (hollow histogram), $\gamma j+j\gamma$ (light solid histogram), and jj (dark solid histogram) contributions. The spectra are shown for the following di-photon variables: $m_{\gamma\gamma}$ (top left), $p_{T,\gamma\gamma}$ (top right), $\Delta\phi_{\gamma\gamma}$ (bottom left), $\cos\theta_{\gamma\gamma}^*$ (bottom right).

Several sources of systematic uncertainty on the signal yield, estimated after the jet background subtraction, are considered. The dominant uncertainty originates from the choice of the background control regions and accounts for both the uncertainty on the background transverse isolation energy distribution and its correlation with the identification criteria. It is first estimated by varying the number of relaxed criteria in the non-tight definition. For the integrated di-photon yield, the effect is found to be $^{+3}_{-6}\%$. In some bins of the $m_{\gamma\gamma}$ and $p_{T,\gamma\gamma}$ spectra where the size of the control samples is small, neighbouring bins are grouped together to extract the jet background templates. Since the background transverse isolation energies depend mildly on these kinematic variables, a systematic uncertainty is evaluated by repeating the yield extraction with jet templates from the adjacent groups of neighbouring bins. The uncertainty on the estimated signal yield is at most $\pm 9\%$.

In the nominal result, the photon isolation templates are taken from the SHERPA di-photon sample. A systematic uncertainty is evaluated by using alternative templates from the PYTHIA di-photon sample, and from data. The data-driven template for the leading (subleading) photon is obtained by selecting events where the requirement $E_T^{\text{iso}} < 8$ GeV is

removed for the leading (subleading) photon candidate, and normalizing the leading (subleading) photon isolation distribution in $\tilde{\mathbf{T}}\text{-}\mathbf{TI}$ ($\mathbf{TI}\text{-}\tilde{\mathbf{T}}$) events, where the leading (subleading) candidate fails the tight identification while the other candidate passes tight identification and isolation criteria, to the isolation distribution of leading (subleading) candidates in $\mathbf{T}\text{-}\mathbf{T}$ events in the $7 < E_{\mathbf{T}}^{\text{iso}} < 17$ GeV region. The difference between the two distributions is used as an estimate of the photon distribution. The PYTHIA di-photon sample exhibits higher tails than SHERPA at large values of $E_{\mathbf{T}}^{\text{iso}}$. The data-driven template, on the other hand, is characterized by smaller tails than the SHERPA template, since it is obtained by assuming that the isolation region above 7 GeV is fully populated by background. The corresponding uncertainty on the signal yield is estimated to be ${}_{-3}^{+2}\%$ of the integrated di-photon yield. It is rather uniform as a function of $m_{\gamma\gamma}$, $p_{\mathbf{T},\gamma\gamma}$, $\Delta\phi_{\gamma\gamma}$ and $\cos\theta_{\gamma\gamma}^*$ and always below 4%, except at very low $m_{\gamma\gamma}$ where it reaches $\pm 5\%$. The photon isolation template is, to a large extent, independent of the variables under study. Repeating the background subtraction procedure using photon isolation templates extracted in bins of the di-photon variable under study leads to variations of the estimated signal yield within ${}_{-4}^{+2}\%$.

Other systematic effects have been considered, and found to be smaller than those previously discussed. The bias created by neglecting the dependence of the identification and isolation efficiencies on η and $E_{\mathbf{T}}$ is estimated to be of $+0.02\%$ and -0.3% respectively. The effect of assuming identical templates for photons in di-photon and in γ -jet events is evaluated by using instead templates from ALPGEN γ -jet samples for photons in the γj and $j\gamma$ components. The uncertainty on the shifts applied to the MC photon templates (± 10 MeV for the leading photons and ± 5 MeV for the subleading ones, as determined from the scan) is propagated to the di-photon yields. The impact of the identification efficiencies on the signal leakage correction is estimated by neglecting in the simulation the correction factors nominally applied to the shower shape variables to account for the observed differences between data and MC simulation. These effects produce systematic uncertainties of at most 0.5% on the differential spectra. Finally, no significant effect is observed due to the imperfect modelling of the material in front of the calorimeters.

5.2 Electron background subtraction

Isolated electrons from W or Z boson decays can be misidentified as photons, since the two particles (e and γ) generate similar electromagnetic showers in the ECAL. Usually a track is reconstructed in the inner detector pointing to the electron ECAL cluster, thus isolated electrons misidentified as photons are mostly classified as converted candidates. Pairs of misidentified, isolated electrons and positrons (ee) from processes such as Drell-Yan, $Z \rightarrow ee$, $WW \rightarrow e\nu e\nu$, or of photons and e^\pm from diboson production ($\gamma W \rightarrow \gamma e\nu$, $\gamma Z \rightarrow \gamma ee$), provide a background that cannot be distinguished from the di-photon signal based on the photon identification and isolation variables and must therefore be estimated in a separate way. The same procedure exploited in ref. [5], based on the number of γe ($N_{\gamma e}$) and ee (N_{ee}) events observed in data, is used to estimate their contributions to the di-photon yield $N_{\gamma\gamma}$ after jet background subtraction.

For a given bin i of the variable X ($X = m_{\gamma\gamma}$, $p_{\mathbf{T},\gamma\gamma}$, $\Delta\phi_{\gamma\gamma}$, or $\cos\theta_{\gamma\gamma}^*$), the signal

component $N_{\gamma\gamma}^{\text{sig}}$ in the $N_{\gamma\gamma}$ sample can be evaluated:

$$N_{\gamma\gamma}^{\text{sig}} = \frac{N_{\gamma\gamma} - [f_{e\rightarrow\gamma}N_{\gamma e} - (f_{e\rightarrow\gamma})^2N_{ee}]}{(1 - f_{e\rightarrow\gamma}f_{\gamma\rightarrow e})^2} \quad (5.1)$$

The fake rates $f_{e\rightarrow\gamma}$ and $f_{\gamma\rightarrow e}$ are measured using Z boson decays in data. $Z \rightarrow ee$ decays are used to estimate $f_{e\rightarrow\gamma}$ as $N_{\gamma e}^Z/(2N_{ee}^Z)$, where $N_{\gamma e}^Z$ and N_{ee}^Z are the numbers of γe and ee pairs with invariant mass within 1.5σ of the Z boson mass. $Z \rightarrow \gamma ee$ decays are similarly used to estimate $f_{\gamma\rightarrow e}$ as $N_{ee\gamma}^Z/N_{\gamma ee}^Z$. The numbers of continuum background events are estimated from the sidebands of the ee , γe , eee or γee invariant mass distributions (51 – 61 GeV and 121 – 131 GeV), and subtracted from N_{ee}^Z , $N_{\gamma e}^Z$, N_{eee}^Z and $N_{\gamma ee}^Z$, respectively. Electrons must satisfy identification criteria based on their shower shape in the electromagnetic calorimeter, quality criteria for the associated track in the ID, and an isolation requirement $E_{\text{T}}^{\text{iso}} < 4$ GeV. The measured fake rates, including statistical and systematic uncertainties, are $f_{e\rightarrow\gamma} = 0.062_{-0.010}^{+0.040}$ and $f_{\gamma\rightarrow e} = 0.038_{-0.007}^{+0.024}$, where the systematic uncertainty is dominated by the dependence on the transverse energy of the candidate photon. Other sources include the uncertainties on N_{ee}^Z , $N_{\gamma e}^Z$, N_{eee}^Z and $N_{\gamma ee}^Z$ which are evaluated by changing the definition of the Z boson mass window to $\pm 2\sigma$ and $\pm 1\sigma$, and shifting the sidebands by ± 5 GeV. The fraction of electron background as a function of $m_{\gamma\gamma}$, $p_{\text{T},\gamma\gamma}$, $\Delta\phi_{\gamma\gamma}$, and $\cos\theta_{\gamma\gamma}^*$ is shown in figure 3. The enhancements at $m_{\gamma\gamma} \approx m_Z$, low $p_{\text{T},\gamma\gamma}$ and $\Delta\phi_{\gamma\gamma} \approx \pi$ are due to the large Z boson production cross section.

6 Cross section measurement

This section describes the extraction of the final cross sections. The background-subtracted differential spectra are first unfolded to the generated-particle level, to take into account reconstruction and selection efficiencies estimated from the simulation, and then divided by the integrated luminosity of the data sample and the trigger efficiency relative to the offline selection.

6.1 Efficiency and unfolding

The background-subtracted differential distributions obtained from the data are unfolded to obtain the particle-level spectra by dividing the signal yield in each bin of the di-photon observable under study by a “bin-by-bin” correction, which accounts for signal reconstruction and selection efficiencies and for finite resolution effects. The bin-by-bin nominal corrections are evaluated from the SHERPA di-photon simulated sample as the number of simulated di-photon events satisfying the selection criteria (excluding the trigger requirement) and for which the reconstructed value of the variable X under consideration is in bin i , divided by the number of simulated di-photon events satisfying the nominal acceptance criteria at generator-level and for which the generated value of X is in the same bin i . The generator-level photon transverse isolation energy is computed from the true four-momenta of the generated particles (excluding muons and neutrinos) inside a cone of radius 0.4 around the photon direction. The pileup contribution is removed using an analogous method to the one for the experimental isolation variable, by subtracting the product of the area of the

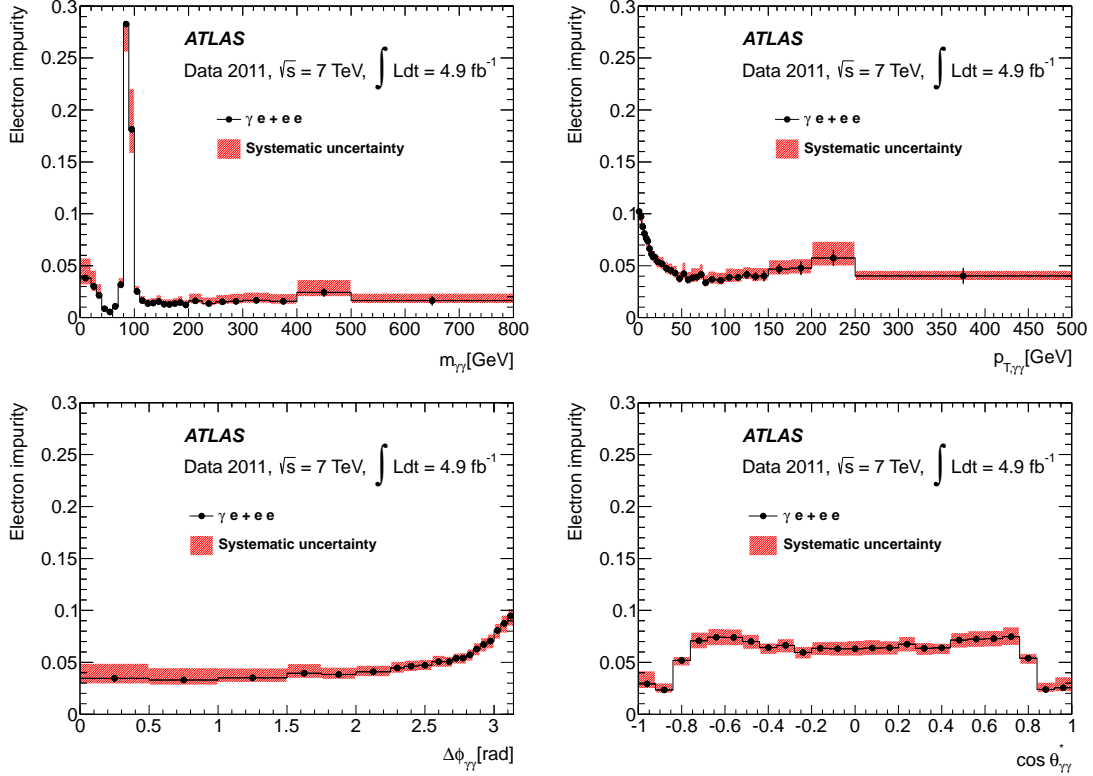


Figure 3. Fraction of electron background (impurity) as a function of $m_{\gamma\gamma}$, $p_{T,\gamma\gamma}$, $\Delta\phi_{\gamma\gamma}$, and $\cos\theta_{\gamma\gamma}^*$.

isolation cone and the median transverse energy density of the low-transverse-momentum truth-particle jets.

Alternative corrections are calculated with the PYTHIA di-photon sample or using a simulated di-photon sample which contains additional material upstream of the calorimeter. The variations induced on the measured cross sections by the alternative corrections are taken as systematic uncertainties, due to the uncertainty on the generated kinematic distributions, on the relative fraction of direct and fragmentation di-photon production, and on the amount of material in the ATLAS detector. The effect on the total cross section is within $^{+2}_{-5}\%$ for $m_{\gamma\gamma}$, $\pm 3\%$ for $p_{T,\gamma\gamma}$, $^{+3}_{-4}\%$ for $\Delta\phi_{\gamma\gamma}$ and $^{+2}_{-3}\%$ for $\cos\theta_{\gamma\gamma}^*$.

The effect of the uncertainty on the efficiency of the photon identification criteria is estimated by varying the identification efficiency in the simulation by its uncertainty [28]. The uncertainties on the electromagnetic (photon) energy scale and resolution are also propagated to the final measurement by varying them within their uncertainties [25]. The effect on the differential cross section is typically $^{+1}_{-2}\%$. Other uncertainties, related to the dependence on the average number of pile-up interactions of the efficiencies of the photon identification and transverse isolation energy requirements and to the observed data–MC shift in the photon transverse isolation energy distributions, are found to be negligible.

A closure test has been performed by unfolding the differential spectra of di-photon

events selected in the PYTHIA signal sample with the bin-by-bin coefficients determined using the SHERPA sample, and comparing the unfolded spectra to the truth-level spectra in the same PYTHIA sample. Non-closure effects of at most 2% have been found and included in the final systematic uncertainty.

More sophisticated unfolding methods which account for migrations between bins, either based on the repeated (iterative) application of Bayes' theorem [29] or on a least-square minimization followed by a regularization of the resulting spectra [30] have also been investigated. The differences between the unfolded spectra obtained with these methods and the spectra extracted with the bin-by-bin corrections are negligible compared to the other uncertainties and therefore the bin-by-bin method was chosen for the final results.

6.2 Trigger efficiency correction

The unfolded spectra are then corrected for the event-level trigger efficiency, defined as the fraction of di-photon events – satisfying all the selection criteria – that pass the di-photon trigger used to collect the data. The trigger efficiency is measured in data using a bootstrap technique [31] from samples selected with fully efficient unbiased triggers with a lower threshold, and taking into account kinematic correlations between the photon candidates. The differences between the measured di-photon trigger efficiency and the efficiency estimated with simulated di-photon samples, or by applying the bootstrap technique to single-photon triggers and neglecting correlations between the two photon candidates, have been assigned as systematic uncertainties. The total trigger efficiency is then:

$$\varepsilon_{\text{trig}} = (97.8^{+0.8}_{-1.5}(\text{stat.}) \pm 0.8(\text{syst.})) \% \quad (6.1)$$

Using di-photon simulated samples, the trigger efficiency has been estimated to be constant, within the total uncertainties, as a function of the four di-photon observables under investigation.

6.3 Results

The differential cross sections as a function of $m_{\gamma\gamma}$, $p_{T,\gamma\gamma}$, $\Delta\phi_{\gamma\gamma}$, and $\cos\theta_{\gamma\gamma}^*$ are extracted following the unfolding procedure described in section 6.1 and using the trigger efficiency quoted in eq. (6.1). The numerical results are listed in Appendix A.

The integrated cross section is measured by dividing the global $\gamma\gamma$ yield (obtained after subtracting the electron contribution from the two-dimensional fit result in table 1) by the product of the average event selection efficiency (from the simulation), trigger efficiency and integrated luminosity. The selection efficiency is defined as the number of reconstructed simulated di-photon events satisfying the detector-level selection criteria divided by the number of generated events satisfying the equivalent truth-level criteria, thus correcting for reconstructed events with true photons failing the acceptance cuts. It is computed from simulated di-photon events, reweighting the spectrum of one of the four di-photon variables under study in order to match the differential background-subtracted di-photon spectrum observed in data. Choosing different variables for the reweighting of the simulated events leads to slightly different but consistent efficiencies, with an average value of 49.6% and

an RMS of 0.2%. Including systematic uncertainties on the photon reconstruction and identification efficiencies, from the same sources described in section 6.1, the event selection efficiency is estimated to be $49.6_{-1.7}^{+1.9}\%$. The dominant contributions to the efficiency uncertainty are from the photon identification efficiency uncertainty ($\pm 1.2\%$), the energy scale uncertainty ($_{-0.5}^{+1.2}\%$), and the choice of the MC generator and the detector simulation ($\pm 0.9\%$). Negligible uncertainties are found to arise from the energy resolution, the isolation requirement (evaluated by shifting the isolation variable by the observed data–MC difference) and from the different pile-up dependence of the efficiency in data and MC simulation. With an integrated luminosity of $(4.9 \pm 0.2) \text{ fb}^{-1}$ at $\sqrt{s} = 7 \text{ TeV}$, we obtain an integrated cross section of $44.0_{-4.2}^{+3.2} \text{ pb}$, where the dominant uncertainties are the event selection efficiency and the jet subtraction systematic uncertainties. As a cross-check, the integrals of the one-dimensional differential cross sections are also computed. They are consistent with the measured integrated cross section quoted above.

7 Comparison with theoretical predictions

The results are compared both to fixed-order NLO and NNLO calculations, obtained with parton-level MC generators (DIPHOX+GAMMA2MC and 2γ NNLO), and to the generated-particle-level di-photon spectra predicted by leading-order (LO) parton-shower MC generators used in the ATLAS full simulation (PYTHIA and SHERPA). The contribution from the particle recently discovered by ATLAS and CMS in the search for the Standard Model Higgs boson is not included in the predictions: it is expected to be around 1% of the signal in the $120 < m_{\gamma\gamma} < 130 \text{ GeV}$ interval, and negligible elsewhere. The contribution from multiple parton interactions is also neglected: measurements by D0 [32] and ATLAS⁵ show that events with two jets (in γ +jets or W+jets) have a contamination between 5% and 10% from double parton interactions. In our data sample, the fraction of selected di-photon candidates with at least two additional jets not overlapping with the photons and not from pile-up is around 8%, thus the overall contribution to the signal from multiple parton interactions is estimated to be lower than 1%.

The main differences between the four predictions are the following:

- 2γ NNLO provides a NNLO calculation of the direct part of the di-photon production cross section, but neglects completely the contribution from the fragmentation component, where one or both photons are produced in the soft collinear fragmentation of coloured partons.
- DIPHOX provides a NLO calculation of both the direct and the fragmentation parts of the di-photon production cross section. It also includes the contribution from the box diagram ($gg \rightarrow \gamma\gamma$), which is in principle a term of the NNLO expansion in the strong coupling constant α_s , but – due to the large gluon luminosity at the LHC [33] – gives a contribution comparable to that of the LO terms. For these reasons, higher-order contributions to the box diagrams, technically at NNNLO but of size similar to that of NLO terms, are also included in our calculation by using GAMMA2MC.

⁵article in preparation

- PYTHIA provides LO matrix elements for di-photon production and models the higher-order terms through γ -jet and di-jet production in combination with initial-state and/or final-state radiation. It also features parton showering and an underlying event model;
- SHERPA has features similar to those of PYTHIA, and in addition includes the di-photon higher-order real-emission matrix elements. For this study, up to two additional QCD partons are generated.

The nominal factorization (μ_F), renormalization (μ_R), and – in the case of DIPHOX and GAMMA2MC – fragmentation (μ_f) scales are set in all cases to the di-photon invariant mass, $m_{\gamma\gamma}$. Different PDF sets are used by each program: CT10 NLO [34] for DIPHOX and GAMMA2MC, MSTW2008 NNLO [35] for 2γ NNLO, CTEQ6L1 for SHERPA and MRST2007 LO* for PYTHIA. The theoretical uncertainty error bands for PYTHIA and SHERPA include only statistical uncertainties. The theory uncertainty error bands for the NLO and NNLO predictions include in addition PDF and scale uncertainties. PDF uncertainties are estimated by varying each of the eigenvalues of the PDFs by $\pm 1\sigma$ and summing in quadrature separately positive and negative variations of the cross section. For DIPHOX and GAMMA2MC, scale uncertainties are evaluated by varying each scale to $m_{\gamma\gamma}/2$ and $2m_{\gamma\gamma}$, and the envelope of all variations is taken as a systematic error; the final uncertainty is dominated by the configurations in which the scales are varied incoherently. For 2γ NNLO, the scale uncertainty is evaluated by considering the variation of the predicted cross sections in the two cases $\mu_R = m_{\gamma\gamma}/2$, $\mu_F = 2m_{\gamma\gamma}$ and $\mu_R = 2m_{\gamma\gamma}$, $\mu_F = m_{\gamma\gamma}/2$.

Fixed-order predictions calculated at parton level do not include underlying event, pile-up or hadronization effects. While the ambient-energy density corrections to the photon isolation are expected to remove most of these effects from the photon isolation energy, it is not guaranteed that they correct the experimental isolation back to exactly the parton-level isolation computed from the elementary-process partons. To estimate these residual effects, PYTHIA and SHERPA di-photon samples are used to evaluate the ratio of generator-level cross sections with and without hadronization and the underlying event, and subsequently, the parton-level cross sections are multiplied bin-by-bin by this ratio. The central value of the envelope of the PYTHIA and SHERPA distributions is taken as the nominal correction and half of the difference between PYTHIA and SHERPA as the systematic uncertainty. The typical correction factor is around 0.95.

Both PYTHIA and SHERPA are expected to underestimate the total cross section, because of the missing NLO (and higher-order) contributions. At low $p_{T,\gamma\gamma}$ and for $\Delta\phi_{\gamma\gamma}$ near π where multiple soft gluon emission is important, PYTHIA and SHERPA are expected to better describe the shape of the differential distributions, thanks to the effective all-order resummation of the leading logs performed by the parton shower. On the other hand, in the same regions fixed-order calculations are expected to exhibit infrared divergences. Finally, 2γ NNLO is expected to underestimate the data in regions populated by the contribution from fragmentation (low $\Delta\phi_{\gamma\gamma}$ and $m_{\gamma\gamma}$, and $\cos\theta_{\gamma\gamma}^* \approx 1$).

The total cross section estimated by PYTHIA and SHERPA with the ATLAS simulation settings is 36 pb, and underestimates the measured cross section by 20%. The

DIPHOX+GAMMA2MC total cross section is 39_{-6}^{+7} pb and the 2γ NNLO total cross section is 44_{-5}^{+6} pb, where the uncertainty is dominated by the choice of the nominal scales.

The comparisons between the experimental cross sections and the predictions by PYTHIA and SHERPA are shown in figure 4. In order to compare the shapes of the MC differential distributions to the data, their cross sections are rescaled by a factor 1.2 to match the total cross section measured in data. PYTHIA misses higher order contributions, as clearly seen for low values of $\Delta\phi_{\gamma\gamma}$, but this is compensated by the parton shower for $\Delta\phi_{\gamma\gamma}$ near π and at low $p_{T,\gamma\gamma}$. It is worth noting that the shoulder expected (and observed) in the $p_{T,\gamma\gamma}$ cross section around the sum of the E_T thresholds of the two photons [36] is almost absent in PYTHIA, while SHERPA correctly reproduces the data in this region. This is interpreted as being due to the additional NLO contributions in SHERPA combined with differences in the parton showers. Overall, SHERPA reproduces the data rather well, except at large $m_{\gamma\gamma}$ and large $|\cos\theta_{\gamma\gamma}^*|$.

The comparisons between the data cross sections and the predictions by 2γ NNLO and DIPHOX+GAMMA2MC are shown in figure 5. In the $\Delta\phi_{\gamma\gamma} \simeq \pi$, low $p_{T,\gamma\gamma}$ region, DIPHOX+GAMMA2MC fails to match the data. This is expected because initial-state soft gluon radiation is divergent at NLO, without soft gluon resummation. Everywhere else DIPHOX+GAMMA2MC is missing NNLO contributions and clearly underestimates the data.

With higher order calculations included, 2γ NNLO is very close to the data within the uncertainties. However, the excess at $\Delta\phi_{\gamma\gamma} \simeq \pi$ and low $p_{T,\gamma\gamma}$ is still present, as expected for a fixed-order calculation. Since the fragmentation component is not calculated in 2γ NNLO, the data is slightly underestimated by 2γ NNLO in the regions where this component is larger: at low $\Delta\phi_{\gamma\gamma}$, low mass, intermediate $p_{T,\gamma\gamma}$ (between 20 GeV and 150 GeV) and large $|\cos\theta_{\gamma\gamma}^*|$.

8 Conclusion

A measurement of the production cross section of isolated-photon pairs in pp collisions at a centre-of-mass energy $\sqrt{s} = 7$ TeV is presented. The measurement uses an integrated luminosity of 4.9 fb^{-1} collected by the ATLAS detector at the LHC in 2011. The two photons are required to be isolated in the calorimeters, to be in the acceptance of the electromagnetic calorimeter ($|\eta| < 2.37$ with the exclusion of the barrel-endcap transition region $1.37 < |\eta| < 1.52$) and to have an angular separation $\Delta R > 0.4$ in the η, ϕ plane. Both photons have transverse energies $E_T > 22$ GeV, and at least one of them has $E_T > 25$ GeV.

The total cross section within the acceptance is $44.0_{-4.2}^{+3.2}$ pb. It is underestimated by SHERPA and PYTHIA, which both predict a value of 36 pb with the current ATLAS simulation tune. The central value of the cross section predicted by DIPHOX+GAMMA2MC, 39 pb, is lower than the data but it is consistent with data within the theoretical ($_{-6}^{+7}$ pb) and experimental errors. The NNLO calculation of 2γ NNLO ($\sigma_{\text{NNLO}} = 44_{-5}^{+6}$ pb) is in excellent agreement with the data.

The differential cross sections, as a function of the di-photon invariant mass, transverse momentum, azimuthal separation and of the cosine of the polar angle of the photon with largest transverse energy in the Collins–Soper di-photon rest frame, are also measured.

Rather good agreement is found with Monte Carlo generators, after rescaling the PYTHIA and SHERPA distributions by a factor 1.2 in order to match the integrated cross section measured in data and fixed-order calculations, in the regions of phase space studied. All generators tend to underestimate the data at large $|\cos\theta_{\gamma\gamma}^*|$. SHERPA performs rather well for most differential spectra, except for high $m_{\gamma\gamma}$. PYTHIA is missing higher order contributions, but this is compensated by the parton shower for $\Delta\phi_{\gamma\gamma}$ near π and at low $p_{T,\gamma\gamma}$. In these same regions the fixed-order calculations do not reproduce the data, due to the known infrared divergences from initial-state soft gluon radiation. Everywhere else DIPHOX+GAMMA2MC is missing NNLO contributions and clearly underestimates the data. On the other hand, with inclusion of NNLO terms, 2γ NNLO is able to match the data very closely within the uncertainties, except in limited regions where the fragmentation component – neglected in the 2γ NNLO calculation – is still significant after the photon isolation requirement.

Acknowledgments

We thank the 2γ NNLO authors for providing theoretical predictions of the NNLO di-photon cross section based on their code. We thank Leandro Cieri, Stefano Catani, Daniel De Florian, Michel Fontannaz, Jean-Philippe Guillet, Eric Pilon and Carl Schmidt, for fruitful discussions on the theoretical calculations and their uncertainties.

We thank CERN for the very successful operation of the LHC, as well as the support staff from our institutions without whom ATLAS could not be operated efficiently.

We acknowledge the support of ANPCyT, Argentina; YerPhI, Armenia; ARC, Australia; BMWF and FWF, Austria; ANAS, Azerbaijan; SSTC, Belarus; CNPq and FAPESP, Brazil; NSERC, NRC and CFI, Canada; CERN; CONICYT, Chile; CAS, MOST and NSFC, China; COLCIENCIAS, Colombia; MSMT CR, MPO CR and VSC CR, Czech Republic; DNRF, DNSRC and Lundbeck Foundation, Denmark; EPLANET, ERC and NSRF, European Union; IN2P3-CNRS, CEA-DSM/IRFU, France; GNSF, Georgia; BMBF, DFG, HGF, MPG and AvH Foundation, Germany; GSRT and NSRF, Greece; ISF, MINERVA, GIF, DIP and Benoziyo Center, Israel; INFN, Italy; MEXT and JSPS, Japan; CNRST, Morocco; FOM and NWO, Netherlands; BRF and RCN, Norway; MNiSW, Poland; GRICES and FCT, Portugal; MERYS (MECTS), Romania; MES of Russia and ROSATOM, Russian Federation; JINR; MSTD, Serbia; MSSR, Slovakia; ARRS and MVZT, Slovenia; DST/NRF, South Africa; MICINN, Spain; SRC and Wallenberg Foundation, Sweden; SER, SNSF and Cantons of Bern and Geneva, Switzerland; NSC, Taiwan; TAEK, Turkey; STFC, the Royal Society and Leverhulme Trust, United Kingdom; DOE and NSF, United States of America.

The crucial computing support from all WLCG partners is acknowledged gratefully, in particular from CERN and the ATLAS Tier-1 facilities at TRIUMF (Canada), NDGF (Denmark, Norway, Sweden), CC-IN2P3 (France), KIT/GridKA (Germany), INFN-CNAF (Italy), NL-T1 (Netherlands), PIC (Spain), ASGC (Taiwan), RAL (UK) and BNL (USA) and in the Tier-2 facilities worldwide.

References

- [1] L. Randall and R. Sundrum, *A Large Mass Hierarchy from a Small Extra Dimension*, *Phys. Rev. Lett.* **83** (1999) 3370, [[hep-ph/9905221](#)].
- [2] S. D. N. Arkani-Hamed and G. R. Dvali, *The Hierarchy Problem and New Dimensions at a Millimeter*, *Phys. Lett. B* **429** (1998) 263, [[hep-ph/9803315](#)].
- [3] DØ Collaboration, V. M. Abazov et al., *Measurement of direct photon pair production cross sections in $p\bar{p}$ collisions at $\sqrt{s} = 1.96$ TeV*, *Phys. Lett. B* **690** (2010) 108, [[arXiv:1002.4917](#)].
- [4] CDF Collaboration, T. Aaltonen et al., *Measurement of the Cross Section for Prompt Isolated Diphoton Production in $p\bar{p}$ Collisions at $\sqrt{s} = 1.96$ TeV*, *Phys. Rev. D* **84** (2011) 052006, [[arXiv:1106.5131](#)].
- [5] ATLAS Collaboration, *Measurement of the isolated di-photon cross-section in pp collisions at $\sqrt{s} = 7$ TeV with the ATLAS detector*, *Phys. Rev. D* **85** (2012) 012003, [[arXiv:1107.0581](#)].
- [6] CMS Collaboration, *Measurement of the Production Cross Section for Pairs of Isolated Photons in pp collisions at $\sqrt{s} = 7$ TeV*, *JHEP* **1201** (2012) 133, [[arXiv:1110.6461](#)].
- [7] ATLAS Collaboration, *Luminosity Determination in pp Collisions at $\sqrt{s} = 7$ TeV Using the ATLAS Detector at the LHC*, *Eur. Phys. J. C* **71** (2011) 1630, [[arXiv:1101.2185](#)].
- [8] ATLAS Collaboration, *Luminosity Determination in pp Collisions at $\sqrt{s} = 7$ TeV using the ATLAS Detector in 2011*, *ATLAS-CONF-2011-116* (2011).
- [9] J. C. Collins and D. E. Soper, *Angular distribution of dileptons in high-energy hadron collisions*, *Phys. Rev. D* **16** (1977) 2219.
- [10] T. Sjöstrand et al., *High-Energy-Physics Event Generation with PYTHIA 6.1*, *Comput. Phys. Commun.* **135** (2001) 238, [[hep-ph/0010017](#)].
- [11] T. Gleisberg et al., *Event generation with SHERPA 1.1*, *JHEP* (2009) [[arXiv:0811.4622](#)].
- [12] T. Binoth, J. P. Guillet, E. Pilon, and M. Werlen, *A full next-to-leading order study of direct photon pair production in hadronic collisions*, *Eur. Phys. J. C* **16** (2000) 311–330, [[hep-ph/9911340](#)].
- [13] Z. Bern, L. Dixon, and C. Schmidt, *Isolating a light Higgs boson from the diphoton background at the LHC*, *Phys. Rev. D* **66** (2002) 074018, [[hep-ph/0206194](#)].
- [14] S. Catani, L. Cieri, D. de Florian, G. Ferrera, and M. Grazzini, *Diphoton production at hadron colliders: a fully-differential QCD calculation at NNLO*, *Phys. Rev. Lett.* **108** (2012) 072001, [[arXiv:1110.2375](#)].
- [15] ATLAS Collaboration, *Observation of a new particle in the search for the Standard Model Higgs boson with the ATLAS detector at the LHC*, *Phys. Lett. B* **716** (2012) 1, [[arXiv:1207.7214](#)].
- [16] CMS Collaboration, *Observation of a new boson at a mass of 125 GeV with the CMS experiment at the LHC*, *Phys. Lett. B* **716** (2012) 30, [[arXiv:1207.7235](#)].
- [17] ATLAS Collaboration, *The ATLAS experiment at the CERN Large Hadron Collider*, *JINST* **3** (2008) S08003.
- [18] GEANT4 Collaboration, S. Agostinelli et al., *Geant4 - a simulation toolkit*, *Nucl. Instrum. Methods A* **506** (2003) 250.

- [19] ATLAS Collaboration, *The ATLAS Simulation Infrastructure*, *Eur. Phys. J. C* **70** (2010) 823–874, [[arXiv:1005.4568](#)].
- [20] A. Sherstnev and R. S. Thorne, *Parton distributions for LO generators*, *Eur. Phys. J. C* **55** (2008) 553, [[arXiv:0711.2473](#)].
- [21] J. Pumplin et al., *New Generation of Parton Distributions with Uncertainties from Global QCD Analysis*, *JHEP* **07** (2002) 012, [[hep-ph/0201195](#)].
- [22] ATLAS Collaboration, *ATLAS tunes of PYTHIA 6 and Pythia 8 for MC11*, *ATL-PHYS-PUB-2011-009* (2011).
- [23] M. Mangano et al., *ALPGEN, a generator for hard multiparton processes in hadronic collisions*, *JHEP* **0307** (2003) 001, [[hep-ph/0206293](#)].
- [24] ATLAS Collaboration, *Measurement of the inclusive isolated photon cross section in pp collisions at $\sqrt{s} = 7$ TeV with the ATLAS detector*, *Phys. Rev. D* **83** (2011) 052005, [[arXiv:1012.4389](#)].
- [25] ATLAS Collaboration, *Electron performance measurements with the ATLAS detector using the 2010 LHC proton-proton collision data*, *Eur. Phys. J. C* **72** (2012) 1909, [[arXiv:1110.3174](#)].
- [26] M. Cacciari, G. P. Salam, and G. Soyez, *The catchment area of jets*, *JHEP* **04** (2008) 005, [[arXiv:0802.1188](#)].
- [27] M. Cacciari, G. P. Salam, and S. Sapeta, *On the characterisation of the underlying event*, *JHEP* **04** (2010) 065, [[arXiv:0912.4926](#)].
- [28] ATLAS Collaboration, *Measurements of the photon identification efficiency with the ATLAS detector using 4.9 fb^{-1} of pp collision data collected in 2011*, *ATLAS-CONF-2012-123* (2012).
- [29] G. D’Agostini, *A multidimensional unfolding method based on Bayes’ theorem*, *Nucl. Instrum. Methods A* **362** (1995) 487.
- [30] S. Schmitt, *TUnfold: an algorithm for correcting migration effects in high energy physics*, *JINST* **7** (2012) T10003, [[arXiv:1205.6201](#)].
- [31] ATLAS Collaboration, *Performance of the ATLAS Trigger System in 2010*, *Eur. Phys. J. C* **72** (2012) 1849, [[arXiv:1110.1530](#)].
- [32] DØ Collaboration, V. M. Abazov et al., *Azimuthal decorrelations and multiple parton interactions in photon+2 jet and photon+3 jet events in $p\bar{p}$ collisions at $\sqrt{s} = 1.96$ TeV*, *Phys. Rev. D* **83**, 052008 (2011), [[arXiv:1101.1509](#)].
- [33] L. Ametller, E. Gava, N. Paver, and D. Treleani, *Role of the QCD induced gluon-gluon coupling to gauge boson pairs in the multi-TeV region*, *Phys. Rev. D* **32** (1985) 1699.
- [34] H.-L. Lai, M. Guzzi, J. Huston, Z. Li, P. M. Nadolsky, et al., *New parton distributions for collider physics*, *Phys. Rev. D* **82** (2010) 074024, [[arXiv:1007.2241](#)].
- [35] A. Martin, W. Stirling, R. Thorne, and G. Watt, *Parton distributions for the LHC*, *Eur. Phys. J. C* **63** (2009) 189–285, [[arXiv:0901.0002](#)].
- [36] T. Binoth, J. P. Guillet, E. Pilon, and M. Werlen, *Beyond leading order effects in photon pair production at the Fermilab Tevatron*, *Phys. Rev. D* **63** (2001) 114016, [[hep-ph/0012191](#)].

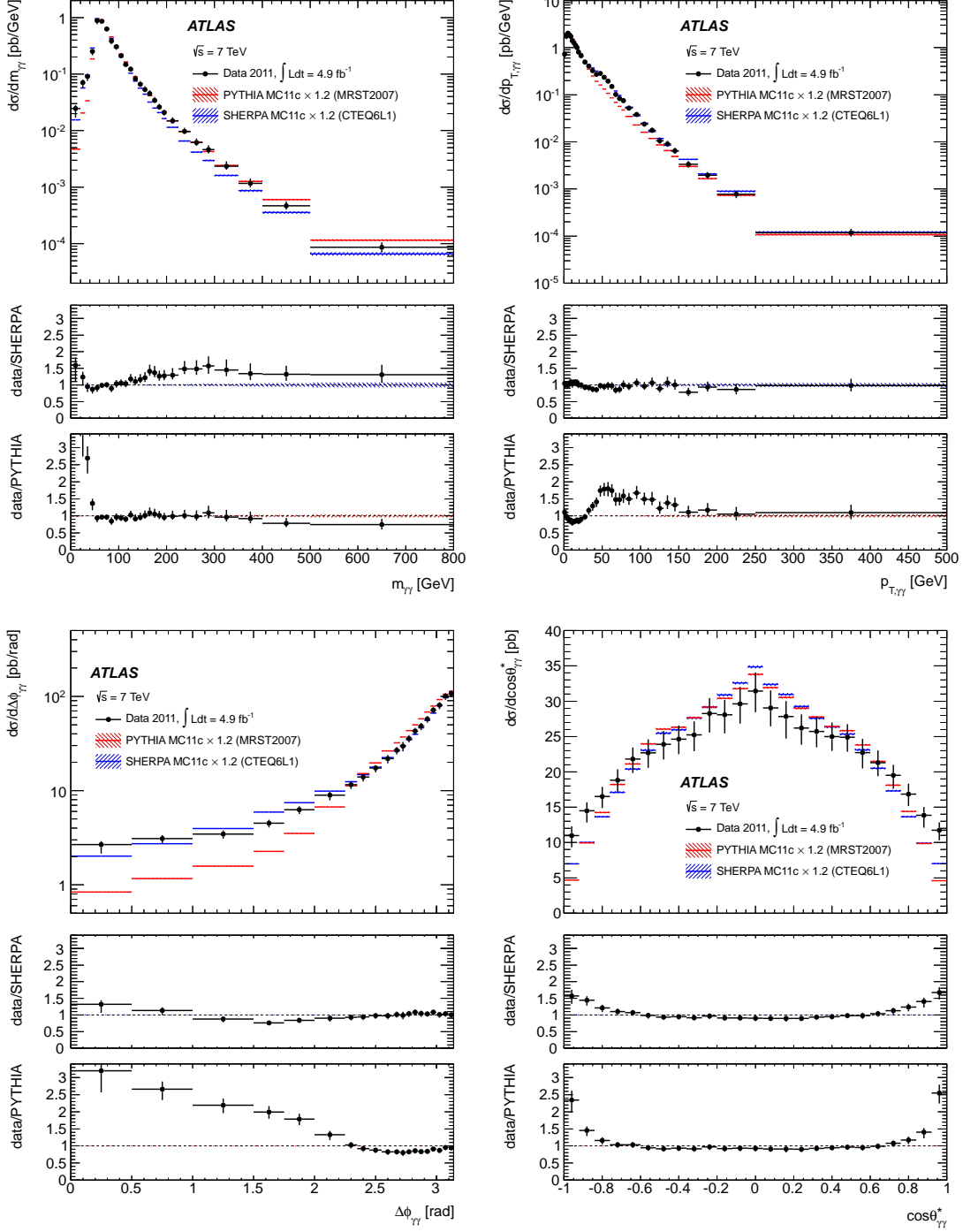


Figure 4. Comparison between the experimental cross sections and the predictions obtained with parton-shower LO simulations: $m_{\gamma\gamma}$ (top left), $p_{T,\gamma\gamma}$ (top right), $\Delta\phi_{\gamma\gamma}$ (bottom left), $\cos\theta_{\gamma\gamma}^*$ (bottom right). The LO cross sections have been scaled to the total data cross section, by a factor 1.2. Black dots correspond to data with error bars for their total uncertainties, which are dominated by the systematic component. The simulated cross sections include only statistical uncertainties.

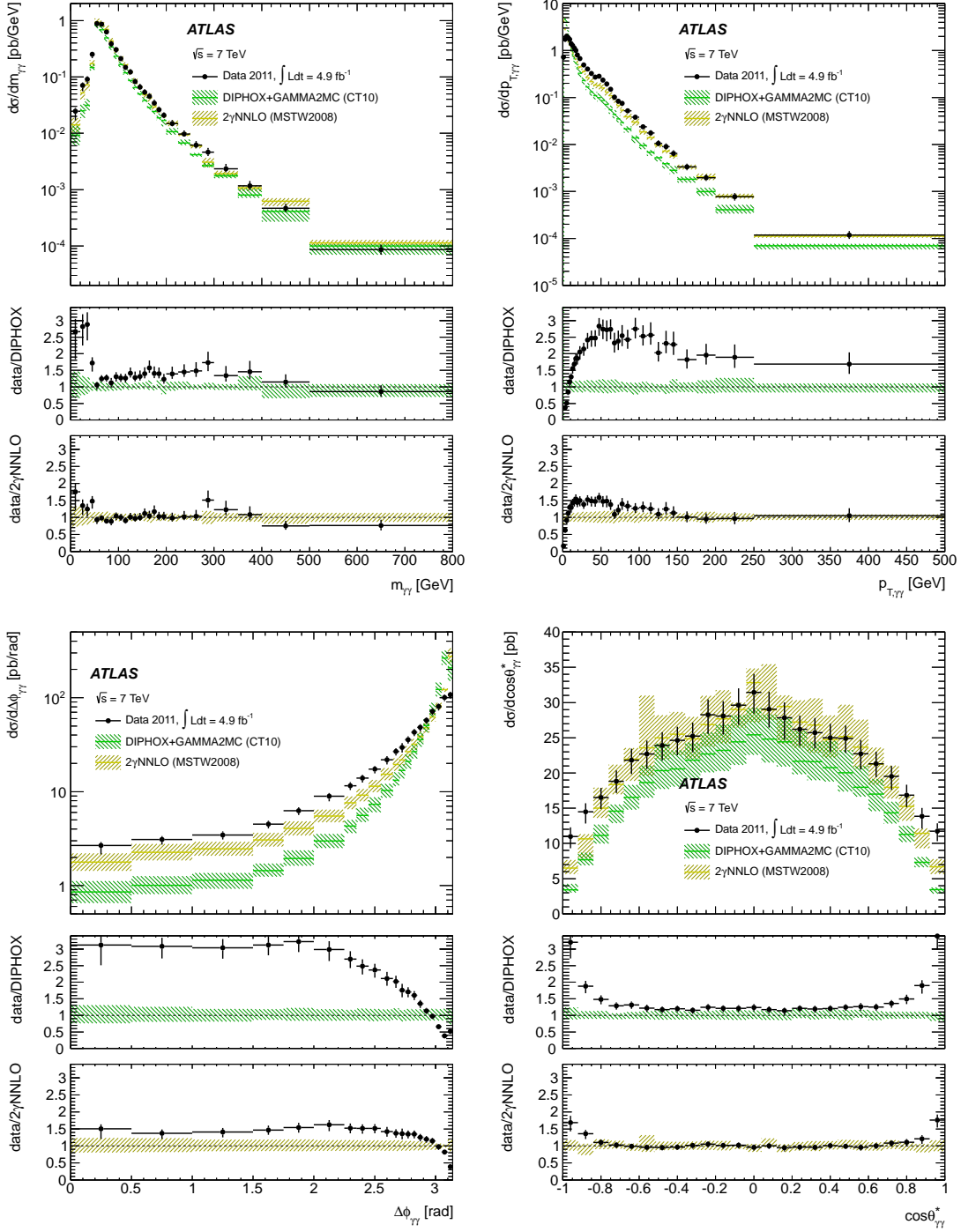


Figure 5. Comparison between the experimental cross sections and the predictions obtained with DIPHOX+GAMMA2MC (NLO) and 2γ NNLO (NNLO): $m_{\gamma\gamma}$ (top left), $p_{T,\gamma\gamma}$ (top right), $\Delta\phi_{\gamma\gamma}$ (bottom left), $\cos\theta_{\gamma\gamma}^*$ (bottom right). Black dots correspond to data with error bars for their total uncertainties, which are dominated by the systematic component. The theoretical uncertainties include contributions from the limited size of the simulated sample, from the scale choice and from uncertainties on the parton distribution functions and on the hadronization and underlying event corrections.

A Experimental differential cross section

The numerical values of the differential cross sections displayed in figures 4 and 5 are quoted in tables 2-5. For each bin of the $m_{\gamma\gamma}$, $p_{T,\gamma\gamma}$, $\Delta\phi_{\gamma\gamma}$, and $\cos\theta_{\gamma\gamma}^*$ variables, the cross section is given together with its statistical, systematic and total uncertainties. All values are divided by the bin width.

$m_{\gamma\gamma}$ [GeV]	$d\sigma/dm_{\gamma\gamma}$ [pb/GeV]	Statistical error		Systematic errors		Total error	
		high	low	high	low	high	low
[0, 20)	0.0247	+0.0015	-0.0015	+0.0032	-0.0076	+0.0036	-0.0077
[20, 30)	0.0704	+0.0032	-0.0032	+0.0087	-0.0140	+0.0093	-0.0144
[30, 40)	0.091	+0.004	-0.004	+0.011	-0.015	+0.012	-0.015
[40, 50)	0.252	+0.006	-0.006	+0.025	-0.037	+0.026	-0.037
[50, 60)	0.880	+0.012	-0.012	+0.073	-0.120	+0.074	-0.120
[60, 70)	0.857	+0.010	-0.010	+0.071	-0.068	+0.071	-0.068
[70, 80)	0.626	+0.008	-0.008	+0.051	-0.052	+0.051	-0.053
[80, 90)	0.384	+0.008	-0.008	+0.049	-0.048	+0.050	-0.049
[90, 100)	0.305	+0.006	-0.006	+0.031	-0.034	+0.032	-0.035
[100, 110)	0.212	+0.004	-0.004	+0.021	-0.021	+0.021	-0.021
[110, 120)	0.148	+0.004	-0.004	+0.015	-0.014	+0.015	-0.015
[120, 130)	0.122	+0.003	-0.003	+0.015	-0.010	+0.015	-0.011
[130, 140)	0.0829	+0.0025	-0.0025	+0.0112	-0.0073	+0.0115	-0.0077
[140, 150)	0.0656	+0.0022	-0.0022	+0.0088	-0.0057	+0.0091	-0.0061
[150, 160)	0.0535	+0.0019	-0.0019	+0.0072	-0.0051	+0.0075	-0.0054
[160, 170)	0.0451	+0.0017	-0.0017	+0.0063	-0.0038	+0.0065	-0.0042
[170, 180)	0.0343	+0.0015	-0.0015	+0.0050	-0.0031	+0.0052	-0.0035
[180, 190)	0.0262	+0.0013	-0.0013	+0.0032	-0.0024	+0.0035	-0.0027
[190, 200)	0.0209	+0.0011	-0.0011	+0.0025	-0.0019	+0.0028	-0.0022
[200, 225)	0.0149	+0.0006	-0.0006	+0.0023	-0.0014	+0.0024	-0.0015
[225, 250)	0.00970	+0.00049	-0.00049	+0.00150	-0.00086	+0.00158	-0.00099
[250, 275)	0.00616	+0.00039	-0.00039	+0.00104	-0.00064	+0.00111	-0.00075
[275, 300)	0.00464	+0.00036	-0.00036	+0.00080	-0.00059	+0.00087	-0.00069
[300, 350)	0.00235	+0.00017	-0.00017	+0.00048	-0.00026	+0.00051	-0.00031
[350, 400)	0.00116	+0.00011	-0.00011	+0.00024	-0.00013	+0.00026	-0.00017
[400, 500)	4.69e-04	+5.0e-05	-5.0e-05	+7.9e-05	-4.7e-05	+9.3e-05	-6.9e-05
[500, 800)	8.6e-05	+1.3e-05	-1.3e-05	+1.5e-05	-1.0e-05	+1.9e-05	-1.6e-05

Table 2. Experimental cross-section values per bin in pb/GeV for $m_{\gamma\gamma}$. The listed total errors are the quadratic sum of statistical and systematic uncertainties.

$p_{T,\gamma\gamma}$ [GeV]	$d\sigma/dp_{T,\gamma\gamma}$ [pb/GeV]	Statistical error		Systematic errors		Total error	
		high	low	high	low	high	low
[0, 2)	0.727	+0.022	-0.022	+0.057	-0.092	+0.061	-0.094
[2, 4)	1.75	+0.04	-0.04	+0.13	-0.23	+0.13	-0.23
[4, 6)	2.03	+0.04	-0.04	+0.15	-0.23	+0.15	-0.23
[6, 8)	1.88	+0.04	-0.04	+0.15	-0.21	+0.16	-0.21
[8, 10)	1.72	+0.03	-0.03	+0.13	-0.19	+0.14	-0.19
[10, 12)	1.40	+0.03	-0.03	+0.12	-0.16	+0.12	-0.16
[12, 14)	1.28	+0.03	-0.03	+0.10	-0.13	+0.11	-0.13
[14, 16)	1.122	+0.026	-0.026	+0.093	-0.114	+0.097	-0.117
[16, 18)	0.999	+0.024	-0.024	+0.086	-0.090	+0.090	-0.093
[18, 20)	0.810	+0.021	-0.021	+0.072	-0.076	+0.075	-0.079
[20, 25)	0.674	+0.012	-0.012	+0.056	-0.074	+0.058	-0.075
[25, 30)	0.492	+0.011	-0.011	+0.041	-0.045	+0.043	-0.047
[30, 35)	0.405	+0.009	-0.009	+0.034	-0.043	+0.035	-0.044
[35, 40)	0.325	+0.009	-0.009	+0.028	-0.034	+0.030	-0.035
[40, 45)	0.272	+0.008	-0.008	+0.024	-0.027	+0.026	-0.028
[45, 50)	0.282	+0.008	-0.008	+0.023	-0.027	+0.024	-0.028
[50, 55)	0.235	+0.007	-0.007	+0.023	-0.025	+0.025	-0.026
[55, 60)	0.194	+0.006	-0.006	+0.019	-0.024	+0.021	-0.024
[60, 65)	0.150	+0.006	-0.006	+0.015	-0.016	+0.016	-0.017
[65, 70)	0.102	+0.005	-0.005	+0.013	-0.012	+0.014	-0.013
[70, 75)	0.0836	+0.0041	-0.0041	+0.0103	-0.0087	+0.0111	-0.0096
[75, 80)	0.0748	+0.0036	-0.0036	+0.0087	-0.0086	+0.0094	-0.0093
[80, 90)	0.0521	+0.0021	-0.0021	+0.0059	-0.0056	+0.0063	-0.0059
[90, 100)	0.0381	+0.0017	-0.0017	+0.0043	-0.0036	+0.0047	-0.0040
[100, 110)	0.0239	+0.0013	-0.0013	+0.0028	-0.0023	+0.0031	-0.0026
[110, 120)	0.0175	+0.0011	-0.0011	+0.0024	-0.0016	+0.0027	-0.0019
[120, 130)	0.0106	+0.0009	-0.0009	+0.0015	-0.0011	+0.0017	-0.0014
[130, 140)	0.0090	+0.0008	-0.0008	+0.0012	-0.0008	+0.0015	-0.0012
[140, 150)	0.00646	+0.00064	-0.00064	+0.00089	-0.00063	+0.00110	-0.00090
[150, 175)	0.00333	+0.00031	-0.00031	+0.00047	-0.00039	+0.00056	-0.00049
[175, 200)	0.00195	+0.00023	-0.00023	+0.00025	-0.00017	+0.00034	-0.00028
[200, 250)	0.00077	+0.00010	-0.00010	+0.00012	-0.00008	+0.00016	-0.00013
[250, 500)	1.18e-04	+1.7e-05	-1.7e-05	+1.8e-05	-1.2e-05	+2.5e-05	-2.1e-05

Table 3. Experimental cross-section values per bin in pb/GeV for $p_{T,\gamma\gamma}$. The listed total errors are the quadratic sum of statistical and systematic uncertainties.

$\Delta\phi_{\gamma\gamma}$ [rad]	$d\sigma/d\Delta\phi_{\gamma\gamma}$ [pb/rad]	Statistical error		Systematic errors		Total error	
		high	low	high	low	high	low
[0.00, 0.50)	2.68	+0.08	-0.08	+0.22	-0.52	+0.24	-0.52
[0.50, 1.00)	3.10	+0.09	-0.09	+0.25	-0.36	+0.26	-0.37
[1.00, 1.50)	3.46	+0.09	-0.09	+0.29	-0.36	+0.31	-0.37
[1.50, 1.75)	4.51	+0.15	-0.15	+0.36	-0.42	+0.39	-0.44
[1.75, 2.00)	6.26	+0.17	-0.17	+0.53	-0.59	+0.55	-0.61
[2.00, 2.25)	8.93	+0.20	-0.20	+0.73	-1.02	+0.76	-1.04
[2.25, 2.35)	11.6	+0.4	-0.4	+0.9	-1.1	+1.0	-1.2
[2.35, 2.45)	13.9	+0.4	-0.4	+1.1	-1.3	+1.1	-1.4
[2.45, 2.55)	17.4	+0.4	-0.4	+1.3	-1.6	+1.4	-1.7
[2.55, 2.65)	21.8	+0.5	-0.5	+2.0	-2.2	+2.0	-2.3
[2.65, 2.70)	26.7	+0.8	-0.8	+2.1	-2.4	+2.3	-2.5
[2.70, 2.75)	29.6	+0.8	-0.8	+3.2	-3.4	+3.3	-3.5
[2.75, 2.80)	35.8	+0.9	-0.9	+2.8	-3.1	+3.0	-3.3
[2.80, 2.85)	42.9	+1.0	-1.0	+3.3	-3.8	+3.4	-3.9
[2.85, 2.90)	48.4	+1.1	-1.1	+3.8	-4.4	+3.9	-4.6
[2.90, 2.95)	57.4	+1.2	-1.2	+4.3	-4.6	+4.4	-4.7
[2.95, 3.00)	71.7	+1.3	-1.3	+5.4	-5.9	+5.6	-6.1
[3.00, 3.05)	80.8	+1.4	-1.4	+6.1	-7.4	+6.3	-7.6
[3.05, 3.10)	100.5	+1.6	-1.6	+7.3	-8.5	+7.4	-8.6
[3.10, 3.14)	107.6	+1.8	-1.8	+7.9	-9.6	+8.1	-9.8

Table 4. Experimental cross-section values per bin in pb/rad for $\Delta\phi_{\gamma\gamma}$. The listed total errors are the quadratic sum of statistical and systematic uncertainties.

$\cos \theta_{\gamma\gamma}^*$	$d\sigma/d\cos \theta_{\gamma\gamma}^*$ [pb]	Statistical error		Systematic errors		Total error	
		high	low	high	low	high	low
[-1.00, -0.92)	11.0	+0.4	-0.4	+1.2	-1.6	+1.3	-1.7
[-0.92, -0.84)	14.5	+0.4	-0.4	+1.1	-1.6	+1.2	-1.6
[-0.84, -0.76)	16.5	+0.5	-0.5	+1.3	-1.6	+1.4	-1.6
[-0.76, -0.68)	18.8	+0.5	-0.5	+1.4	-1.6	+1.5	-1.7
[-0.68, -0.60)	21.8	+0.6	-0.6	+1.5	-1.9	+1.6	-1.9
[-0.60, -0.52)	22.7	+0.6	-0.6	+1.8	-2.0	+1.9	-2.1
[-0.52, -0.44)	23.9	+0.6	-0.6	+1.8	-2.1	+1.9	-2.1
[-0.44, -0.36)	24.6	+0.6	-0.6	+1.8	-2.0	+1.9	-2.1
[-0.36, -0.28)	25.2	+0.6	-0.6	+1.8	-2.2	+1.9	-2.3
[-0.28, -0.20)	28.3	+0.6	-0.6	+2.1	-2.6	+2.2	-2.7
[-0.20, -0.12)	28.1	+0.7	-0.7	+2.0	-2.6	+2.1	-2.6
[-0.12, -0.04)	29.6	+0.7	-0.7	+2.3	-2.7	+2.4	-2.8
[-0.04, 0.04)	31.4	+0.7	-0.7	+2.5	-2.9	+2.6	-3.0
[0.04, 0.12)	29.0	+0.7	-0.7	+2.4	-2.5	+2.5	-2.6
[0.12, 0.20)	27.8	+0.7	-0.7	+2.1	-3.0	+2.2	-3.1
[0.20, 0.28)	26.2	+0.6	-0.6	+1.8	-2.3	+2.0	-2.3
[0.28, 0.36)	25.7	+0.6	-0.6	+2.0	-2.1	+2.1	-2.2
[0.36, 0.44)	25.0	+0.6	-0.6	+1.9	-1.9	+2.0	-2.0
[0.44, 0.52)	24.9	+0.6	-0.6	+1.7	-2.0	+1.8	-2.1
[0.52, 0.60)	22.7	+0.6	-0.6	+1.9	-2.2	+2.0	-2.2
[0.60, 0.68)	21.3	+0.6	-0.6	+1.6	-1.8	+1.7	-1.9
[0.68, 0.76)	19.5	+0.5	-0.5	+1.4	-1.8	+1.5	-1.9
[0.76, 0.84)	16.9	+0.5	-0.5	+1.4	-1.6	+1.5	-1.7
[0.84, 0.92)	13.9	+0.4	-0.4	+1.1	-1.7	+1.2	-1.8
[0.92, 1.00)	11.7	+0.4	-0.4	+1.0	-1.4	+1.1	-1.4

Table 5. Experimental cross-section values per bin in pb for $\cos \theta_{\gamma\gamma}^*$. The listed total errors are the quadratic sum of statistical and systematic uncertainties.

The ATLAS Collaboration

G. Aad⁴⁸, T. Abajyan²¹, B. Abbott¹¹¹, J. Abdallah¹², S. Abdel Khalek¹¹⁵,
A.A. Abdelalim⁴⁹, O. Abdinov¹¹, R. Aben¹⁰⁵, B. Abi¹¹², M. Abolins⁸⁸, O.S. AbouZeid¹⁵⁸,
H. Abramowicz¹⁵³, H. Abreu¹³⁶, B.S. Acharya^{164a,164b,a}, L. Adamczyk³⁸, D.L. Adams²⁵,
T.N. Addy⁵⁶, J. Adelman¹⁷⁶, S. Adomeit⁹⁸, P. Adragna⁷⁵, T. Adye¹²⁹, S. Aefsky²³,
J.A. Aguilar-Saavedra^{124b,b}, M. Agustoni¹⁷, M. Aharrouche⁸¹, S.P. Ahlen²², F. Ahles⁴⁸,
A. Ahmad¹⁴⁸, M. Ahsan⁴¹, G. Aielli^{133a,133b}, T.P.A. Åkesson⁷⁹, G. Akimoto¹⁵⁵,
A.V. Akimov⁹⁴, M.S. Alam², M.A. Alam⁷⁶, J. Albert¹⁶⁹, S. Albrand⁵⁵, M. Aleksa³⁰,
I.N. Aleksandrov⁶⁴, F. Alessandria^{89a}, C. Alexa^{26a}, G. Alexander¹⁵³, G. Alexandre⁴⁹,
T. Alexopoulos¹⁰, M. Alhroob^{164a,164c}, M. Aliev¹⁶, G. Alimonti^{89a}, J. Alison¹²⁰,
B.M.M. Allbrooke¹⁸, P.P. Allport⁷³, S.E. Allwood-Spiers⁵³, J. Almond⁸²,
A. Aloisio^{102a,102b}, R. Alon¹⁷², A. Alonso⁷⁹, F. Alonso⁷⁰, A. Altheimer³⁵,
B. Alvarez Gonzalez⁸⁸, M.G. Alviggi^{102a,102b}, K. Amako⁶⁵, C. Amelung²³,
V.V. Ammosov^{128,*}, S.P. Amor Dos Santos^{124a}, A. Amorim^{124a,c}, N. Amram¹⁵³,
C. Anastopoulos³⁰, L.S. Ancu¹⁷, N. Andari¹¹⁵, T. Andeen³⁵, C.F. Anders^{58b},
G. Anders^{58a}, K.J. Anderson³¹, A. Andreazza^{89a,89b}, V. Andrei^{58a}, M-L. Andrieux⁵⁵,
X.S. Anduaga⁷⁰, S. Angelidakis⁹, P. Anger⁴⁴, A. Angerami³⁵, F. Anghinolfi³⁰,
A. Anisenkov¹⁰⁷, N. Anjos^{124a}, A. Annovi⁴⁷, A. Antonaki⁹, M. Antonelli⁴⁷, A. Antonov⁹⁶,
J. Antos^{144b}, F. Anulli^{132a}, M. Aoki¹⁰¹, S. Aoun⁸³, L. Aperio Bella⁵, R. Apolle^{118,d},
G. Arabidze⁸⁸, I. Aracena¹⁴³, Y. Arai⁶⁵, A.T.H. Arce⁴⁵, S. Arfaoui¹⁴⁸, J-F. Arguin⁹³,
S. Argyropoulos⁴², E. Arik^{19a,*}, M. Arik^{19a}, A.J. Armbruster⁸⁷, O. Arnaez⁸¹, V. Arnal⁸⁰,
A. Artamonov⁹⁵, G. Artoni^{132a,132b}, D. Arutinov²¹, S. Asai¹⁵⁵, S. Ask²⁸,
B. Åsman^{146a,146b}, L. Asquith⁶, K. Assamagan^{25,e}, A. Astbury¹⁶⁹, M. Atkinson¹⁶⁵,
B. Aubert⁵, E. Auge¹¹⁵, K. Augsten¹²⁶, M. Aurousseau^{145a}, G. Avolio³⁰, D. Axen¹⁶⁸,
G. Azuelos^{93,f}, Y. Azuma¹⁵⁵, M.A. Baak³⁰, G. Baccaglioni^{89a}, C. Bacci^{134a,134b},
A.M. Bach¹⁵, H. Bachacou¹³⁶, K. Bachas¹⁵⁴, M. Backes⁴⁹, M. Backhaus²¹,
J. Backus Mayes¹⁴³, E. Badescu^{26a}, P. Bagnaia^{132a,132b}, S. Bahinipati³, Y. Bai^{33a},
D.C. Bailey¹⁵⁸, T. Bain¹⁵⁸, J.T. Baines¹²⁹, O.K. Baker¹⁷⁶, M.D. Baker²⁵, S. Baker⁷⁷,
P. Balek¹²⁷, E. Banas³⁹, P. Banerjee⁹³, Sw. Banerjee¹⁷³, D. Banfi³⁰, A. Bangert¹⁵⁰,
V. Bansal¹⁶⁹, H.S. Bansil¹⁸, L. Barak¹⁷², S.P. Baranov⁹⁴, A. Barbaro Galtieri¹⁵,
T. Barber⁴⁸, E.L. Barberio⁸⁶, D. Barberis^{50a,50b}, M. Barbero²¹, D.Y. Bardin⁶⁴,
T. Barillari⁹⁹, M. Barisonzi¹⁷⁵, T. Barklow¹⁴³, N. Barlow²⁸, B.M. Barnett¹²⁹,
R.M. Barnett¹⁵, A. Baroncelli^{134a}, G. Barone⁴⁹, A.J. Barr¹¹⁸, F. Barreiro⁸⁰,
J. Barreiro Guimarães da Costa⁵⁷, R. Bartoldus¹⁴³, A.E. Barton⁷¹, V. Bartsch¹⁴⁹,
A. Basye¹⁶⁵, R.L. Bates⁵³, L. Batkova^{144a}, J.R. Batley²⁸, A. Battaglia¹⁷, M. Battistin³⁰,
F. Bauer¹³⁶, H.S. Bawa^{143,g}, S. Beale⁹⁸, T. Beau⁷⁸, P.H. Beauchemin¹⁶¹, R. Beccherle^{50a},
P. Bechtel²¹, H.P. Beck¹⁷, K. Becker¹⁷⁵, S. Becker⁹⁸, M. Beckingham¹³⁸, K.H. Becks¹⁷⁵,
A.J. Beddall^{19c}, A. Beddall^{19c}, S. Bedikian¹⁷⁶, V.A. Bednyakov⁶⁴, C.P. Bee⁸³,
L.J. Beamster¹⁰⁵, M. Begel²⁵, S. Behar Harpaz¹⁵², P.K. Behera⁶², M. Beimforde⁹⁹,
C. Belanger-Champagne⁸⁵, P.J. Bell⁴⁹, W.H. Bell⁴⁹, G. Bella¹⁵³, L. Bellagamba^{20a},
M. Bellomo³⁰, A. Belloni⁵⁷, O. Beloborodova^{107,h}, K. Belotskiy⁹⁶, O. Beltramello³⁰,
O. Benary¹⁵³, D. Benchekroun^{135a}, K. Bendtz^{146a,146b}, N. Benekos¹⁶⁵, Y. Benhammou¹⁵³,

E. Benhar Noccioli⁴⁹, J.A. Benitez Garcia^{159b}, D.P. Benjamin⁴⁵, M. Benoit¹¹⁵,
 J.R. Bensingher²³, K. Benslama¹³⁰, S. Bentvelsen¹⁰⁵, D. Berge³⁰, E. Bergeaas Kuutmann⁴²,
 N. Berger⁵, F. Berghaus¹⁶⁹, E. Berglund¹⁰⁵, J. Beringer¹⁵, P. Bernat⁷⁷, R. Bernhard⁴⁸,
 C. Bernius²⁵, T. Berry⁷⁶, C. Bertella⁸³, A. Bertin^{20a,20b}, F. Bertolucci^{122a,122b},
 M.I. Besana^{89a,89b}, G.J. Besjes¹⁰⁴, N. Besson¹³⁶, S. Bethke⁹⁹, W. Bhimji⁴⁶,
 R.M. Bianchi³⁰, L. Bianchini²³, M. Bianco^{72a,72b}, O. Biebel⁹⁸, S.P. Bieniek⁷⁷,
 K. Bierwagen⁵⁴, J. Biesiada¹⁵, M. Biglietti^{134a}, H. Bilokon⁴⁷, M. Bindi^{20a,20b}, S. Binet¹¹⁵,
 A. Bingul^{19c}, C. Bini^{132a,132b}, C. Biscarat¹⁷⁸, B. Bittner⁹⁹, C.W. Black¹⁵⁰, K.M. Black²²,
 R.E. Blair⁶, J.-B. Blanchard¹³⁶, G. Blanchot³⁰, T. Blazek^{144a}, I. Bloch⁴², C. Blocker²³,
 J. Blocki³⁹, A. Blondel⁴⁹, W. Blum⁸¹, U. Blumenschein⁵⁴, G.J. Bobbink¹⁰⁵,
 V.S. Bobrovnikov¹⁰⁷, S.S. Bocchetta⁷⁹, A. Bocci⁴⁵, C.R. Boddy¹¹⁸, M. Boehler⁴⁸,
 J. Boek¹⁷⁵, T.T. Boek¹⁷⁵, N. Boelaert³⁶, J.A. Bogaerts³⁰, A. Bogdanchikov¹⁰⁷,
 A. Bogouch^{90,*}, C. Bohm^{146a}, J. Bohm¹²⁵, V. Boisvert⁷⁶, T. Bold³⁸, V. Boldea^{26a},
 N.M. Bolnet¹³⁶, M. Bomben⁷⁸, M. Bona⁷⁵, M. Boonekamp¹³⁶, S. Bordoni⁷⁸, C. Borer¹⁷,
 A. Borisov¹²⁸, G. Borissov⁷¹, I. Borjanovic^{13a}, M. Borri⁸², S. Borroni⁸⁷, J. Bortfeldt⁹⁸,
 V. Bortolotto^{134a,134b}, K. Bos¹⁰⁵, D. Boscherini^{20a}, M. Bosman¹², H. Boterenbrood¹⁰⁵,
 J. Bouchami⁹³, J. Boudreau¹²³, E.V. Bouhova-Thacker⁷¹, D. Boumediene³⁴,
 C. Bourdarios¹¹⁵, N. Bousson⁸³, A. Boveia³¹, J. Boyd³⁰, I.R. Boyko⁶⁴,
 I. Bozovic-Jelisavcic^{13b}, J. Bracinik¹⁸, P. Branchini^{134a}, A. Brandt⁸, G. Brandt¹¹⁸,
 O. Brandt⁵⁴, U. Bratzler¹⁵⁶, B. Brau⁸⁴, J.E. Brau¹¹⁴, H.M. Braun^{175,*},
 S.F. Brazzale^{164a,164c}, B. Brelief¹⁵⁸, J. Bremer³⁰, K. Brendlinger¹²⁰, R. Brenner¹⁶⁶,
 S. Bressler¹⁷², D. Britton⁵³, F.M. Brochu²⁸, I. Brock²¹, R. Brock⁸⁸, F. Broggi^{89a},
 C. Bromberg⁸⁸, J. Bronner⁹⁹, G. Brooijmans³⁵, T. Brooks⁷⁶, W.K. Brooks^{32b},
 G. Brown⁸², P.A. Bruckman de Renstrom³⁹, D. Bruncko^{144b}, R. Bruneliere⁴⁸, S. Brunet⁶⁰,
 A. Bruni^{20a}, G. Bruni^{20a}, M. Bruschi^{20a}, L. Bryngemark⁷⁹, T. Buanes¹⁴, Q. Buat⁵⁵,
 F. Bucci⁴⁹, J. Buchanan¹¹⁸, P. Buchholz¹⁴¹, R.M. Buckingham¹¹⁸, A.G. Buckley⁴⁶,
 S.I. Buda^{26a}, I.A. Budagov⁶⁴, B. Budick¹⁰⁸, V. Büscher⁸¹, L. Bugge¹¹⁷, O. Bulekov⁹⁶,
 A.C. Bundock⁷³, M. Bunse⁴³, T. Buran¹¹⁷, H. Burckhart³⁰, S. Burdin⁷³, T. Burgess¹⁴,
 S. Burke¹²⁹, E. Busato³⁴, P. Bussey⁵³, C.P. Buszello¹⁶⁶, B. Butler¹⁴³, J.M. Butler²²,
 C.M. Buttar⁵³, J.M. Butterworth⁷⁷, W. Buttinger²⁸, M. Byszewski³⁰,
 S. Cabrera Urbán¹⁶⁷, D. Caforio^{20a,20b}, O. Cakir^{4a}, P. Calafiura¹⁵, G. Calderini⁷⁸,
 P. Calfayan⁹⁸, R. Calkins¹⁰⁶, L.P. Caloba^{24a}, R. Caloi^{132a,132b}, D. Calvet³⁴, S. Calvet³⁴,
 R. Camacho Toro³⁴, P. Camarri^{133a,133b}, D. Cameron¹¹⁷, L.M. Caminada¹⁵,
 R. Caminal Armadans¹², S. Campana³⁰, M. Campanelli⁷⁷, V. Canale^{102a,102b},
 F. Canelli³¹, A. Canepa^{159a}, J. Cantero⁸⁰, R. Cantrill⁷⁶, L. Capasso^{102a,102b},
 M.D.M. Capeans Garrido³⁰, I. Caprini^{26a}, M. Caprini^{26a}, D. Capriotti⁹⁹, M. Capua^{37a,37b},
 R. Caputo⁸¹, R. Cardarelli^{133a}, T. Carli³⁰, G. Carlino^{102a}, L. Carminati^{89a,89b},
 B. Caron⁸⁵, S. Caron¹⁰⁴, E. Carquin^{32b}, G.D. Carrillo-Montoya^{145b}, A.A. Carter⁷⁵,
 J.R. Carter²⁸, J. Carvalho^{124a,i}, D. Casadei¹⁰⁸, M.P. Casado¹², M. Cascella^{122a,122b},
 C. Caso^{50a,50b,*}, A.M. Castaneda Hernandez^{173,j}, E. Castaneda-Miranda¹⁷³,
 V. Castillo Gimenez¹⁶⁷, N.F. Castro^{124a}, G. Cataldi^{72a}, P. Catastini⁵⁷, A. Catinaccio³⁰,
 J.R. Catmore³⁰, A. Cattai³⁰, G. Cattani^{133a,133b}, S. Caughron⁸⁸, V. Cavaliere¹⁶⁵,
 P. Cavalleri⁷⁸, D. Cavalli^{89a}, M. Cavalli-Sforza¹², V. Cavasinni^{122a,122b},

F. Ceradini^{134a,134b}, A.S. Cerqueira^{24b}, A. Cerri¹⁵, L. Cerrito⁷⁵, F. Cerutti¹⁵,
 S.A. Cetin^{19b}, A. Chafaq^{135a}, D. Chakraborty¹⁰⁶, I. Chalupkova¹²⁷, K. Chan³,
 P. Chang¹⁶⁵, B. Chapleau⁸⁵, J.D. Chapman²⁸, J.W. Chapman⁸⁷, D.G. Charlton¹⁸,
 V. Chavda⁸², C.A. Chavez Barajas³⁰, S. Cheatham⁸⁵, S. Chekanov⁶, S.V. Chekulaev^{159a},
 G.A. Chelkov⁶⁴, M.A. Chelstowska¹⁰⁴, C. Chen⁶³, H. Chen²⁵, S. Chen^{33c}, X. Chen¹⁷³,
 Y. Chen³⁵, Y. Cheng³¹, A. Cheplakov⁶⁴, R. Cherkaoui El Moursli^{135e}, V. Chernyatin²⁵,
 E. Cheu⁷, S.L. Cheung¹⁵⁸, L. Chevalier¹³⁶, G. Chiefari^{102a,102b}, L. Chikovani^{51a,*},
 J.T. Childers³⁰, A. Chilingarov⁷¹, G. Chiodini^{72a}, A.S. Chisholm¹⁸, R.T. Chislett⁷⁷,
 A. Chitan^{26a}, M.V. Chizhov⁶⁴, G. Choudalakis³¹, S. Chouridou¹³⁷, I.A. Christidi⁷⁷,
 A. Christov⁴⁸, D. Chromek-Burckhart³⁰, M.L. Chu¹⁵¹, J. Chudoba¹²⁵, G. Ciapetti^{132a,132b},
 A.K. Ciftci^{4a}, R. Ciftci^{4a}, D. Cinca³⁴, V. Cindro⁷⁴, A. Ciocio¹⁵, M. Cirilli⁸⁷,
 P. Cirkovic^{13b}, Z.H. Citron¹⁷², M. Citterio^{89a}, M. Ciubancan^{26a}, A. Clark⁴⁹, P.J. Clark⁴⁶,
 R.N. Clarke¹⁵, W. Cleland¹²³, J.C. Clemens⁸³, B. Clement⁵⁵, C. Clement^{146a,146b},
 Y. Coadou⁸³, M. Cobal^{164a,164c}, A. Coccaro¹³⁸, J. Cochran⁶³, L. Coffey²³, J.G. Cogan¹⁴³,
 J. Coggeshall¹⁶⁵, J. Colas⁵, S. Cole¹⁰⁶, A.P. Colijn¹⁰⁵, N.J. Collins¹⁸, C. Collins-Tooth⁵³,
 J. Collot⁵⁵, T. Colombo^{119a,119b}, G. Colon⁸⁴, G. Compostella⁹⁹, P. Conde Muiño^{124a},
 E. Coniavitis¹⁶⁶, M.C. Conidi¹², S.M. Consonni^{89a,89b}, V. Consorti⁴⁸,
 S. Constantinescu^{26a}, C. Conta^{119a,119b}, G. Conti⁵⁷, F. Conventi^{102a,k}, M. Cooke¹⁵,
 B.D. Cooper⁷⁷, A.M. Cooper-Sarkar¹¹⁸, K. Copic¹⁵, T. Cornelissen¹⁷⁵, M. Corradi^{20a},
 F. Corriveau^{85,l}, A. Cortes-Gonzalez¹⁶⁵, G. Cortiana⁹⁹, G. Costa^{89a}, M.J. Costa¹⁶⁷,
 D. Costanzo¹³⁹, D. Côté³⁰, L. Courneyea¹⁶⁹, G. Cowan⁷⁶, B.E. Cox⁸², K. Cranmer¹⁰⁸,
 F. Crescioli⁷⁸, M. Cristinziani²¹, G. Crosetti^{37a,37b}, S. Crépé-Renaudin⁵⁵,
 C.-M. Cuciuc^{26a}, C. Cuenca Almenar¹⁷⁶, T. Cuhadar Donszelmann¹³⁹, J. Cummings¹⁷⁶,
 M. Curatolo⁴⁷, C.J. Curtis¹⁸, C. Cuthbert¹⁵⁰, P. Cwetanski⁶⁰, H. Czirr¹⁴¹,
 P. Czodrowski⁴⁴, Z. Czyczula¹⁷⁶, S. D'Auria⁵³, M. D'Onofrio⁷³, A. D'Orazio^{132a,132b},
 M.J. Da Cunha Sargedas De Sousa^{124a}, C. Da Via⁸², W. Dabrowski³⁸, A. Dafinca¹¹⁸,
 T. Dai⁸⁷, F. Dallaire⁹³, C. Dallapiccola⁸⁴, M. Dam³⁶, M. Dameri^{50a,50b}, D.S. Damiani¹³⁷,
 H.O. Danielsson³⁰, V. Dao⁴⁹, G. Darbo^{50a}, G.L. Darlea^{26b}, J.A. Dassoulas⁴², W. Davey²¹,
 T. Davidek¹²⁷, N. Davidson⁸⁶, R. Davidson⁷¹, E. Davies^{118,d}, M. Davies⁹³, O. Davignon⁷⁸,
 A.R. Davison⁷⁷, Y. Davygora^{58a}, E. Dawe¹⁴², I. Dawson¹³⁹,
 R.K. Daya-Ishmukhametova²³, K. De⁸, R. de Asmundis^{102a}, S. De Castro^{20a,20b},
 S. De Cecco⁷⁸, J. de Graat⁹⁸, N. De Groot¹⁰⁴, P. de Jong¹⁰⁵, C. De La Taille¹¹⁵,
 H. De la Torre⁸⁰, F. De Lorenzi⁶³, L. de Mora⁷¹, L. De Nooij¹⁰⁵, D. De Pedis^{132a},
 A. De Salvo^{132a}, U. De Sanctis^{164a,164c}, A. De Santo¹⁴⁹, J.B. De Vivie De Regie¹¹⁵,
 G. De Zorzi^{132a,132b}, W.J. Dearnaley⁷¹, R. Debbe²⁵, C. Debenedetti⁴⁶, B. Dechenaux⁵⁵,
 D.V. Dedovich⁶⁴, J. Degenhardt¹²⁰, J. Del Peso⁸⁰, T. Del Prete^{122a,122b}, T. Delemontex⁵⁵,
 M. Deliyergiyev⁷⁴, A. Dell'Acqua³⁰, L. Dell'Asta²², M. Della Pietra^{102a,k},
 D. della Volpe^{102a,102b}, M. Delmastro⁵, P.A. Delsart⁵⁵, C. Deluca¹⁰⁵, S. Demers¹⁷⁶,
 M. Demichev⁶⁴, B. Demirköz^{12,m}, S.P. Denisov¹²⁸, D. Derendarz³⁹, J.E. Derkaoui^{135d},
 F. Derue⁷⁸, P. Dervan⁷³, K. Desch²¹, E. Devetak¹⁴⁸, P.O. Deviveiros¹⁰⁵, A. Dewhurst¹²⁹,
 B. DeWilde¹⁴⁸, S. Dhaliwal¹⁵⁸, R. Dhullipudi^{25,n}, A. Di Ciaccio^{133a,133b}, L. Di Ciaccio⁵,
 C. Di Donato^{102a,102b}, A. Di Girolamo³⁰, B. Di Girolamo³⁰, S. Di Luise^{134a,134b},
 A. Di Mattia¹⁵², B. Di Micco³⁰, R. Di Nardo⁴⁷, A. Di Simone^{133a,133b}, R. Di Sipio^{20a,20b},

M.A. Diaz^{32a}, E.B. Diehl⁸⁷, J. Dietrich⁴², T.A. Dietzsch^{58a}, S. Diglio⁸⁶,
K. Dindar Yagci⁴⁰, J. Dingfelder²¹, F. Dinut^{26a}, C. Dionisi^{132a,132b}, P. Dita^{26a}, S. Dita^{26a},
F. Dittus³⁰, F. Djama⁸³, T. Djobava^{51b}, M.A.B. do Vale^{24c}, A. Do Valle Wemans^{124a,o},
T.K.O. Doan⁵, M. Dobbs⁸⁵, D. Dobos³⁰, E. Dobson^{30,p}, J. Dodd³⁵, C. Doglioni⁴⁹,
T. Doherty⁵³, Y. Doi^{65,*}, J. Dolejsi¹²⁷, Z. Dolezal¹²⁷, B.A. Dolgoshein^{96,*}, T. Dohmae¹⁵⁵,
M. Donadelli^{24d}, J. Donini³⁴, J. Dopke³⁰, A. Doria^{102a}, A. Dos Anjos¹⁷³, A. Dotti^{122a,122b},
M.T. Dova⁷⁰, A.D. Doxiadis¹⁰⁵, A.T. Doyle⁵³, N. Dressnandt¹²⁰, M. Dris¹⁰, J. Dubbert⁹⁹,
S. Dube¹⁵, E. Duchovni¹⁷², G. Duckeck⁹⁸, D. Duda¹⁷⁵, A. Dudarev³⁰, F. Dudziak⁶³,
M. Dührssen³⁰, I.P. Duerdoth⁸², L. Dufflot¹¹⁵, M-A. Dufour⁸⁵, L. Duguid⁷⁶,
M. Dunford^{58a}, H. Duran Yildiz^{4a}, R. Duxfield¹³⁹, M. Dwuznik³⁸, M. Düren⁵²,
W.L. Ebenstein⁴⁵, J. Ebke⁹⁸, S. Eckweiler⁸¹, K. Edmonds⁸¹, W. Edson², C.A. Edwards⁷⁶,
N.C. Edwards⁵³, W. Ehrenfeld⁴², T. Eifert¹⁴³, G. Eigen¹⁴, K. Einsweiler¹⁵,
E. Eisenhandler⁷⁵, T. Ekelof¹⁶⁶, M. El Kacimi^{135c}, M. Ellert¹⁶⁶, S. Elles⁵, F. Ellinghaus⁸¹,
K. Ellis⁷⁵, N. Ellis³⁰, J. Elmsheuser⁹⁸, M. Elsing³⁰, D. Emelianov¹²⁹, R. Engelmann¹⁴⁸,
A. Engl⁹⁸, B. Epp⁶¹, J. Erdmann¹⁷⁶, A. Ereditato¹⁷, D. Eriksson^{146a}, J. Ernst²,
M. Ernst²⁵, J. Ernwein¹³⁶, D. Errede¹⁶⁵, S. Errede¹⁶⁵, E. Ertel⁸¹, M. Escalier¹¹⁵,
H. Esch⁴³, C. Escobar¹²³, X. Espinal Curull¹², B. Esposito⁴⁷, F. Etienne⁸³,
A.I. Etievre¹³⁶, E. Etzion¹⁵³, D. Evangelakou⁵⁴, H. Evans⁶⁰, L. Fabbri^{20a,20b}, C. Fabre³⁰,
R.M. Fakhrutdinov¹²⁸, S. Falciano^{132a}, Y. Fang^{33a}, M. Fanti^{89a,89b}, A. Farbin⁸,
A. Farilla^{134a}, J. Farley¹⁴⁸, T. Farooque¹⁵⁸, S. Farrell¹⁶³, S.M. Farrington¹⁷⁰,
P. Farthouat³⁰, F. Fassi¹⁶⁷, P. Fassnacht³⁰, D. Fassouliotis⁹, B. Fatholahzadeh¹⁵⁸,
A. Favareto^{89a,89b}, L. Fayard¹¹⁵, S. Fazio^{37a,37b}, P. Federic^{144a}, O.L. Fedin¹²¹,
W. Fedorko⁸⁸, M. Fehling-Kaschek⁴⁸, L. Feligioni⁸³, C. Feng^{33d}, E.J. Feng⁶,
A.B. Fenyuk¹²⁸, J. Ferencei^{144b}, W. Fernando⁶, S. Ferrag⁵³, J. Ferrando⁵³, V. Ferrara⁴²,
A. Ferrari¹⁶⁶, P. Ferrari¹⁰⁵, R. Ferrari^{119a}, D.E. Ferreira de Lima⁵³, A. Ferrer¹⁶⁷,
D. Ferrere⁴⁹, C. Ferretti⁸⁷, A. Ferretto Parodi^{50a,50b}, M. Fiascaris³¹, F. Fiedler⁸¹,
A. Filipčič⁷⁴, F. Filthaut¹⁰⁴, M. Fincke-Keeler¹⁶⁹, M.C.N. Fiolhais^{124a,i}, L. Fiorini¹⁶⁷,
A. Firan⁴⁰, G. Fischer⁴², M.J. Fisher¹⁰⁹, M. Flechl⁴⁸, I. Fleck¹⁴¹, J. Fleckner⁸¹,
P. Fleischmann¹⁷⁴, S. Fleischmann¹⁷⁵, T. Flick¹⁷⁵, A. Floderus⁷⁹, L.R. Flores Castillo¹⁷³,
A.C. Florez Bustos^{159b}, M.J. Flowerdew⁹⁹, T. Fonseca Martin¹⁷, A. Formica¹³⁶,
A. Forti⁸², D. Fortin^{159a}, D. Fournier¹¹⁵, A.J. Fowler⁴⁵, H. Fox⁷¹, P. Francavilla¹²,
M. Franchini^{20a,20b}, S. Franchino^{119a,119b}, D. Francis³⁰, T. Frank¹⁷², M. Franklin⁵⁷,
S. Franz³⁰, M. Fraternali^{119a,119b}, S. Fratina¹²⁰, S.T. French²⁸, C. Friedrich⁴²,
F. Friedrich⁴⁴, D. Froidevaux³⁰, J.A. Frost²⁸, C. Fukunaga¹⁵⁶, E. Fullana Torregrosa¹²⁷,
B.G. Fulsom¹⁴³, J. Fuster¹⁶⁷, C. Gabaldon³⁰, O. Gabizon¹⁷², T. Gadfort²⁵,
S. Gadomski⁴⁹, G. Gagliardi^{50a,50b}, P. Gagnon⁶⁰, C. Galea⁹⁸, B. Galhardo^{124a},
E.J. Gallas¹¹⁸, V. Gallo¹⁷, B.J. Gallop¹²⁹, P. Gallus¹²⁵, K.K. Gan¹⁰⁹, Y.S. Gao^{143,g},
A. Gaponenko¹⁵, F. Garbersen¹⁷⁶, M. Garcia-Sciveres¹⁵, C. García¹⁶⁷,
J.E. García Navarro¹⁶⁷, R.W. Gardner³¹, N. Garelli³⁰, H. Garitaonandia¹⁰⁵,
V. Garonne³⁰, C. Gatti⁴⁷, G. Gaudio^{119a}, B. Gaur¹⁴¹, L. Gauthier¹³⁶, P. Gauzzi^{132a,132b},
I.L. Gavrilenko⁹⁴, C. Gay¹⁶⁸, G. Gaycken²¹, E.N. Gazis¹⁰, P. Ge^{33d}, Z. Gecse¹⁶⁸,
C.N.P. Gee¹²⁹, D.A.A. Geerts¹⁰⁵, Ch. Geich-Gimbel²¹, K. Gellerstedt^{146a,146b},
C. Gemme^{50a}, A. Gemmell⁵³, M.H. Genest⁵⁵, S. Gentile^{132a,132b}, M. George⁵⁴,

S. George⁷⁶, D. Gerbaudo¹², P. Gerlach¹⁷⁵, A. Gershon¹⁵³, C. Geweniger^{58a},
 H. Ghazlane^{135b}, N. Ghodbane³⁴, B. Giacobbe^{20a}, S. Giagu^{132a,132b}, V. Giangiobbe¹²,
 F. Gianotti³⁰, B. Gibbard²⁵, A. Gibson¹⁵⁸, S.M. Gibson³⁰, M. Gilchriese¹⁵, D. Gillberg²⁹,
 A.R. Gillman¹²⁹, D.M. Gingrich^{3,f}, J. Ginzburg¹⁵³, N. Giokaris⁹, M.P. Giordani^{164c},
 R. Giordano^{102a,102b}, F.M. Giorgi¹⁶, P. Giovannini⁹⁹, P.F. Giraud¹³⁶, D. Giugni^{89a},
 M. Giunta⁹³, B.K. Gjelsten¹¹⁷, L.K. Gladilin⁹⁷, C. Glasman⁸⁰, J. Glatzer²¹, A. Glazov⁴²,
 K.W. Glitza¹⁷⁵, G.L. Glonti⁶⁴, J.R. Goddard⁷⁵, J. Godfrey¹⁴², J. Godlewski³⁰,
 M. Goebel⁴², T. Göpfert⁴⁴, C. Goeringer⁸¹, C. Gössling⁴³, S. Goldfarb⁸⁷, T. Golling¹⁷⁶,
 D. Golubkov¹²⁸, A. Gomes^{124a,c}, L.S. Gomez Fajardo⁴², R. Gonçalo⁷⁶,
 J. Goncalves Pinto Firmino Da Costa⁴², L. Gonella²¹, S. González de la Hoz¹⁶⁷,
 G. Gonzalez Parra¹², M.L. Gonzalez Silva²⁷, S. Gonzalez-Sevilla⁴⁹, J.J. Goodson¹⁴⁸,
 L. Goossens³⁰, P.A. Gorbounov⁹⁵, H.A. Gordon²⁵, I. Gorelov¹⁰³, G. Gorfine¹⁷⁵,
 B. Gorini³⁰, E. Gorini^{72a,72b}, A. Gorišek⁷⁴, E. Gornicki³⁹, A.T. Goshaw⁶, M. Gosselink¹⁰⁵,
 M.I. Gostkin⁶⁴, I. Gough Eschrich¹⁶³, M. Gouighri^{135a}, D. Goujdami^{135c}, M.P. Goulette⁴⁹,
 A.G. Goussiou¹³⁸, C. Goy⁵, S. Gozpinar²³, I. Grabowska-Bold³⁸, P. Grafström^{20a,20b},
 K.-J. Grahn⁴², E. Gramstad¹¹⁷, F. Grancagnolo^{72a}, S. Grancagnolo¹⁶, V. Grassi¹⁴⁸,
 V. Gratchev¹²¹, N. Grau³⁵, H.M. Gray³⁰, J.A. Gray¹⁴⁸, E. Graziani^{134a},
 O.G. Grebenyuk¹²¹, T. Greenshaw⁷³, Z.D. Greenwood^{25,n}, K. Gregersen³⁶, I.M. Gregor⁴²,
 P. Grenier¹⁴³, J. Griffiths⁸, N. Grigalashvili⁶⁴, A.A. Grillo¹³⁷, S. Grinstein¹², Ph. Gris³⁴,
 Y.V. Grishkevich⁹⁷, J.-F. Grivaz¹¹⁵, E. Gross¹⁷², J. Grosse-Knetter⁵⁴, J. Groth-Jensen¹⁷²,
 K. Grybel¹⁴¹, D. Guest¹⁷⁶, C. Guicheney³⁴, E. Guido^{50a,50b}, S. Guindon⁵⁴, U. Gul⁵³,
 J. Gunther¹²⁵, B. Guo¹⁵⁸, J. Guo³⁵, P. Gutierrez¹¹¹, N. Guttman¹⁵³, O. Gutzwiller¹⁷³,
 C. Guyot¹³⁶, C. Gwenlan¹¹⁸, C.B. Gwilliam⁷³, A. Haas¹⁰⁸, S. Haas³⁰, C. Haber¹⁵,
 H.K. Hadavand⁸, D.R. Hadley¹⁸, P. Haefner²¹, F. Hahn³⁰, Z. Hajduk³⁹, H. Hakobyan¹⁷⁷,
 D. Hall¹¹⁸, K. Hamacher¹⁷⁵, P. Hamal¹¹³, K. Hamano⁸⁶, M. Hamer⁵⁴, A. Hamilton^{145b,q},
 S. Hamilton¹⁶¹, L. Han^{33b}, K. Hanagaki¹¹⁶, K. Hanawa¹⁶⁰, M. Hance¹⁵, C. Handel⁸¹,
 P. Hanke^{58a}, J.R. Hansen³⁶, J.B. Hansen³⁶, J.D. Hansen³⁶, P.H. Hansen³⁶, P. Hansson¹⁴³,
 K. Hara¹⁶⁰, T. Harenberg¹⁷⁵, S. Harkusha⁹⁰, D. Harper⁸⁷, R.D. Harrington⁴⁶,
 O.M. Harris¹³⁸, J. Hartert⁴⁸, F. Hartjes¹⁰⁵, T. Haruyama⁶⁵, A. Harvey⁵⁶, S. Hasegawa¹⁰¹,
 Y. Hasegawa¹⁴⁰, S. Hassani¹³⁶, S. Haug¹⁷, M. Hauschild³⁰, R. Hauser⁸⁸, M. Havranek²¹,
 C.M. Hawkes¹⁸, R.J. Hawkings³⁰, A.D. Hawkins⁷⁹, T. Hayakawa⁶⁶, T. Hayashi¹⁶⁰,
 D. Hayden⁷⁶, C.P. Hays¹¹⁸, H.S. Hayward⁷³, S.J. Haywood¹²⁹, S.J. Head¹⁸, V. Hedberg⁷⁹,
 L. Heelan⁸, S. Heim¹²⁰, B. Heinemann¹⁵, S. Heisterkamp³⁶, L. Helary²², C. Heller⁹⁸,
 M. Heller³⁰, S. Hellman^{146a,146b}, D. Hellmich²¹, C. Hensens¹², R.C.W. Henderson⁷¹,
 M. Henke^{58a}, A. Henrichs¹⁷⁶, A.M. Henriques Correia³⁰, S. Henrot-Versille¹¹⁵,
 C. Hensel⁵⁴, C.M. Hernandez⁸, Y. Hernández Jiménez¹⁶⁷, R. Herrberg¹⁶, G. Herten⁴⁸,
 R. Hertenberger⁹⁸, L. Hervas³⁰, G.G. Hesketh⁷⁷, N.P. Hessey¹⁰⁵, E. Higón-Rodriguez¹⁶⁷,
 J.C. Hill²⁸, K.H. Hiller⁴², S. Hillert²¹, S.J. Hillier¹⁸, I. Hinchliffe¹⁵, E. Hines¹²⁰,
 M. Hirose¹¹⁶, F. Hirsch⁴³, D. Hirschbuehl¹⁷⁵, J. Hobbs¹⁴⁸, N. Hod¹⁵³,
 M.C. Hodgkinson¹³⁹, P. Hodgson¹³⁹, A. Hoecker³⁰, M.R. Hoferkamp¹⁰³, J. Hoffman⁴⁰,
 D. Hoffmann⁸³, M. Hohlfeld⁸¹, M. Holder¹⁴¹, S.O. Holmgren^{146a}, T. Holy¹²⁶,
 J.L. Holzbauer⁸⁸, T.M. Hong¹²⁰, L. Hooft van Huysduynen¹⁰⁸, S. Horner⁴⁸,
 J.-Y. Hostachy⁵⁵, S. Hou¹⁵¹, A. Hoummada^{135a}, J. Howard¹¹⁸, J. Howarth⁸², I. Hristova¹⁶,

J. Hrivnac¹¹⁵, T. Hryn'ova⁵, P.J. Hsu⁸¹, S.-C. Hsu¹³⁸, D. Hu³⁵, Z. Hubacek¹²⁶,
 F. Hubaut⁸³, F. Huegging²¹, A. Huettmann⁴², T.B. Huffman¹¹⁸, E.W. Hughes³⁵,
 G. Hughes⁷¹, M. Huhtinen³⁰, M. Hurwitz¹⁵, N. Huseynov^{64,r}, J. Huston⁸⁸, J. Huth⁵⁷,
 G. Iacobucci⁴⁹, G. Iakovidis¹⁰, M. Ibbotson⁸², I. Ibragimov¹⁴¹, L. Iconomidou-Fayard¹¹⁵,
 J. Idarraga¹¹⁵, P. Iengo^{102a}, O. Igonkina¹⁰⁵, Y. Ikegami⁶⁵, M. Ikeno⁶⁵, D. Iliadis¹⁵⁴,
 N. Ilic¹⁵⁸, T. Ince⁹⁹, P. Ioannou⁹, M. Iodice^{134a}, K. Iordanidou⁹, V. Ippolito^{132a,132b},
 A. Irls Quiles¹⁶⁷, C. Isaksson¹⁶⁶, M. Ishino⁶⁷, M. Ishitsuka¹⁵⁷, R. Ishmukhametov¹⁰⁹,
 C. Issever¹¹⁸, S. Istin^{19a}, A.V. Ivashin¹²⁸, W. Iwanski³⁹, H. Iwasaki⁶⁵, J.M. Izen⁴¹,
 V. Izzo^{102a}, B. Jackson¹²⁰, J.N. Jackson⁷³, P. Jackson¹, M.R. Jaekel³⁰, V. Jain²,
 K. Jakobs⁴⁸, S. Jakobsen³⁶, T. Jakoubek¹²⁵, J. Jakubek¹²⁶, D.O. Jamin¹⁵¹, D.K. Jana¹¹¹,
 E. Jansen⁷⁷, H. Jansen³⁰, J. Janssen²¹, A. Jantsch⁹⁹, M. Janus⁴⁸, R.C. Jared¹⁷³,
 G. Jarlskog⁷⁹, L. Jeanty⁵⁷, I. Jen-La Plante³¹, D. Jennens⁸⁶, P. Jenni³⁰,
 A.E. Loevschall-Jensen³⁶, P. Jež³⁶, S. Jézéquel⁵, M.K. Jha^{20a}, H. Ji¹⁷³, W. Ji⁸¹, J. Jia¹⁴⁸,
 Y. Jiang^{33b}, M. Jimenez Belenguer⁴², S. Jin^{33a}, O. Jinnouchi¹⁵⁷, M.D. Joergensen³⁶,
 D. Joffe⁴⁰, M. Johansen^{146a,146b}, K.E. Johansson^{146a}, P. Johansson¹³⁹, S. Johnert⁴²,
 K.A. Johns⁷, K. Jon-And^{146a,146b}, G. Jones¹⁷⁰, R.W.L. Jones⁷¹, T.J. Jones⁷³, C. Joram³⁰,
 P.M. Jorge^{124a}, K.D. Joshi⁸², J. Jovicevic¹⁴⁷, T. Jovin^{13b}, X. Ju¹⁷³, C.A. Jung⁴³,
 R.M. Jungst³⁰, V. Juranek¹²⁵, P. Jussel⁶¹, A. Juste Rozas¹², S. Kabana¹⁷, M. Kaci¹⁶⁷,
 A. Kaczmarska³⁹, P. Kadlecik³⁶, M. Kado¹¹⁵, H. Kagan¹⁰⁹, M. Kagan⁵⁷,
 E. Kajomovitz¹⁵², S. Kalinin¹⁷⁵, L.V. Kalinovskaya⁶⁴, S. Kama⁴⁰, N. Kanaya¹⁵⁵,
 M. Kaneda³⁰, S. Kaneti²⁸, T. Kanno¹⁵⁷, V.A. Kantserov⁹⁶, J. Kanzaki⁶⁵, B. Kaplan¹⁰⁸,
 A. Kapliy³¹, J. Kaplon³⁰, D. Kar⁵³, M. Karagounis²¹, K. Karakostas¹⁰, M. Karneviskiy^{58b},
 V. Kartvelishvili⁷¹, A.N. Karyukhin¹²⁸, L. Kashif¹⁷³, G. Kasieczka^{58b}, R.D. Kass¹⁰⁹,
 A. Kastanas¹⁴, M. Kataoka⁵, Y. Kataoka¹⁵⁵, J. Katzy⁴², V. Kaushik⁷, K. Kawagoe⁶⁹,
 T. Kawamoto¹⁵⁵, G. Kawamura⁸¹, M.S. Kayl¹⁰⁵, S. Kazama¹⁵⁵, V.F. Kazanin¹⁰⁷,
 M.Y. Kazarinov⁶⁴, R. Keeler¹⁶⁹, P.T. Keener¹²⁰, R. Kehoe⁴⁰, M. Keil⁵⁴, G.D. Kekelidze⁶⁴,
 J.S. Keller¹³⁸, M. Kenyon⁵³, O. Kepka¹²⁵, N. Kerschen³⁰, B.P. Kerševan⁷⁴, S. Kersten¹⁷⁵,
 K. Kessoku¹⁵⁵, J. Keung¹⁵⁸, F. Khalil-zada¹¹, H. Khandanyan^{146a,146b}, A. Khanov¹¹²,
 D. Kharchenko⁶⁴, A. Khodinov⁹⁶, A. Khomich^{58a}, T.J. Khoo²⁸, G. Khoraiuli²¹,
 A. Khoroshilov¹⁷⁵, V. Khovanskiy⁹⁵, E. Khramov⁶⁴, J. Klubua^{51b}, H. Kim^{146a,146b},
 S.H. Kim¹⁶⁰, N. Kimura¹⁷¹, O. Kind¹⁶, B.T. King⁷³, M. King⁶⁶, R.S.B. King¹¹⁸,
 J. Kirk¹²⁹, A.E. Kiryunin⁹⁹, T. Kishimoto⁶⁶, D. Kisielewska³⁸, T. Kitamura⁶⁶,
 T. Kittelmann¹²³, K. Kiuchi¹⁶⁰, E. Kladiva^{144b}, M. Klein⁷³, U. Klein⁷³, K. Kleinknecht⁸¹,
 M. Klemetti⁸⁵, A. Klier¹⁷², P. Klimek^{146a,146b}, A. Klimentov²⁵, R. Klingenberg⁴³,
 J.A. Klinger⁸², E.B. Klinkby³⁶, T. Klioutchnikova³⁰, P.F. Klok¹⁰⁴, S. Klous¹⁰⁵,
 E.-E. Kluge^{58a}, T. Kluge⁷³, P. Kluit¹⁰⁵, S. Kluth⁹⁹, E. Kneringer⁶¹, E.B.F.G. Knoops⁸³,
 A. Knue⁵⁴, B.R. Ko⁴⁵, T. Kobayashi¹⁵⁵, M. Kobel⁴⁴, M. Kocian¹⁴³, P. Kodys¹²⁷,
 K. Köneke³⁰, A.C. König¹⁰⁴, S. Koenig⁸¹, L. Köpke⁸¹, F. Koetsveld¹⁰⁴, P. Koevesarki²¹,
 T. Koffas²⁹, E. Koffeman¹⁰⁵, L.A. Kogan¹¹⁸, S. Kohlmann¹⁷⁵, F. Kohn⁵⁴, Z. Kohout¹²⁶,
 T. Kohriki⁶⁵, T. Koi¹⁴³, G.M. Kolachev^{107,*}, H. Kolanoski¹⁶, V. Kolesnikov⁶⁴,
 I. Koletsou^{89a}, J. Koll⁸⁸, A.A. Komar⁹⁴, Y. Komori¹⁵⁵, T. Kondo⁶⁵, T. Kono^{42,s},
 A.I. Kononov⁴⁸, R. Konoplich^{108,t}, N. Konstantinidis⁷⁷, R. Kopeliansky¹⁵², S. Koperny³⁸,
 K. Korcyl³⁹, K. Kordas¹⁵⁴, A. Korn¹¹⁸, A. Korol¹⁰⁷, I. Korolkov¹², E.V. Korolkova¹³⁹,

V.A. Korotkov¹²⁸, O. Kortner⁹⁹, S. Kortner⁹⁹, V.V. Kostyukhin²¹, S. Kotov⁹⁹,
 V.M. Kotov⁶⁴, A. Kotwal⁴⁵, C. Kourkouvelis⁹, V. Kouskoura¹⁵⁴, A. Koutsman^{159a},
 R. Kowalewski¹⁶⁹, T.Z. Kowalski³⁸, W. Kozanecki¹³⁶, A.S. Kozhin¹²⁸, V. Kral¹²⁶,
 V.A. Kramarenko⁹⁷, G. Kramberger⁷⁴, M.W. Krasny⁷⁸, A. Krasznahorkay¹⁰⁸,
 J.K. Kraus²¹, A. Kravchenko²⁵, S. Kreiss¹⁰⁸, F. Krejci¹²⁶, J. Kretzschmar⁷³,
 K. Kreutzfeldt⁵², N. Krieger⁵⁴, P. Krieger¹⁵⁸, K. Kroeninger⁵⁴, H. Kroha⁹⁹, J. Kroll¹²⁰,
 J. Kroseberg²¹, J. Krstic^{13a}, U. Kruchonak⁶⁴, H. Krüger²¹, T. Kruker¹⁷, N. Krumnack⁶³,
 Z.V. Krumshteyn⁶⁴, M.K. Kruse⁴⁵, T. Kubota⁸⁶, S. Kудay^{4a}, S. Kuehn⁴⁸, A. Kugel^{58c},
 T. Kuhl⁴², D. Kuhn⁶¹, V. Kukhtin⁶⁴, Y. Kulchitsky⁹⁰, S. Kuleshov^{32b}, C. Kummer⁹⁸,
 M. Kuna⁷⁸, J. Kunkle¹²⁰, A. Kupco¹²⁵, H. Kurashige⁶⁶, M. Kurata¹⁶⁰, Y.A. Kurochkin⁹⁰,
 V. Kus¹²⁵, E.S. Kuwertz¹⁴⁷, M. Kuze¹⁵⁷, J. Kvitá¹⁴², R. Kwee¹⁶, A. La Rosa⁴⁹,
 L. La Rotonda^{37a,37b}, L. Labarga⁸⁰, S. Lablak^{135a}, C. Lacasta¹⁶⁷, F. Lacava^{132a,132b},
 J. Lacey²⁹, H. Lacker¹⁶, D. Lacour⁷⁸, V.R. Lacuesta¹⁶⁷, E. Ladygin⁶⁴, R. Lafaye⁵,
 B. Laforge⁷⁸, T. Lagouri¹⁷⁶, S. Lai⁴⁸, E. Laisne⁵⁵, L. Lambourne⁷⁷, C.L. Lampen⁷,
 W. Lampl⁷, E. Lancon¹³⁶, U. Landgraf⁴⁸, M.P.J. Landon⁷⁵, V.S. Lang^{58a}, C. Lange⁴²,
 A.J. Lankford¹⁶³, F. Lanni²⁵, K. Lantzschi¹⁷⁵, A. Lanza^{119a}, S. Laplace⁷⁸, C. Lapoire²¹,
 J.F. Laporte¹³⁶, T. Lari^{89a}, A. Larner¹¹⁸, M. Lassnig³⁰, P. Laurelli⁴⁷, V. Lavorini^{37a,37b},
 W. Lavrijsen¹⁵, P. Laycock⁷³, O. Le Dortz⁷⁸, E. Le Guirriec⁸³, E. Le Menedeu¹²,
 T. LeCompte⁶, F. Ledroit-Guillon⁵⁵, H. Lee¹⁰⁵, J.S.H. Lee¹¹⁶, S.C. Lee¹⁵¹, L. Lee¹⁷⁶,
 M. Lefebvre¹⁶⁹, M. Legendre¹³⁶, F. Legger⁹⁸, C. Leggett¹⁵, M. Lehmacher²¹,
 G. Lehmann Miotto³⁰, A.G. Leister¹⁷⁶, M.A.L. Leite^{24d}, R. Leitner¹²⁷, D. Lellouch¹⁷²,
 B. Lemmer⁵⁴, V. Lendermann^{58a}, K.J.C. Leney^{145b}, T. Lenz¹⁰⁵, G. Lenzen¹⁷⁵, B. Lenzi³⁰,
 K. Leonhardt⁴⁴, S. Leontsinis¹⁰, F. Lepold^{58a}, C. Leroy⁹³, J-R. Lessard¹⁶⁹, C.G. Lester²⁸,
 C.M. Lester¹²⁰, J. Levêque⁵, D. Levin⁸⁷, L.J. Levinson¹⁷², A. Lewis¹¹⁸, G.H. Lewis¹⁰⁸,
 A.M. Leyko²¹, M. Leyton¹⁶, B. Li^{33b}, B. Li⁸³, H. Li¹⁴⁸, H.L. Li³¹, S. Li^{33b,u}, X. Li⁸⁷,
 Z. Liang^{118,v}, H. Liao³⁴, B. Liberti^{133a}, P. Lichard³⁰, M. Lichtnecker⁹⁸, K. Lie¹⁶⁵,
 W. Liebig¹⁴, C. Limbach²¹, A. Limosani⁸⁶, M. Limper⁶², S.C. Lin^{151,w}, F. Linde¹⁰⁵,
 J.T. Linnemann⁸⁸, E. Lipeles¹²⁰, A. Lipniacka¹⁴, T.M. Liss¹⁶⁵, D. Lissauer²⁵, A. Lister⁴⁹,
 A.M. Litke¹³⁷, C. Liu²⁹, D. Liu¹⁵¹, J.B. Liu⁸⁷, L. Liu⁸⁷, M. Liu^{33b}, Y. Liu^{33b},
 M. Livan^{119a,119b}, S.S.A. Livermore¹¹⁸, A. Lleres⁵⁵, J. Llorente Merino⁸⁰, S.L. Lloyd⁷⁵,
 E. Lobodzinska⁴², P. Loch⁷, W.S. Lockman¹³⁷, T. Loddenkoetter²¹, F.K. Loebinger⁸²,
 A. Loginov¹⁷⁶, C.W. Loh¹⁶⁸, T. Lohse¹⁶, K. Lohwasser⁴⁸, M. Lokajicek¹²⁵,
 V.P. Lombardo⁵, R.E. Long⁷¹, L. Lopes^{124a}, D. Lopez Mateos⁵⁷, J. Lorenz⁹⁸,
 N. Lorenzo Martinez¹¹⁵, M. Losada¹⁶², P. Loscutoff¹⁵, F. Lo Sterzo^{132a,132b},
 M.J. Losty^{159a,*}, X. Lou⁴¹, A. Lounis¹¹⁵, K.F. Loureiro¹⁶², J. Love⁶, P.A. Love⁷¹,
 A.J. Lowe^{143.g}, F. Lu^{33a}, H.J. Lubatti¹³⁸, C. Luci^{132a,132b}, A. Lucotte⁵⁵, A. Ludwig⁴⁴,
 D. Ludwig⁴², I. Ludwig⁴⁸, J. Ludwig⁴⁸, F. Luehring⁶⁰, G. Luijckx¹⁰⁵, W. Lukas⁶¹,
 L. Luminari^{132a}, E. Lund¹¹⁷, B. Lund-Jensen¹⁴⁷, B. Lundberg⁷⁹, J. Lundberg^{146a,146b},
 O. Lundberg^{146a,146b}, J. Lundquist³⁶, M. Lungwitz⁸¹, D. Lynn²⁵, E. Lytken⁷⁹, H. Ma²⁵,
 L.L. Ma¹⁷³, G. Maccarrone⁴⁷, A. Macchiolo⁹⁹, B. Maček⁷⁴, J. Machado Miguens^{124a},
 D. Macina³⁰, R. Mackeprang³⁶, R.J. Madaras¹⁵, H.J. Maddocks⁷¹, W.F. Mader⁴⁴,
 R. Maenner^{58c}, T. Maeno²⁵, P. Mättig¹⁷⁵, S. Mättig⁴², L. Magnoni¹⁶³, E. Magradze⁵⁴,
 K. Mahboubi⁴⁸, J. Mahlstedt¹⁰⁵, S. Mahmoud⁷³, G. Mahout¹⁸, C. Maiani¹³⁶,

C. Maidantchik^{24a}, A. Maio^{124a,c}, S. Majewski²⁵, Y. Makida⁶⁵, N. Makovec¹¹⁵, P. Mal¹³⁶,
 B. Malaescu³⁰, Pa. Malecki³⁹, P. Malecki³⁹, V.P. Maleev¹²¹, F. Malek⁵⁵, U. Mallik⁶²,
 D. Malon⁶, C. Malone¹⁴³, S. Maltezos¹⁰, V. Malyshev¹⁰⁷, S. Malyukov³⁰, J. Mamuzic^{13b},
 A. Manabe⁶⁵, L. Mandelli^{89a}, I. Mandić⁷⁴, R. Mandrysch⁶², J. Maneira^{124a},
 A. Manfredini⁹⁹, L. Manhaes de Andrade Filho^{24b}, J.A. Manjarres Ramos¹³⁶, A. Mann⁹⁸,
 P.M. Manning¹³⁷, A. Manousakis-Katsikakis⁹, B. Mansoulie¹³⁶, A. Mapelli³⁰,
 L. Mapelli³⁰, L. March¹⁶⁷, J.F. Marchand²⁹, F. Marchese^{133a,133b}, G. Marchiori⁷⁸,
 M. Marcisovsky¹²⁵, C.P. Marino¹⁶⁹, F. Marroquim^{24a}, Z. Marshall³⁰, L.F. Marti¹⁷,
 S. Marti-Garcia¹⁶⁷, B. Martin³⁰, B. Martin⁸⁸, J.P. Martin⁹³, T.A. Martin¹⁸,
 V.J. Martin⁴⁶, B. Martin dit Latour⁴⁹, S. Martin-Haugh¹⁴⁹, M. Martinez¹²,
 V. Martinez Outschoorn⁵⁷, A.C. Martyniuk¹⁶⁹, M. Marx⁸², F. Marzano^{132a}, A. Marzin¹¹¹,
 L. Masetti⁸¹, T. Mashimo¹⁵⁵, R. Mashinistov⁹⁴, J. Masik⁸², A.L. Maslennikov¹⁰⁷,
 I. Massa^{20a,20b}, G. Massaro¹⁰⁵, N. Massol⁵, P. Mastrandrea¹⁴⁸, A. Mastroberardino^{37a,37b},
 T. Masubuchi¹⁵⁵, H. Matsunaga¹⁵⁵, T. Matsushita⁶⁶, C. Mattravers^{118,d}, J. Maurer⁸³,
 S.J. Maxfield⁷³, D.A. Maximov^{107,h}, A. Mayne¹³⁹, R. Mazini¹⁵¹, M. Mazur²¹,
 L. Mazzaferro^{133a,133b}, M. Mazzanti^{89a}, J. Mc Donald⁸⁵, S.P. Mc Kee⁸⁷, A. McCarn¹⁶⁵,
 R.L. McCarthy¹⁴⁸, T.G. McCarthy²⁹, N.A. McCubbin¹²⁹, K.W. McFarlane^{56,*},
 J.A. MCFayden¹³⁹, G. Mchedlize^{51b}, T. McLaughlan¹⁸, S.J. McMahon¹²⁹,
 R.A. McPherson^{169,l}, A. Meade⁸⁴, J. Mechnich¹⁰⁵, M. Mechtel¹⁷⁵, M. Medinnis⁴²,
 S. Meehan³¹, R. Meera-Lebbai¹¹¹, T. Meguro¹¹⁶, S. Mehlhase³⁶, A. Mehta⁷³, K. Meier^{58a},
 B. Meirose⁷⁹, C. Melachrinou³¹, B.R. Mellado Garcia¹⁷³, F. Meloni^{89a,89b},
 L. Mendoza Navas¹⁶², Z. Meng^{151,x}, A. Mengarelli^{20a,20b}, S. Menke⁹⁹, E. Meoni¹⁶¹,
 K.M. Mercurio⁵⁷, P. Mermod⁴⁹, L. Merola^{102a,102b}, C. Meroni^{89a}, F.S. Merritt³¹,
 H. Merritt¹⁰⁹, A. Messina^{30,y}, J. Metcalfe²⁵, A.S. Mete¹⁶³, C. Meyer⁸¹, C. Meyer³¹,
 J-P. Meyer¹³⁶, J. Meyer¹⁷⁴, J. Meyer⁵⁴, S. Michal³⁰, L. Micu^{26a}, R.P. Middleton¹²⁹,
 S. Migas⁷³, L. Mijović¹³⁶, G. Mikenberg¹⁷², M. Mikestikova¹²⁵, M. Mikuz⁷⁴,
 D.W. Miller³¹, R.J. Miller⁸⁸, W.J. Mills¹⁶⁸, C. Mills⁵⁷, A. Milov¹⁷²,
 D.A. Milstead^{146a,146b}, D. Milstein¹⁷², A.A. Minaenko¹²⁸, M. Miñano Moya¹⁶⁷,
 I.A. Minashvili⁶⁴, A.I. Mincer¹⁰⁸, B. Mindur³⁸, M. Mineev⁶⁴, Y. Ming¹⁷³, L.M. Mir¹²,
 G. Mirabelli^{132a}, J. Mitrevski¹³⁷, V.A. Mitsou¹⁶⁷, S. Mitsui⁶⁵, P.S. Miyagawa¹³⁹,
 J.U. Mjörnmark⁷⁹, T. Moa^{146a,146b}, V. Moeller²⁸, K. Mönig⁴², N. Möser²¹,
 S. Mohapatra¹⁴⁸, W. Mohr⁴⁸, R. Moles-Valls¹⁶⁷, A. Molfetas³⁰, J. Monk⁷⁷, E. Monnier⁸³,
 J. Montejo Berlingen¹², F. Monticelli⁷⁰, S. Monzani^{20a,20b}, R.W. Moore³,
 G.F. Moorhead⁸⁶, C. Mora Herrera⁴⁹, A. Moraes⁵³, N. Morange¹³⁶, J. Morel⁵⁴,
 G. Morello^{37a,37b}, D. Moreno⁸¹, M. Moreno Llácer¹⁶⁷, P. Morettini^{50a}, M. Morgenstern⁴⁴,
 M. Morii⁵⁷, A.K. Morley³⁰, G. Mornacchi³⁰, J.D. Morris⁷⁵, L. Morvaj¹⁰¹, H.G. Moser⁹⁹,
 M. Mosidze^{51b}, J. Moss¹⁰⁹, R. Mount¹⁴³, E. Mountricha^{10,z}, S.V. Mouraviev^{94,*},
 E.J.W. Moyse⁸⁴, F. Mueller^{58a}, J. Mueller¹²³, K. Mueller²¹, T.A. Müller⁹⁸, T. Mueller⁸¹,
 D. Muenstermann³⁰, Y. Munwes¹⁵³, W.J. Murray¹²⁹, I. Mussche¹⁰⁵, E. Musto¹⁵²,
 A.G. Myagkov¹²⁸, M. Myska¹²⁵, O. Nackenhorst⁵⁴, J. Nadal¹², K. Nagai¹⁶⁰, R. Nagai¹⁵⁷,
 K. Nagano⁶⁵, A. Nagarkar¹⁰⁹, Y. Nagasaka⁵⁹, M. Nagel⁹⁹, A.M. Nairz³⁰, Y. Nakahama³⁰,
 K. Nakamura¹⁵⁵, T. Nakamura¹⁵⁵, I. Nakano¹¹⁰, G. Nanava²¹, A. Napier¹⁶¹,
 R. Narayan^{58b}, M. Nash^{77,d}, T. Nattermann²¹, T. Naumann⁴², G. Navarro¹⁶²,

H.A. Neal⁸⁷, P.Yu. Nechaeva⁹⁴, T.J. Neep⁸², A. Negri^{119a,119b}, G. Negri³⁰, M. Negrini^{20a},
 S. Nektarijevic⁴⁹, A. Nelson¹⁶³, T.K. Nelson¹⁴³, S. Nemecek¹²⁵, P. Nemethy¹⁰⁸,
 A.A. Nepomuceno^{24a}, M. Nessi^{30,aa}, M.S. Neubauer¹⁶⁵, M. Neumann¹⁷⁵, A. Neusiedl⁸¹,
 R.M. Neves¹⁰⁸, P. Nevski²⁵, F.M. Newcomer¹²⁰, P.R. Newman¹⁸, V. Nguyen Thi Hong¹³⁶,
 R.B. Nickerson¹¹⁸, R. Nicolaidou¹³⁶, B. Nicquevert³⁰, F. Niedercorn¹¹⁵, J. Nielsen¹³⁷,
 N. Nikiforou³⁵, A. Nikiforov¹⁶, V. Nikolaenko¹²⁸, I. Nikolic-Audit⁷⁸, K. Nikolics⁴⁹,
 K. Nikolopoulos¹⁸, H. Nilsen⁴⁸, P. Nilsson⁸, Y. Ninomiya¹⁵⁵, A. Nisati^{132a}, R. Nisius⁹⁹,
 T. Nobe¹⁵⁷, L. Nodulman⁶, M. Nomachi¹¹⁶, I. Nomidis¹⁵⁴, S. Norberg¹¹¹, M. Nordberg³⁰,
 P.R. Norton¹²⁹, J. Novakova¹²⁷, M. Nozaki⁶⁵, L. Nozka¹¹³, I.M. Nugent^{159a},
 A.-E. Nuncio-Quiroz²¹, G. Nunes Hanninger⁸⁶, T. Nunnemann⁹⁸, E. Nurse⁷⁷,
 B.J. O'Brien⁴⁶, D.C. O'Neil¹⁴², V. O'Shea⁵³, L.B. Oakes⁹⁸, F.G. Oakham^{29.f},
 H. Oberlack⁹⁹, J. Ocariz⁷⁸, A. Ochi⁶⁶, S. Oda⁶⁹, S. Odaka⁶⁵, J. Odier⁸³, H. Ogren⁶⁰,
 A. Oh⁸², S.H. Oh⁴⁵, C.C. Ohm³⁰, T. Ohshima¹⁰¹, W. Okamura¹¹⁶, H. Okawa²⁵,
 Y. Okumura³¹, T. Okuyama¹⁵⁵, A. Olariu^{26a}, A.G. Olchevski⁶⁴, S.A. Olivares Pino^{32a},
 M. Oliveira^{124a,i}, D. Oliveira Damazio²⁵, E. Oliver Garcia¹⁶⁷, D. Olivito¹²⁰,
 A. Olszewski³⁹, J. Olszowska³⁹, A. Onofre^{124a,ab}, P.U.E. Onyisi^{31,ac}, C.J. Oram^{159a},
 M.J. Oreglia³¹, Y. Oren¹⁵³, D. Orestano^{134a,134b}, N. Orlando^{72a,72b}, I. Orlov¹⁰⁷,
 C. Oropeza Barrera⁵³, R.S. Orr¹⁵⁸, B. Osculati^{50a,50b}, R. Ospanov¹²⁰, C. Osuna¹²,
 G. Otero y Garzon²⁷, J.P. Ottersbach¹⁰⁵, M. Ouchrif^{135d}, E.A. Ouellette¹⁶⁹,
 F. Ould-Saada¹¹⁷, A. Ouraou¹³⁶, Q. Ouyang^{33a}, A. Ovcharova¹⁵, M. Owen⁸², S. Owen¹³⁹,
 V.E. Ozcan^{19a}, N. Ozturk⁸, A. Pacheco Pages¹², C. Padilla Aranda¹², S. Pagan Griso¹⁵,
 E. Paganis¹³⁹, C. Pahl⁹⁹, F. Paige²⁵, P. Pais⁸⁴, K. Pajchel¹¹⁷, G. Palacino^{159b},
 C.P. Paleari⁷, S. Palestini³⁰, D. Pallin³⁴, A. Palma^{124a}, J.D. Palmer¹⁸, Y.B. Pan¹⁷³,
 E. Panagiotopoulou¹⁰, J.G. Panduro Vazquez⁷⁶, P. Pani¹⁰⁵, N. Panikashvili⁸⁷,
 S. Panitkin²⁵, D. Pantea^{26a}, A. Papadelis^{146a}, Th.D. Papadopoulou¹⁰, A. Paramonov⁶,
 D. Paredes Hernandez³⁴, W. Park^{25,ad}, M.A. Parker²⁸, F. Parodi^{50a,50b}, J.A. Parsons³⁵,
 U. Parzefall⁴⁸, S. Pashapour⁵⁴, E. Pasqualucci^{132a}, S. Passaggio^{50a}, A. Passeri^{134a},
 F. Pastore^{134a,134b,*}, Fr. Pastore⁷⁶, G. Pásztor^{49,ae}, S. Patarraia¹⁷⁵, N. Patel¹⁵⁰,
 J.R. Pater⁸², S. Patricelli^{102a,102b}, T. Pauly³⁰, M. Pecsny^{144a}, S. Pedraza Lopez¹⁶⁷,
 M.I. Pedraza Morales¹⁷³, S.V. Peleganchuk¹⁰⁷, D. Pelikan¹⁶⁶, H. Peng^{33b}, B. Penning³¹,
 A. Penson³⁵, J. Penwell⁶⁰, M. Perantoni^{24a}, K. Perez^{35,af}, T. Perez Cavalcanti⁴²,
 E. Perez Codina^{159a}, M.T. Pérez García-Estañ¹⁶⁷, V. Perez Reale³⁵, L. Perini^{89a,89b},
 H. Pernegger³⁰, R. Perrino^{72a}, P. Perrodo⁵, V.D. Peshekhonov⁶⁴, K. Peters³⁰,
 B.A. Petersen³⁰, J. Petersen³⁰, T.C. Petersen³⁶, E. Petit⁵, A. Petridis¹⁵⁴, C. Petridou¹⁵⁴,
 E. Petrolo^{132a}, F. Petrucci^{134a,134b}, D. Petschull⁴², M. Petteni¹⁴², R. Pezoa^{32b}, A. Phan⁸⁶,
 P.W. Phillips¹²⁹, G. Piacquadio³⁰, A. Picazio⁴⁹, E. Piccaro⁷⁵, M. Piccinini^{20a,20b},
 S.M. Piec⁴², R. Piegai²⁷, D.T. Pignotti¹⁰⁹, J.E. Pilcher³¹, A.D. Pilkington⁸²,
 J. Pina^{124a,c}, M. Pinamonti^{164a,164c}, A. Pinder¹¹⁸, J.L. Pinfold³, A. Pingel³⁶, B. Pinto^{124a},
 C. Pizio^{89a,89b}, M.-A. Pleier²⁵, E. Plotnikova⁶⁴, A. Poblaguev²⁵, S. Poddar^{58a},
 F. Podlyski³⁴, L. Poggioli¹¹⁵, D. Pohl²¹, M. Pohl⁴⁹, G. Polesello^{119a}, A. Policicchio^{37a,37b},
 A. Polini^{20a}, J. Poll⁷⁵, V. Polychronakos²⁵, D. Pomeroy²³, K. Pommès³⁰,
 L. Pontecorvo^{132a}, B.G. Pope⁸⁸, G.A. Popeneciu^{26a}, D.S. Popovic^{13a}, A. Poppleton³⁰,
 X. Portell Bueso³⁰, G.E. Pospelov⁹⁹, S. Pospisil¹²⁶, I.N. Potrap⁹⁹, C.J. Potter¹⁴⁹,

C.T. Potter¹¹⁴, G. Poulard³⁰, J. Poveda⁶⁰, V. Pozdnyakov⁶⁴, R. Prabhu⁷⁷, P. Pralavorio⁸³,
 A. Pranko¹⁵, S. Prasad³⁰, R. Pravahan²⁵, S. Prell⁶³, K. Pretzl¹⁷, D. Price⁶⁰, J. Price⁷³,
 L.E. Price⁶, D. Prieur¹²³, M. Primavera^{72a}, K. Prokofiev¹⁰⁸, F. Prokoshin^{32b},
 S. Protopopescu²⁵, J. Proudfoot⁶, X. Prudent⁴⁴, M. Przybycien³⁸, H. Przysieszniak⁵,
 S. Psoroulas²¹, E. Ptacek¹¹⁴, E. Pueschel⁸⁴, J. Purdham⁸⁷, M. Purohit^{25,ad}, P. Puzo¹¹⁵,
 Y. Pylypchenko⁶², J. Qian⁸⁷, A. Quadt⁵⁴, D.R. Quarrie¹⁵, W.B. Quayle¹⁷³, M. Raas¹⁰⁴,
 V. Radeka²⁵, V. Radescu⁴², P. Radloff¹¹⁴, F. Ragusa^{89a,89b}, G. Rahal¹⁷⁸, A.M. Rahimi¹⁰⁹,
 D. Rahm²⁵, S. Rajagopalan²⁵, M. Rammensee⁴⁸, M. Rammes¹⁴¹, A.S. Randle-Conde⁴⁰,
 K. Randrianarivony²⁹, K. Rao¹⁶³, F. Rauscher⁹⁸, T.C. Rave⁴⁸, M. Raymond³⁰,
 A.L. Read¹¹⁷, D.M. Rebuzzi^{119a,119b}, A. Redelbach¹⁷⁴, G. Redlinger²⁵, R. Reece¹²⁰,
 K. Reeves⁴¹, A. Reinsch¹¹⁴, I. Reisinger⁴³, C. Rembser³⁰, Z.L. Ren¹⁵¹, A. Renaud¹¹⁵,
 M. Rescigno^{132a}, S. Resconi^{89a}, B. Resende¹³⁶, P. Reznicek⁹⁸, R. Rezvani¹⁵⁸, R. Richter⁹⁹,
 E. Richter-Was^{5,ag}, M. Ridel⁷⁸, M. Rijpstra¹⁰⁵, M. Rijssenbeek¹⁴⁸, A. Rimoldi^{119a,119b},
 L. Rinaldi^{20a}, R.R. Rios⁴⁰, I. Riu¹², G. Rivoltella^{89a,89b}, F. Rizatdinova¹¹², E. Rizvi⁷⁵,
 S.H. Robertson^{85,l}, A. Robichaud-Veronneau¹¹⁸, D. Robinson²⁸, J.E.M. Robinson⁸²,
 A. Robson⁵³, J.G. Rocha de Lima¹⁰⁶, C. Roda^{122a,122b}, D. Roda Dos Santos³⁰, A. Roe⁵⁴,
 S. Roe³⁰, O. Røhne¹¹⁷, S. Rolli¹⁶¹, A. Romaniouk⁹⁶, M. Romano^{20a,20b}, G. Romeo²⁷,
 E. Romero Adam¹⁶⁷, N. Rompotis¹³⁸, L. Roos⁷⁸, E. Ros¹⁶⁷, S. Rosati^{132a}, K. Rosbach⁴⁹,
 A. Rose¹⁴⁹, M. Rose⁷⁶, G.A. Rosenbaum¹⁵⁸, E.I. Rosenberg⁶³, P.L. Rosendahl¹⁴,
 O. Rosenthal¹⁴¹, L. Rosselet⁴⁹, V. Rossetti¹², E. Rossi^{132a,132b}, L.P. Rossi^{50a},
 M. Rotaru^{26a}, I. Roth¹⁷², J. Rothberg¹³⁸, D. Rousseau¹¹⁵, C.R. Royon¹³⁶, A. Rozanov⁸³,
 Y. Rozen¹⁵², X. Ruan^{33a,ah}, F. Rubbo¹², I. Rubinskiy⁴², N. Ruckstuhl¹⁰⁵, V.I. Rud⁹⁷,
 C. Rudolph⁴⁴, G. Rudolph⁶¹, F. Rühr⁷, A. Ruiz-Martinez⁶³, L. Rumyantsev⁶⁴,
 Z. Rurikova⁴⁸, N.A. Rusakovich⁶⁴, A. Ruschke⁹⁸, J.P. Rutherford⁷, P. Ruzicka¹²⁵,
 Y.F. Ryabov¹²¹, M. Rybar¹²⁷, G. Rybkin¹¹⁵, N.C. Ryder¹¹⁸, A.F. Saavedra¹⁵⁰,
 I. Sadeh¹⁵³, H.F.W. Sadrozinski¹³⁷, R. Sadykov⁶⁴, F. Safai Tehrani^{132a}, H. Sakamoto¹⁵⁵,
 G. Salamanna⁷⁵, A. Salamon^{133a}, M. Saleem¹¹¹, D. Salek³⁰, D. Salihagic⁹⁹, A. Salnikov¹⁴³,
 J. Salt¹⁶⁷, B.M. Salvachua Ferrando⁶, D. Salvatore^{37a,37b}, F. Salvatore¹⁴⁹, A. Salvucci¹⁰⁴,
 A. Salzburger³⁰, D. Sampsonidis¹⁵⁴, B.H. Samset¹¹⁷, A. Sanchez^{102a,102b},
 V. Sanchez Martinez¹⁶⁷, H. Sandaker¹⁴, H.G. Sander⁸¹, M.P. Sanders⁹⁸, M. Sandhoff¹⁷⁵,
 T. Sandoval²⁸, C. Sandoval¹⁶², R. Sandstroem⁹⁹, D.P.C. Sankey¹²⁹, A. Sansoni⁴⁷,
 C. Santamarina Rios⁸⁵, C. Santoni³⁴, R. Santonico^{133a,133b}, H. Santos^{124a},
 I. Santoyo Castillo¹⁴⁹, J.G. Saraiva^{124a}, T. Sarangi¹⁷³, E. Sarkisyan-Grinbaum⁸,
 B. Sarrazin²¹, F. Sarri^{122a,122b}, G. Sartiso¹⁷⁵, O. Sasaki⁶⁵, Y. Sasaki¹⁵⁵, N. Sasao⁶⁷,
 I. Satsounkevitch⁹⁰, G. Sauvage^{5,*}, E. Sauvan⁵, J.B. Sauvan¹¹⁵, P. Savard^{158,f},
 V. Savinov¹²³, D.O. Savu³⁰, L. Sawyer^{25,n}, D.H. Saxon⁵³, J. Saxon¹²⁰, C. Sbarra^{20a},
 A. Sbrizzi^{20a,20b}, D.A. Scannicchio¹⁶³, M. Scarcella¹⁵⁰, J. Schaarschmidt¹¹⁵, P. Schacht⁹⁹,
 D. Schaefer¹²⁰, U. Schäfer⁸¹, A. Schaelicke⁴⁶, S. Schaepe²¹, S. Schaetzel^{58b},
 A.C. Schaffer¹¹⁵, D. Schaile⁹⁸, R.D. Schamberger¹⁴⁸, A.G. Schamov¹⁰⁷, V. Scharf^{58a},
 V.A. Schegelsky¹²¹, D. Scheirich⁸⁷, M. Schernau¹⁶³, M.I. Scherzer³⁵, C. Schiavi^{50a,50b},
 J. Schieck⁹⁸, M. Schioppa^{37a,37b}, S. Schlenker³⁰, E. Schmidt⁴⁸, K. Schmieden²¹,
 C. Schmitt⁸¹, S. Schmitt^{58b}, B. Schneider¹⁷, U. Schnoor⁴⁴, L. Schoeffel¹³⁶,
 A. Schoening^{58b}, A.L.S. Schorlemmer⁵⁴, M. Schott³⁰, D. Schouten^{159a}, J. Schovancova¹²⁵,

M. Schram⁸⁵, C. Schroeder⁸¹, N. Schroer^{58c}, M.J. Schultens²¹, J. Schultes¹⁷⁵,
H.-C. Schultz-Coulon^{58a}, H. Schulz¹⁶, M. Schumacher⁴⁸, B.A. Schumm¹³⁷, Ph. Schune¹³⁶,
A. Schwartzman¹⁴³, Ph. Schwegler⁹⁹, Ph. Schwemling⁷⁸, R. Schwienhorst⁸⁸, R. Schwierz⁴⁴,
J. Schwindling¹³⁶, T. Schwindt²¹, M. Schwoerer⁵, F.G. Sciacca¹⁷, G. Sciolla²³,
W.G. Scott¹²⁹, J. Searcy¹¹⁴, G. Sedov⁴², E. Sedykh¹²¹, S.C. Seidel¹⁰³, A. Seiden¹³⁷,
F. Seifert⁴⁴, J.M. Seixas^{24a}, G. Sekhniaidze^{102a}, S.J. Sekula⁴⁰, K.E. Selbach⁴⁶,
D.M. Seliverstov¹²¹, B. Sellden^{146a}, G. Sellers⁷³, M. Seman^{144b}, N. Semprini-Cesari^{20a,20b},
C. Serfon⁹⁸, L. Serin¹¹⁵, L. Serkin⁵⁴, R. Seuster^{159a}, H. Severini¹¹¹, A. Sfyrla³⁰,
E. Shabalina⁵⁴, M. Shamim¹¹⁴, L.Y. Shan^{33a}, J.T. Shank²², Q.T. Shao⁸⁶, M. Shapiro¹⁵,
P.B. Shatalov⁹⁵, K. Shaw^{164a,164c}, D. Sherman¹⁷⁶, P. Sherwood⁷⁷, S. Shimizu¹⁰¹,
M. Shimojima¹⁰⁰, T. Shin⁵⁶, M. Shiyakova⁶⁴, A. Shmeleva⁹⁴, M.J. Shochet³¹, D. Short¹¹⁸,
S. Shrestha⁶³, E. Shulga⁹⁶, M.A. Shupe⁷, P. Sicho¹²⁵, A. Sidoti^{132a}, F. Siegert⁴⁸,
Dj. Sijacki^{13a}, O. Silbert¹⁷², J. Silva^{124a}, Y. Silver¹⁵³, D. Silverstein¹⁴³,
S.B. Silverstein^{146a}, V. Simak¹²⁶, O. Simard¹³⁶, Lj. Simic^{13a}, S. Simion¹¹⁵, E. Simioni⁸¹,
B. Simmons⁷⁷, R. Simoniello^{89a,89b}, M. Simonyan³⁶, P. Sinervo¹⁵⁸, N.B. Sinev¹¹⁴,
V. Sipica¹⁴¹, G. Siragusa¹⁷⁴, A. Sircar²⁵, A.N. Sisakyan^{64,*}, S.Yu. Sivoklokov⁹⁷,
J. Sjölin^{146a,146b}, T.B. Sjursen¹⁴, L.A. Skinnari¹⁵, H.P. Skottowe⁵⁷, K. Skovpen¹⁰⁷,
P. Skubic¹¹¹, M. Slater¹⁸, T. Slavicek¹²⁶, K. Sliwa¹⁶¹, V. Smakhtin¹⁷², B.H. Smart⁴⁶,
L. Smestad¹¹⁷, S.Yu. Smirnov⁹⁶, Y. Smirnov⁹⁶, L.N. Smirnova⁹⁷, O. Smirnova⁷⁹,
B.C. Smith⁵⁷, D. Smith¹⁴³, K.M. Smith⁵³, M. Smizanska⁷¹, K. Smolek¹²⁶,
A.A. Snesarev⁹⁴, S.W. Snow⁸², J. Snow¹¹¹, S. Snyder²⁵, R. Sobie^{169,l}, J. Sodomka¹²⁶,
A. Soffer¹⁵³, C.A. Solans¹⁶⁷, M. Solar¹²⁶, J. Solc¹²⁶, E.Yu. Soldatov⁹⁶, U. Soldevila¹⁶⁷,
E. Solfaroli Camillocci^{132a,132b}, A.A. Solodkov¹²⁸, O.V. Solovyanov¹²⁸, V. Solovyev¹²¹,
N. Soni¹, A. Sood¹⁵, V. Sopko¹²⁶, B. Sopko¹²⁶, M. Sosebee⁸, R. Soualah^{164a,164c},
P. Soueid⁹³, A. Soukharev¹⁰⁷, S. Spagnolo^{72a,72b}, F. Spanò⁷⁶, R. Spighi^{20a}, G. Spigo³⁰,
R. Spiwox³⁰, M. Spousta^{127,ai}, T. Spreitzer¹⁵⁸, B. Spurlock⁸, R.D. St. Denis⁵³,
J. Stahlman¹²⁰, R. Stamen^{58a}, E. Stanecka³⁹, R.W. Stanek⁶, C. Stanescu^{134a},
M. Stanescu-Bellu⁴², M.M. Stanitzki⁴², S. Stapnes¹¹⁷, E.A. Starchenko¹²⁸, J. Stark⁵⁵,
P. Staroba¹²⁵, P. Starovoitov⁴², R. Staszewski³⁹, A. Staude⁹⁸, P. Stavina^{144a,*}, G. Steele⁵³,
P. Steinbach⁴⁴, P. Steinberg²⁵, I. Stekl¹²⁶, B. Stelzer¹⁴², H.J. Stelzer⁸⁸,
O. Stelzer-Chilton^{159a}, H. Stenzel⁵², S. Stern⁹⁹, G.A. Stewart³⁰, J.A. Stillings²¹,
M.C. Stockton⁸⁵, K. Stoerig⁴⁸, G. Stoicea^{26a}, S. Stonjek⁹⁹, P. Strachota¹²⁷,
A.R. Stradling⁸, A. Straessner⁴⁴, J. Strandberg¹⁴⁷, S. Strandberg^{146a,146b}, A. Strandlie¹¹⁷,
M. Strang¹⁰⁹, E. Strauss¹⁴³, M. Strauss¹¹¹, P. Strizenec^{144b}, R. Ströhmer¹⁷⁴,
D.M. Strom¹¹⁴, J.A. Strong^{76,*}, R. Stroynowski⁴⁰, B. Stugu¹⁴, I. Stumer^{25,*}, J. Stupak¹⁴⁸,
P. Sturm¹⁷⁵, N.A. Styles⁴², D.A. Soh^{151,v}, D. Su¹⁴³, HS. Subramania³, R. Subramaniam²⁵,
A. Succuro¹², Y. Sugaya¹¹⁶, C. Suhr¹⁰⁶, M. Suk¹²⁷, V.V. Sulin⁹⁴, S. Sultansoy^{4d},
T. Sumida⁶⁷, X. Sun⁵⁵, J.E. Sundermann⁴⁸, K. Suruliz¹³⁹, G. Susinno^{37a,37b},
M.R. Sutton¹⁴⁹, Y. Suzuki⁶⁵, Y. Suzuki⁶⁶, M. Svatos¹²⁵, S. Swedish¹⁶⁸, I. Sykora^{144a},
T. Sykora¹²⁷, J. Sánchez¹⁶⁷, D. Ta¹⁰⁵, K. Tackmann⁴², A. Taffard¹⁶³, R. Tafirout^{159a},
N. Taiblum¹⁵³, Y. Takahashi¹⁰¹, H. Takai²⁵, R. Takashima⁶⁸, H. Takeda⁶⁶,
T. Takeshita¹⁴⁰, Y. Takubo⁶⁵, M. Talby⁸³, A. Talyshev^{107,h}, M.C. Tamsett²⁵, K.G. Tan⁸⁶,
J. Tanaka¹⁵⁵, R. Tanaka¹¹⁵, S. Tanaka¹³¹, S. Tanaka⁶⁵, A.J. Tanasijczuk¹⁴², K. Tani⁶⁶,

N. Tannoury⁸³, S. Tapprogge⁸¹, D. Tardif¹⁵⁸, S. Tarem¹⁵², F. Tarrade²⁹,
 G.F. Tartarelli^{89a}, P. Tas¹²⁷, M. Tasevsky¹²⁵, E. Tassi^{37a,37b}, Y. Tayalati^{135d}, C. Taylor⁷⁷,
 F.E. Taylor⁹², G.N. Taylor⁸⁶, W. Taylor^{159b}, M. Teinturier¹¹⁵, F.A. Teischinger³⁰,
 M. Teixeira Dias Castanheira⁷⁵, P. Teixeira-Dias⁷⁶, K.K. Temming⁴⁸, H. Ten Kate³⁰,
 P.K. Teng¹⁵¹, S. Terada⁶⁵, K. Terashi¹⁵⁵, J. Terron⁸⁰, M. Testa⁴⁷, R.J. Teuscher^{158,l},
 J. Therhaag²¹, T. Theveneaux-Pelzer⁷⁸, S. Thoma⁴⁸, J.P. Thomas¹⁸, E.N. Thompson³⁵,
 P.D. Thompson¹⁸, P.D. Thompson¹⁵⁸, A.S. Thompson⁵³, L.A. Thomsen³⁶,
 E. Thomson¹²⁰, M. Thomson²⁸, W.M. Thong⁸⁶, R.P. Thun⁸⁷, F. Tian³⁵, M.J. Tibbetts¹⁵,
 T. Tic¹²⁵, V.O. Tikhomirov⁹⁴, Y.A. Tikhonov^{107,h}, S. Timoshenko⁹⁶, E. Tiouchichine⁸³,
 P. Tipton¹⁷⁶, S. Tisserant⁸³, T. Todorov⁵, S. Todorova-Nova¹⁶¹, B. Toggerson¹⁶³,
 J. Tojo⁶⁹, S. Tokár^{144a}, K. Tokushuku⁶⁵, K. Tollefson⁸⁸, M. Tomoto¹⁰¹, L. Tompkins³¹,
 K. Toms¹⁰³, A. Tonoyan¹⁴, C. Topfel¹⁷, N.D. Topilin⁶⁴, E. Torrence¹¹⁴, H. Torres⁷⁸,
 E. Torró Pastor¹⁶⁷, J. Toth^{83,ae}, F. Touchard⁸³, D.R. Tovey¹³⁹, T. Trefzger¹⁷⁴,
 L. Tremblet³⁰, A. Tricoli³⁰, I.M. Trigger^{159a}, S. Trincaz-Duvoid⁷⁸, M.F. Tripiana⁷⁰,
 N. Triplett²⁵, W. Trischuk¹⁵⁸, B. Trocmé⁵⁵, C. Troncon^{89a}, M. Trottier-McDonald¹⁴²,
 P. True⁸⁸, M. Trzebinski³⁹, A. Trzupke³⁹, C. Tsarouchas³⁰, J.C-L. Tseng¹¹⁸,
 M. Tsiakiris¹⁰⁵, P.V. Tsiareshka⁹⁰, D. Tsionou^{5,aj}, G. Tsipolitis¹⁰, S. Tsiskaridze¹²,
 V. Tsiskaridze⁴⁸, E.G. Tskhadadze^{51a}, I.I. Tsukerman⁹⁵, V. Tsulaia¹⁵, J.-W. Tsung²¹,
 S. Tsuno⁶⁵, D. Tsybychev¹⁴⁸, A. Tua¹³⁹, A. Tudorache^{26a}, V. Tudorache^{26a},
 J.M. Tuggle³¹, M. Turala³⁹, D. Turecek¹²⁶, I. Turk Cakir^{4e}, E. Turlay¹⁰⁵, R. Turra^{89a,89b},
 P.M. Tuts³⁵, A. Tykhonov⁷⁴, M. Tylmad^{146a,146b}, M. Tyndel¹²⁹, G. Tzanakos⁹,
 K. Uchida²¹, I. Ueda¹⁵⁵, R. Ueno²⁹, M. Ughetto⁸³, M. Ugland¹⁴, M. Uhlenbrock²¹,
 M. Uhrmacher⁵⁴, F. Ukegawa¹⁶⁰, G. Unal³⁰, A. Undrus²⁵, G. Unel¹⁶³, Y. Unno⁶⁵,
 D. Urbaniec³⁵, P. Urquijo²¹, G. Usai⁸, M. Uslenghi^{119a,119b}, L. Vacavant⁸³, V. Vacek¹²⁶,
 B. Vachon⁸⁵, S. Vahsen¹⁵, J. Valenta¹²⁵, S. Valentinetti^{20a,20b}, A. Valero¹⁶⁷, S. Valkar¹²⁷,
 E. Valladolid Gallego¹⁶⁷, S. Vallecorsa¹⁵², J.A. Valls Ferrer¹⁶⁷, R. Van Berg¹²⁰,
 P.C. Van Der Deijl¹⁰⁵, R. van der Geer¹⁰⁵, H. van der Graaf¹⁰⁵, R. Van Der Leeuw¹⁰⁵,
 E. van der Poel¹⁰⁵, D. van der Ster³⁰, N. van Eldik³⁰, P. van Gemmeren⁶,
 J. Van Nieuwkoop¹⁴², I. van Vulpen¹⁰⁵, M. Vanadia⁹⁹, W. Vandelli³⁰, A. Vaniachine⁶,
 P. Vankov⁴², F. Vannucci⁷⁸, R. Vari^{132a}, E.W. Varnes⁷, T. Varol⁸⁴, D. Varouchas¹⁵,
 A. Vartapetian⁸, K.E. Varvell¹⁵⁰, V.I. Vassilakopoulos⁵⁶, F. Vazeille³⁴,
 T. Vazquez Schroeder⁵⁴, G. Vegni^{89a,89b}, J.J. Veillet¹¹⁵, F. Veloso^{124a}, R. Veness³⁰,
 S. Veneziano^{132a}, A. Ventura^{72a,72b}, D. Ventura⁸⁴, M. Venturi⁴⁸, N. Venturi¹⁵⁸,
 V. Vercesi^{119a}, M. Verducci¹³⁸, W. Verkerke¹⁰⁵, J.C. Vermeulen¹⁰⁵, A. Vest⁴⁴,
 M.C. Vetterli^{142,f}, I. Vichou¹⁶⁵, T. Vickey^{145b,ak}, O.E. Vickey Boeriu^{145b},
 G.H.A. Viehhauser¹¹⁸, S. Viel¹⁶⁸, M. Villa^{20a,20b}, M. Villaplana Perez¹⁶⁷, E. Vilucchi⁴⁷,
 M.G. Vincker²⁹, E. Vinek³⁰, V.B. Vinogradov⁶⁴, M. Virchaux^{136,*}, J. Virzi¹⁵,
 O. Vitells¹⁷², M. Viti⁴², I. Vivarelli⁴⁸, F. Vives Vaque³, S. Vlachos¹⁰, D. Vladoiu⁹⁸,
 M. Vlasak¹²⁶, A. Vogel²¹, P. Vokac¹²⁶, G. Volpi⁴⁷, M. Volpi⁸⁶, G. Volpini^{89a},
 H. von der Schmitt⁹⁹, H. von Radziewski⁴⁸, E. von Toerne²¹, V. Vorobel¹²⁷, V. Vorwerk¹²,
 M. Vos¹⁶⁷, R. Voss³⁰, J.H. Vosseveld⁷³, N. Vranjes¹³⁶, M. Vranjes Milosavljevic¹⁰⁵,
 V. Vrba¹²⁵, M. Vreeswijk¹⁰⁵, T. Vu Anh⁴⁸, R. Vuillermet³⁰, I. Vukotic³¹, W. Wagner¹⁷⁵,
 P. Wagner¹²⁰, H. Wahlen¹⁷⁵, S. Wahrenmund⁴⁴, J. Wakabayashi¹⁰¹, S. Walch⁸⁷, J. Walder⁷¹,

R. Walker⁹⁸, W. Walkowiak¹⁴¹, R. Wall¹⁷⁶, P. Waller⁷³, B. Walsh¹⁷⁶, C. Wang⁴⁵,
H. Wang¹⁷³, H. Wang⁴⁰, J. Wang¹⁵¹, J. Wang^{33a}, R. Wang¹⁰³, S.M. Wang¹⁵¹, T. Wang²¹,
A. Warburton⁸⁵, C.P. Ward²⁸, D.R. Wardrope⁷⁷, M. Warsinsky⁴⁸, A. Washbrook⁴⁶,
C. Wasicki⁴², I. Watanabe⁶⁶, P.M. Watkins¹⁸, A.T. Watson¹⁸, I.J. Watson¹⁵⁰,
M.F. Watson¹⁸, G. Watts¹³⁸, S. Watts⁸², A.T. Waugh¹⁵⁰, B.M. Waugh⁷⁷, M.S. Weber¹⁷,
J.S. Webster³¹, A.R. Weidberg¹¹⁸, P. Weigell⁹⁹, J. Weingarten⁵⁴, C. Weiser⁴⁸,
P.S. Wells³⁰, T. Wenaus²⁵, D. Wendland¹⁶, Z. Weng^{151,v}, T. Wengler³⁰, S. Wenig³⁰,
N. Vermes²¹, M. Werner⁴⁸, P. Werner³⁰, M. Werth¹⁶³, M. Wessels^{58a}, J. Wetter¹⁶¹,
C. Weydert⁵⁵, K. Whalen²⁹, A. White⁸, M.J. White⁸⁶, S. White^{122a,122b},
S.R. Whitehead¹¹⁸, D. Whiteson¹⁶³, D. Whittington⁶⁰, D. Wicke¹⁷⁵, F.J. Wickens¹²⁹,
W. Wiedenmann¹⁷³, M. Wielers¹²⁹, P. Wienemann²¹, C. Wiglesworth⁷⁵,
L.A.M. Wiik-Fuchs²¹, P.A. Wijeratne⁷⁷, A. Wildauer⁹⁹, M.A. Wildt^{42,s}, I. Wilhelm¹²⁷,
H.G. Wilkens³⁰, J.Z. Will⁹⁸, E. Williams³⁵, H.H. Williams¹²⁰, S. Williams²⁸, W. Willis³⁵,
S. Willocq⁸⁴, J.A. Wilson¹⁸, M.G. Wilson¹⁴³, A. Wilson⁸⁷, I. Wingerter-Seez⁵,
S. Winkelmann⁴⁸, F. Winklmeier³⁰, M. Wittgen¹⁴³, S.J. Wollstadt⁸¹, M.W. Wolter³⁹,
H. Wolters^{124a,i}, W.C. Wong⁴¹, G. Wooden⁸⁷, B.K. Wosiek³⁹, J. Wotschack³⁰,
M.J. Woudstra⁸², K.W. Wozniak³⁹, K. Wraight⁵³, M. Wright⁵³, B. Wrona⁷³, S.L. Wu¹⁷³,
X. Wu⁴⁹, Y. Wu^{33b,al}, E. Wulf³⁵, B.M. Wynne⁴⁶, S. Xella³⁶, M. Xiao¹³⁶, S. Xie⁴⁸,
C. Xu^{33b,z}, D. Xu^{33a}, L. Xu^{33b}, B. Yabsley¹⁵⁰, S. Yacoob^{145a,am}, M. Yamada⁶⁵,
H. Yamaguchi¹⁵⁵, A. Yamamoto⁶⁵, K. Yamamoto⁶³, S. Yamamoto¹⁵⁵, T. Yamamura¹⁵⁵,
T. Yamanaka¹⁵⁵, T. Yamazaki¹⁵⁵, Y. Yamazaki⁶⁶, Z. Yan²², H. Yang⁸⁷, U.K. Yang⁸²,
Y. Yang¹⁰⁹, Z. Yang^{146a,146b}, S. Yanush⁹¹, L. Yao^{33a}, Y. Yasu⁶⁵, E. Yatsenko⁴², J. Ye⁴⁰,
S. Ye²⁵, A.L. Yen⁵⁷, M. Yilmaz^{4c}, R. Yoosofmiya¹²³, K. Yorita¹⁷¹, R. Yoshida⁶,
K. Yoshihara¹⁵⁵, C. Young¹⁴³, C.J. Young¹¹⁸, S. Youssef²², D. Yu²⁵, D.R. Yu¹⁵, J. Yu⁸,
J. Yu¹¹², L. Yuan⁶⁶, A. Yurkewicz¹⁰⁶, B. Zabinski³⁹, R. Zaidan⁶², A.M. Zaitsev¹²⁸,
L. Zanello^{132a,132b}, D. Zanzi⁹⁹, A. Zaytsev²⁵, C. Zeitnitz¹⁷⁵, M. Zeman¹²⁵, A. Zemla³⁹,
O. Zenin¹²⁸, T. Ženiš^{144a}, Z. Zinonos^{122a,122b}, D. Zerwas¹¹⁵, G. Zevi della Porta⁵⁷,
D. Zhang⁸⁷, H. Zhang⁸⁸, J. Zhang⁶, X. Zhang^{33d}, Z. Zhang¹¹⁵, L. Zhao¹⁰⁸, Z. Zhao^{33b},
A. Zhemchugov⁶⁴, J. Zhong¹¹⁸, B. Zhou⁸⁷, N. Zhou¹⁶³, Y. Zhou¹⁵¹, C.G. Zhu^{33d},
H. Zhu⁴², J. Zhu⁸⁷, Y. Zhu^{33b}, X. Zhuang⁹⁸, V. Zhuravlov⁹⁹, A. Zibell⁹⁸, D. Zieminska⁶⁰,
N.I. Zimin⁶⁴, R. Zimmermann²¹, S. Zimmermann²¹, S. Zimmermann⁴⁸, M. Ziolkowski¹⁴¹,
R. Zitoun⁵, L. Živković³⁵, V.V. Zmouchko^{128,*}, G. Zobernig¹⁷³, A. Zoccoli^{20a,20b},
M. zur Nedden¹⁶, V. Zutshi¹⁰⁶, L. Zwalinski³⁰.

¹ School of Chemistry and Physics, University of Adelaide, Adelaide, Australia

² Physics Department, SUNY Albany, Albany NY, United States of America

³ Department of Physics, University of Alberta, Edmonton AB, Canada

⁴ ^(a) Department of Physics, Ankara University, Ankara; ^(b) Department of Physics, Dumlupinar University, Kutahya; ^(c) Department of Physics, Gazi University, Ankara; ^(d) Division of Physics, TOBB University of Economics and Technology, Ankara; ^(e) Turkish Atomic Energy Authority, Ankara, Turkey

⁵ LAPP, CNRS/IN2P3 and Université de Savoie, Annecy-le-Vieux, France

⁶ High Energy Physics Division, Argonne National Laboratory, Argonne IL, United States

of America

⁷ Department of Physics, University of Arizona, Tucson AZ, United States of America

⁸ Department of Physics, The University of Texas at Arlington, Arlington TX, United States of America

⁹ Physics Department, University of Athens, Athens, Greece

¹⁰ Physics Department, National Technical University of Athens, Zografou, Greece

¹¹ Institute of Physics, Azerbaijan Academy of Sciences, Baku, Azerbaijan

¹² Institut de Física d'Altes Energies and Departament de Física de la Universitat Autònoma de Barcelona and ICREA, Barcelona, Spain

¹³ ^(a) Institute of Physics, University of Belgrade, Belgrade; ^(b) Vinca Institute of Nuclear Sciences, University of Belgrade, Belgrade, Serbia

¹⁴ Department for Physics and Technology, University of Bergen, Bergen, Norway

¹⁵ Physics Division, Lawrence Berkeley National Laboratory and University of California, Berkeley CA, United States of America

¹⁶ Department of Physics, Humboldt University, Berlin, Germany

¹⁷ Albert Einstein Center for Fundamental Physics and Laboratory for High Energy Physics, University of Bern, Bern, Switzerland

¹⁸ School of Physics and Astronomy, University of Birmingham, Birmingham, United Kingdom

¹⁹ ^(a) Department of Physics, Bogazici University, Istanbul; ^(b) Division of Physics, Dogus University, Istanbul; ^(c) Department of Physics Engineering, Gaziantep University, Gaziantep; ^(d) Department of Physics, Istanbul Technical University, Istanbul, Turkey

²⁰ ^(a) INFN Sezione di Bologna; ^(b) Dipartimento di Fisica, Università di Bologna, Bologna, Italy

²¹ Physikalisches Institut, University of Bonn, Bonn, Germany

²² Department of Physics, Boston University, Boston MA, United States of America

²³ Department of Physics, Brandeis University, Waltham MA, United States of America

²⁴ ^(a) Universidade Federal do Rio De Janeiro COPPE/EE/IF, Rio de Janeiro; ^(b) Federal University of Juiz de Fora (UFJF), Juiz de Fora; ^(c) Federal University of Sao Joao del Rei (UFSJ), Sao Joao del Rei; ^(d) Instituto de Fisica, Universidade de Sao Paulo, Sao Paulo, Brazil

²⁵ Physics Department, Brookhaven National Laboratory, Upton NY, United States of America

²⁶ ^(a) National Institute of Physics and Nuclear Engineering, Bucharest; ^(b) University Politehnica Bucharest, Bucharest; ^(c) West University in Timisoara, Timisoara, Romania

²⁷ Departamento de Física, Universidad de Buenos Aires, Buenos Aires, Argentina

²⁸ Cavendish Laboratory, University of Cambridge, Cambridge, United Kingdom

²⁹ Department of Physics, Carleton University, Ottawa ON, Canada

³⁰ CERN, Geneva, Switzerland

³¹ Enrico Fermi Institute, University of Chicago, Chicago IL, United States of America

³² ^(a) Departamento de Física, Pontificia Universidad Católica de Chile, Santiago; ^(b) Departamento de Física, Universidad Técnica Federico Santa María, Valparaíso, Chile

³³ ^(a) Institute of High Energy Physics, Chinese Academy of Sciences, Beijing; ^(b)

Department of Modern Physics, University of Science and Technology of China, Anhui; ^(c) Department of Physics, Nanjing University, Jiangsu; ^(d) School of Physics, Shandong University, Shandong; ^(e) Physics Department, Shanghai Jiao Tong University, Shanghai, China

³⁴ Laboratoire de Physique Corpusculaire, Clermont Université and Université Blaise Pascal and CNRS/IN2P3, Clermont-Ferrand, France

³⁵ Nevis Laboratory, Columbia University, Irvington NY, United States of America

³⁶ Niels Bohr Institute, University of Copenhagen, Kobenhavn, Denmark

³⁷ ^(a) INFN Gruppo Collegato di Cosenza; ^(b) Dipartimento di Fisica, Università della Calabria, Arcavata di Rende, Italy

³⁸ AGH University of Science and Technology, Faculty of Physics and Applied Computer Science, Krakow, Poland

³⁹ The Henryk Niewodniczanski Institute of Nuclear Physics, Polish Academy of Sciences, Krakow, Poland

⁴⁰ Physics Department, Southern Methodist University, Dallas TX, United States of America

⁴¹ Physics Department, University of Texas at Dallas, Richardson TX, United States of America

⁴² DESY, Hamburg and Zeuthen, Germany

⁴³ Institut für Experimentelle Physik IV, Technische Universität Dortmund, Dortmund, Germany

⁴⁴ Institut für Kern- und Teilchenphysik, Technical University Dresden, Dresden, Germany

⁴⁵ Department of Physics, Duke University, Durham NC, United States of America

⁴⁶ SUPA - School of Physics and Astronomy, University of Edinburgh, Edinburgh, United Kingdom

⁴⁷ INFN Laboratori Nazionali di Frascati, Frascati, Italy

⁴⁸ Fakultät für Mathematik und Physik, Albert-Ludwigs-Universität, Freiburg, Germany

⁴⁹ Section de Physique, Université de Genève, Geneva, Switzerland

⁵⁰ ^(a) INFN Sezione di Genova; ^(b) Dipartimento di Fisica, Università di Genova, Genova, Italy

⁵¹ ^(a) E. Andronikashvili Institute of Physics, Iv. Javakhishvili Tbilisi State University, Tbilisi; ^(b) High Energy Physics Institute, Tbilisi State University, Tbilisi, Georgia

⁵² II Physikalisches Institut, Justus-Liebig-Universität Giessen, Giessen, Germany

⁵³ SUPA - School of Physics and Astronomy, University of Glasgow, Glasgow, United Kingdom

⁵⁴ II Physikalisches Institut, Georg-August-Universität, Göttingen, Germany

⁵⁵ Laboratoire de Physique Subatomique et de Cosmologie, Université Joseph Fourier and CNRS/IN2P3 and Institut National Polytechnique de Grenoble, Grenoble, France

⁵⁶ Department of Physics, Hampton University, Hampton VA, United States of America

⁵⁷ Laboratory for Particle Physics and Cosmology, Harvard University, Cambridge MA, United States of America

⁵⁸ ^(a) Kirchhoff-Institut für Physik, Ruprecht-Karls-Universität Heidelberg, Heidelberg; ^(b) Physikalisches Institut, Ruprecht-Karls-Universität Heidelberg, Heidelberg; ^(c) ZITI

Institut für technische Informatik, Ruprecht-Karls-Universität Heidelberg, Mannheim, Germany

⁵⁹ Faculty of Applied Information Science, Hiroshima Institute of Technology, Hiroshima, Japan

⁶⁰ Department of Physics, Indiana University, Bloomington IN, United States of America

⁶¹ Institut für Astro- und Teilchenphysik, Leopold-Franzens-Universität, Innsbruck, Austria

⁶² University of Iowa, Iowa City IA, United States of America

⁶³ Department of Physics and Astronomy, Iowa State University, Ames IA, United States of America

⁶⁴ Joint Institute for Nuclear Research, JINR Dubna, Dubna, Russia

⁶⁵ KEK, High Energy Accelerator Research Organization, Tsukuba, Japan

⁶⁶ Graduate School of Science, Kobe University, Kobe, Japan

⁶⁷ Faculty of Science, Kyoto University, Kyoto, Japan

⁶⁸ Kyoto University of Education, Kyoto, Japan

⁶⁹ Department of Physics, Kyushu University, Fukuoka, Japan

⁷⁰ Instituto de Física La Plata, Universidad Nacional de La Plata and CONICET, La Plata, Argentina

⁷¹ Physics Department, Lancaster University, Lancaster, United Kingdom

⁷² ^(a) INFN Sezione di Lecce; ^(b) Dipartimento di Matematica e Fisica, Università del Salento, Lecce, Italy

⁷³ Oliver Lodge Laboratory, University of Liverpool, Liverpool, United Kingdom

⁷⁴ Department of Physics, Jožef Stefan Institute and University of Ljubljana, Ljubljana, Slovenia

⁷⁵ School of Physics and Astronomy, Queen Mary University of London, London, United Kingdom

⁷⁶ Department of Physics, Royal Holloway University of London, Surrey, United Kingdom

⁷⁷ Department of Physics and Astronomy, University College London, London, United Kingdom

⁷⁸ Laboratoire de Physique Nucléaire et de Hautes Energies, UPMC and Université Paris-Diderot and CNRS/IN2P3, Paris, France

⁷⁹ Fysiska institutionen, Lunds universitet, Lund, Sweden

⁸⁰ Departamento de Física Teórica C-15, Universidad Autónoma de Madrid, Madrid, Spain

⁸¹ Institut für Physik, Universität Mainz, Mainz, Germany

⁸² School of Physics and Astronomy, University of Manchester, Manchester, United Kingdom

⁸³ CPPM, Aix-Marseille Université and CNRS/IN2P3, Marseille, France

⁸⁴ Department of Physics, University of Massachusetts, Amherst MA, United States of America

⁸⁵ Department of Physics, McGill University, Montreal QC, Canada

⁸⁶ School of Physics, University of Melbourne, Victoria, Australia

⁸⁷ Department of Physics, The University of Michigan, Ann Arbor MI, United States of

America

⁸⁸ Department of Physics and Astronomy, Michigan State University, East Lansing MI, United States of America

⁸⁹ ^(a) INFN Sezione di Milano; ^(b) Dipartimento di Fisica, Università di Milano, Milano, Italy

⁹⁰ B.I. Stepanov Institute of Physics, National Academy of Sciences of Belarus, Minsk, Republic of Belarus

⁹¹ National Scientific and Educational Centre for Particle and High Energy Physics, Minsk, Republic of Belarus

⁹² Department of Physics, Massachusetts Institute of Technology, Cambridge MA, United States of America

⁹³ Group of Particle Physics, University of Montreal, Montreal QC, Canada

⁹⁴ P.N. Lebedev Institute of Physics, Academy of Sciences, Moscow, Russia

⁹⁵ Institute for Theoretical and Experimental Physics (ITEP), Moscow, Russia

⁹⁶ Moscow Engineering and Physics Institute (MEPhI), Moscow, Russia

⁹⁷ Skobeltsyn Institute of Nuclear Physics, Lomonosov Moscow State University, Moscow, Russia

⁹⁸ Fakultät für Physik, Ludwig-Maximilians-Universität München, München, Germany

⁹⁹ Max-Planck-Institut für Physik (Werner-Heisenberg-Institut), München, Germany

¹⁰⁰ Nagasaki Institute of Applied Science, Nagasaki, Japan

¹⁰¹ Graduate School of Science and Kobayashi-Maskawa Institute, Nagoya University, Nagoya, Japan

¹⁰² ^(a) INFN Sezione di Napoli; ^(b) Dipartimento di Scienze Fisiche, Università di Napoli, Napoli, Italy

¹⁰³ Department of Physics and Astronomy, University of New Mexico, Albuquerque NM, United States of America

¹⁰⁴ Institute for Mathematics, Astrophysics and Particle Physics, Radboud University Nijmegen/Nikhef, Nijmegen, Netherlands

¹⁰⁵ Nikhef National Institute for Subatomic Physics and University of Amsterdam, Amsterdam, Netherlands

¹⁰⁶ Department of Physics, Northern Illinois University, DeKalb IL, United States of America

¹⁰⁷ Budker Institute of Nuclear Physics, SB RAS, Novosibirsk, Russia

¹⁰⁸ Department of Physics, New York University, New York NY, United States of America

¹⁰⁹ Ohio State University, Columbus OH, United States of America

¹¹⁰ Faculty of Science, Okayama University, Okayama, Japan

¹¹¹ Homer L. Dodge Department of Physics and Astronomy, University of Oklahoma, Norman OK, United States of America

¹¹² Department of Physics, Oklahoma State University, Stillwater OK, United States of America

¹¹³ Palacký University, RCPTM, Olomouc, Czech Republic

¹¹⁴ Center for High Energy Physics, University of Oregon, Eugene OR, United States of America

- 115 LAL, Université Paris-Sud and CNRS/IN2P3, Orsay, France
- 116 Graduate School of Science, Osaka University, Osaka, Japan
- 117 Department of Physics, University of Oslo, Oslo, Norway
- 118 Department of Physics, Oxford University, Oxford, United Kingdom
- 119 ^(a) INFN Sezione di Pavia; ^(b) Dipartimento di Fisica, Università di Pavia, Pavia, Italy
- 120 Department of Physics, University of Pennsylvania, Philadelphia PA, United States of America
- 121 Petersburg Nuclear Physics Institute, Gatchina, Russia
- 122 ^(a) INFN Sezione di Pisa; ^(b) Dipartimento di Fisica E. Fermi, Università di Pisa, Pisa, Italy
- 123 Department of Physics and Astronomy, University of Pittsburgh, Pittsburgh PA, United States of America
- 124 ^(a) Laboratório de Instrumentação e Física Experimental de Partículas - LIP, Lisboa, Portugal; ^(b) Departamento de Física Teórica y del Cosmos and CAFPE, Universidad de Granada, Granada, Spain
- 125 Institute of Physics, Academy of Sciences of the Czech Republic, Praha, Czech Republic
- 126 Czech Technical University in Prague, Praha, Czech Republic
- 127 Faculty of Mathematics and Physics, Charles University in Prague, Praha, Czech Republic
- 128 State Research Center Institute for High Energy Physics, Protvino, Russia
- 129 Particle Physics Department, Rutherford Appleton Laboratory, Didcot, United Kingdom
- 130 Physics Department, University of Regina, Regina SK, Canada
- 131 Ritsumeikan University, Kusatsu, Shiga, Japan
- 132 ^(a) INFN Sezione di Roma I; ^(b) Dipartimento di Fisica, Università La Sapienza, Roma, Italy
- 133 ^(a) INFN Sezione di Roma Tor Vergata; ^(b) Dipartimento di Fisica, Università di Roma Tor Vergata, Roma, Italy
- 134 ^(a) INFN Sezione di Roma Tre; ^(b) Dipartimento di Fisica, Università Roma Tre, Roma, Italy
- 135 ^(a) Faculté des Sciences Ain Chock, Réseau Universitaire de Physique des Hautes Energies - Université Hassan II, Casablanca; ^(b) Centre National de l'Energie des Sciences Techniques Nucleaires, Rabat; ^(c) Faculté des Sciences Semlalia, Université Cadi Ayyad, LPHEA-Marrakech; ^(d) Faculté des Sciences, Université Mohamed Premier and LPTPM, Oujda; ^(e) Faculté des sciences, Université Mohammed V-Agdal, Rabat, Morocco
- 136 DSM/IRFU (Institut de Recherches sur les Lois Fondamentales de l'Univers), CEA Saclay (Commissariat à l'Energie Atomique), Gif-sur-Yvette, France
- 137 Santa Cruz Institute for Particle Physics, University of California Santa Cruz, Santa Cruz CA, United States of America
- 138 Department of Physics, University of Washington, Seattle WA, United States of America
- 139 Department of Physics and Astronomy, University of Sheffield, Sheffield, United

Kingdom

¹⁴⁰ Department of Physics, Shinshu University, Nagano, Japan

¹⁴¹ Fachbereich Physik, Universität Siegen, Siegen, Germany

¹⁴² Department of Physics, Simon Fraser University, Burnaby BC, Canada

¹⁴³ SLAC National Accelerator Laboratory, Stanford CA, United States of America

¹⁴⁴ ^(a) Faculty of Mathematics, Physics & Informatics, Comenius University, Bratislava;

^(b) Department of Subnuclear Physics, Institute of Experimental Physics of the Slovak Academy of Sciences, Kosice, Slovak Republic

¹⁴⁵ ^(a) Department of Physics, University of Johannesburg, Johannesburg; ^(b) School of Physics, University of the Witwatersrand, Johannesburg, South Africa

¹⁴⁶ ^(a) Department of Physics, Stockholm University; ^(b) The Oskar Klein Centre, Stockholm, Sweden

¹⁴⁷ Physics Department, Royal Institute of Technology, Stockholm, Sweden

¹⁴⁸ Departments of Physics & Astronomy and Chemistry, Stony Brook University, Stony Brook NY, United States of America

¹⁴⁹ Department of Physics and Astronomy, University of Sussex, Brighton, United

Kingdom

¹⁵⁰ School of Physics, University of Sydney, Sydney, Australia

¹⁵¹ Institute of Physics, Academia Sinica, Taipei, Taiwan

¹⁵² Department of Physics, Technion: Israel Institute of Technology, Haifa, Israel

¹⁵³ Raymond and Beverly Sackler School of Physics and Astronomy, Tel Aviv University, Tel Aviv, Israel

¹⁵⁴ Department of Physics, Aristotle University of Thessaloniki, Thessaloniki, Greece

¹⁵⁵ International Center for Elementary Particle Physics and Department of Physics, The University of Tokyo, Tokyo, Japan

¹⁵⁶ Graduate School of Science and Technology, Tokyo Metropolitan University, Tokyo, Japan

¹⁵⁷ Department of Physics, Tokyo Institute of Technology, Tokyo, Japan

¹⁵⁸ Department of Physics, University of Toronto, Toronto ON, Canada

¹⁵⁹ ^(a) TRIUMF, Vancouver BC; ^(b) Department of Physics and Astronomy, York University, Toronto ON, Canada

¹⁶⁰ Faculty of Pure and Applied Sciences, University of Tsukuba, Tsukuba, Japan

¹⁶¹ Department of Physics and Astronomy, Tufts University, Medford MA, United States of America

¹⁶² Centro de Investigaciones, Universidad Antonio Narino, Bogota, Colombia

¹⁶³ Department of Physics and Astronomy, University of California Irvine, Irvine CA, United States of America

¹⁶⁴ ^(a) INFN Gruppo Collegato di Udine; ^(b) ICTP, Trieste; ^(c) Dipartimento di Chimica, Fisica e Ambiente, Università di Udine, Udine, Italy

¹⁶⁵ Department of Physics, University of Illinois, Urbana IL, United States of America

¹⁶⁶ Department of Physics and Astronomy, University of Uppsala, Uppsala, Sweden

¹⁶⁷ Instituto de Física Corpuscular (IFIC) and Departamento de Física Atómica, Molecular y Nuclear and Departamento de Ingeniería Electrónica and Instituto de

Microelectrónica de Barcelona (IMB-CNM), University of Valencia and CSIC, Valencia, Spain

¹⁶⁸ Department of Physics, University of British Columbia, Vancouver BC, Canada

¹⁶⁹ Department of Physics and Astronomy, University of Victoria, Victoria BC, Canada

¹⁷⁰ Department of Physics, University of Warwick, Coventry, United Kingdom

¹⁷¹ Waseda University, Tokyo, Japan

¹⁷² Department of Particle Physics, The Weizmann Institute of Science, Rehovot, Israel

¹⁷³ Department of Physics, University of Wisconsin, Madison WI, United States of America

¹⁷⁴ Fakultät für Physik und Astronomie, Julius-Maximilians-Universität, Würzburg, Germany

¹⁷⁵ Fachbereich C Physik, Bergische Universität Wuppertal, Wuppertal, Germany

¹⁷⁶ Department of Physics, Yale University, New Haven CT, United States of America

¹⁷⁷ Yerevan Physics Institute, Yerevan, Armenia

¹⁷⁸ Centre de Calcul de l'Institut National de Physique Nucléaire et de Physique des Particules (IN2P3), Villeurbanne, France

^a Also at Department of Physics, King's College London, London, United Kingdom

^b Also at Laboratório de Instrumentação e Física Experimental de Partículas - LIP, Lisboa, Portugal

^c Also at Faculdade de Ciências and CFNUL, Universidade de Lisboa, Lisboa, Portugal

^d Also at Particle Physics Department, Rutherford Appleton Laboratory, Didcot, United Kingdom

^e Also at Department of Physics, University of Johannesburg, Johannesburg, South Africa

^f Also at TRIUMF, Vancouver BC, Canada

^g Also at Department of Physics, California State University, Fresno CA, United States of America

^h Also at Novosibirsk State University, Novosibirsk, Russia

ⁱ Also at Department of Physics, University of Coimbra, Coimbra, Portugal

^j Also at Department of Physics, UASLP, San Luis Potosi, Mexico

^k Also at Università di Napoli Parthenope, Napoli, Italy

^l Also at Institute of Particle Physics (IPP), Canada

^m Also at Department of Physics, Middle East Technical University, Ankara, Turkey

ⁿ Also at Louisiana Tech University, Ruston LA, United States of America

^o Also at Dep Física and CEFITEC of Faculdade de Ciências e Tecnologia, Universidade Nova de Lisboa, Caparica, Portugal

^p Also at Department of Physics and Astronomy, University College London, London, United Kingdom

^q Also at Department of Physics, University of Cape Town, Cape Town, South Africa

^r Also at Institute of Physics, Azerbaijan Academy of Sciences, Baku, Azerbaijan

^s Also at Institut für Experimentalphysik, Universität Hamburg, Hamburg, Germany

^t Also at Manhattan College, New York NY, United States of America

^u Also at CPPM, Aix-Marseille Université and CNRS/IN2P3, Marseille, France

^v Also at School of Physics and Engineering, Sun Yat-sen University, Guanzhou, China

- ^w Also at Academia Sinica Grid Computing, Institute of Physics, Academia Sinica, Taipei, Taiwan
- ^x Also at School of Physics, Shandong University, Shandong, China
- ^y Also at Dipartimento di Fisica, Università La Sapienza, Roma, Italy
- ^z Also at DSM/IRFU (Institut de Recherches sur les Lois Fondamentales de l'Univers), CEA Saclay (Commissariat à l'Energie Atomique), Gif-sur-Yvette, France
- ^{aa} Also at Section de Physique, Université de Genève, Geneva, Switzerland
- ^{ab} Also at Departamento de Fisica, Universidade de Minho, Braga, Portugal
- ^{ac} Also at Department of Physics, The University of Texas at Austin, Austin TX, United States of America
- ^{ad} Also at Department of Physics and Astronomy, University of South Carolina, Columbia SC, United States of America
- ^{ae} Also at Institute for Particle and Nuclear Physics, Wigner Research Centre for Physics, Budapest, Hungary
- ^{af} Also at California Institute of Technology, Pasadena CA, United States of America
- ^{ag} Also at Institute of Physics, Jagiellonian University, Krakow, Poland
- ^{ah} Also at LAL, Université Paris-Sud and CNRS/IN2P3, Orsay, France
- ^{ai} Also at Nevis Laboratory, Columbia University, Irvington NY, United States of America
- ^{aj} Also at Department of Physics and Astronomy, University of Sheffield, Sheffield, United Kingdom
- ^{ak} Also at Department of Physics, Oxford University, Oxford, United Kingdom
- ^{al} Also at Department of Physics, The University of Michigan, Ann Arbor MI, United States of America
- ^{am} Also at Discipline of Physics, University of KwaZulu-Natal, Durban, South Africa
- * Deceased